UNIVERSITATEA POLITEHNICA TIMIŞOARA

FACULTATEA DE CONSTRUCŢII
DEPARTAMENTUL DE CONSTRUCŢII METALICE ŞI MECANICA CONSTRUCŢIILOR
Ioan Curea 1, 300224 Timişoara, ROMÂNIA

HABILITATION THESIS

Contributions to the behavior of structures under extreme loading

Contribuţii la studiul comportarii structurilor solicitate la actiuni extreme

Assoc. Prof. Florea DINU, PhD
Civil Engineering Faculty
The "Politehnica" University of Timişoara

15.03.2013

Table of content

2

(a) Abstract

The research activity of the candidate started in November 1994, when he was first employed at The Romanian Academy, Timisoara Branch, then continued with the enrolment for the PhD in 1995, under the coordination of Acad. Dan Mateescu, the founder of the Steel Structure Research School in Timisoara.

In 2004 the candidate defended the PhD Thesis at The "Politehnica" University of Timişoara. The PhD thesis investigated the behaviour of MR steel frames with semirigid joints, focusing mainly on the seismic behaviour of such structures and taking into account the real behaviour of beam-to-column joints. In the thesis were also investigated factors that may affect the local ductility of MR steel frames and which may be key factors when a structure is loaded beyond normal conditions, e.g. strain rate, welding detail. It was also proposed a methodology for performance based design and evaluation of buildings based on partial seismic reduction factors, q. The main results of the thesis were presented in several international conferences and in national or international journals. Candidate has been also involved, as member or coordinator, in several national research grants sponsored by Ministry of Education and Research and international research programs. In 2003 the candidate has been awarded by the European Convention for Constructional Steelwork for the application of new structural systems to seismic resistant structures. Since 2005, he is a full member of the Department of Steel Structures and Structural Mechanics from the Civil Engineering Faculty, Politehnica University of Timisoara.

The thesis presents the activity of the candidate after defending the PhD Thesis at The "Politehnica" University of Timişoara, which was confirmed by The Ministry of Education and Research, on the basis of Order no. 1300/112/C, dated 23.12.2004.

Within all this period, the research activity extended the previous research that has been developed during the PhD period (which focused mainly on seismic behavior of steel framed buildings). Starting from the performance based seismic design methodology and the factors that affect one of the key properties, i.e. ductility of members and connections, the research activity extended to other extreme actions, with the aim of providing a complete set of design requirements under any type of extreme loading. These new topics partially continued the previous activity, but there were also new topics that emerged from the previous activity. As a direct consequence of the research activity, a great effort has been paid to bring these new concepts into real applications. Thus, there were several projects that may be viewed as innovative, from the point of view of the structural system, connections, detailing and use of materials or analysis techniques. For their innovative character, applications have been awarded by prestigious national and international organizations.

A great support for the activity that followed after the PhD, may be attributed to the participation of the candidate to national and international projects and also to the cooperation with industrial partners. This can be justified by the publication of more than 40 papers, mostly in international conferences and journals. The main achievements and results are presented in detail in Chapter (b-i): *Scientific, professional and academic achievements.*

In what concerns the future research and development plans that are related to the fields of research presented above, the following research topics will be further developed or will start:
<u>Robustness based design of buildings</u>
- Experimental program on beam-to-column joints under column loss scenario
- Experimental program on 3D assemblies under column loss scenario
- Experimental program on macro-components and welding details under extreme loading

- o Validation of numerical models for members and connections to evaluate the progressive collapse resistance of framed buildings
- o Improved details for progressive collapse resistance
- o Guidelines for the collapse control performance based design of multi-story frame buildings against accidental actions

Improved structural systems and application to buildings
- o New structural systems based on removable dissipative members
- o New hysteretic devices with improved damping characteristics (eg. visco-elastic dampers)
- o Application of new braced systems (steel panels, buckling restrained braces) to design of new buildings
- o Application of new braced systems (steel panels, buckling restrained braces) for refurbishing existing buildings.

Durability of structures under climate change effects
- o Evaluation of the reliability and durability of structures along the designed lifetime
- o Methodologies for Performance Based Evaluation / Design of construction for progressive climate action exposures;
- o Intervention strategies and adaptive building technologies

A short description of each topic is given in Chapter (b-ii): *Scientific, professional and academic future development plans.*

(b) ACHIEVEMENTS AND DEVELOPMENT PLANS

(b-i) Scientific, professional and academic achievements

1   INTRODUCTION

The research activity of the candidate started in November 1994, when he was first employed at The Romanian Academy, Timisoara Branch, then continued with the enrolment for the PhD in 1995, under the coordination of Acad. Dan Mateescu, the founder of the Steel Structure Research School in Timisoara.

In 2004 the candidate defended the PhD Thesis at The "Politehnica" University of Timişoara. The PhD thesis investigated the behaviour of MR steel frames with semirigid joints, focusing mainly on the seismic behaviour of framed structures and taking into account the real behaviour of beam-to-column joints. He proposed a methodology for performance based design and evaluation of buildings based on partial seismic reduction factors, q. In the thesis were also investigated factors that may affect the local ductility of MR steel frames, e.g. strain rate, welding detail, which may be key factors when a structure is loaded beyond normal conditions. The main results of the thesis were presented in several international conferences and published in national and international journals. Candidate has been also involved, as member or coordinator, in several national research grants sponsored by Ministry of Education and Research and international research programs.

Since 2005, he is a full member of the Department of Steel Structures and Structural Mechanics from the Civil Engineering Faculty.

The thesis presents the activity of the candidate after defending the PhD Thesis at The "Politehnica" University of Timişoara, which was confirmed by The Ministry of Education and Research, on the basis of Order no. 1300/112/C, dated 23.12.2004.

Within all this period, the research activity extended the previous research that has been developed during the PhD period. Starting from the performance based seismic design methodology and the factors that affect one of the key properties, i.e. ductility of members and connections, the research activity extended to other extreme actions, with the aim of providing a complete set of design requirements under any type of extreme loading. These new topics partially continued the previous activity, but there were also new topics that emerged from the previous activity. The research activities developed by the candidate after defending the PhD Thesis, can therefore be divided in three main components:

- Models and methods for the control, design and evaluation of structural performance of building frames:
    - Factors affecting local ductility of beam-to-column connections: this topic, which refers to factors affecting local ductility, has been one of the key parameters investigated within the PhD activity - *This activity has continued and extended to other factors, like the design failure mode of the connection and the strain rate associated or not with the elevated temperature.*
    - Collapse control design methodology for prevention of collapse in case of extreme loading:
        - Effect of local ductility on the progressive collapse resistance and development of catenary action (improved beam-to-column connections, composite beams, membrane action of composite floors)

- New modeling techniques for extreme events on buildings (the Applied Element Method may be used for blast and explosion, and can model the initiation and propagation of cracks until complete separation).
  This topic, which refers to the design approach for reducing the risk of collapse, is an extension of the previous research devoted to the performance based design, now extended to other types of actions and using different analysis techniques.
  - Tools for practical design evaluation of dissipation capacity - behavior factor q, modeling parameters and acceptance criteria – *This topic also continued the activity developed during the PhD period. The innovative character of this last research is evaluation of q factor for new and existing structures based on experimental tests.*

- <u>Improved structural systems and detailing for increasing the robustness under extreme loading:</u>
  - Dual steel structural systems, dual steel frame connections
  - Systems with removable dissipative members and improved recentring capacity (dual frames with removable steel panels, dual frames with removable buckling restrained braces, frames with coupling beams)

  This research topic can be considered partially as a new topic. Thus, the dual steel solutions, both at local level (connections) or global level (members), may help adjusting the mechanical characteristics to fit better with the demands. For example, by using lower steel grade for dissipative parts or members, the over strength demand on non-dissipative ones may be reduced.

- <u>The applications for buildings, can be divided in two main groups:</u>
  - Low rise commercial buildings made with steel or composite structures
  - Design of multistory frame buildings. Two example will be presented in the thesis:
    - Design and performance based evaluation of a 26 storey building located in Bucharest
    - Design and performance based evaluation of a 6 storey building located in Constanta

  As a direct consequence of the research activity, a great effort has been paid to bring these new concepts into real applications. Thus, the third topic may be considered as the application of all this concepts and studies to design and construction of low rise to high rise buildings. There were several projects that may be viewed as innovative, from the point of view of the structural system, connections, detailing, and use of materials or analysis techniques. For their innovative character, many applications have been awarded by prestigious national and international organizations.

A great support for the activity that followed after the PhD, may be attributed to the participation of the candidate to national and international projects and also to the cooperation with industrial partners. This can be justified by the publication of more than 40 papers, mostly in international conferences and journals, and the awards from national and international professional organizations. The main achievements and results are presented in detail in Chapter (b-i): *Scientific, professional and academic achievements.*

In what concerns the future research and development plans that are related to the fields of research presented above, the following research topics will be further developed or will start:

- <u>Robustness based design of buildings</u>
  - Experimental program on beam-to-column joints under column loss scenario

- Experimental program on 3D assemblies under column loss scenario
- Experimental program on macro-components and welding details under extreme loading
- Validation of numerical models for members and connections to evaluate the progressive collapse resistance of framed buildings
- Improved details for progressive collapse resistance
- Guidelines for the collapse control performance based design of multi-story frame buildings against accidental actions

- Improved structural systems and application to buildings
  - New structural systems based on removable disipative members
  - New hysteretic devices with improved damping characteristics (eg. visco-elastic dampers)
  - Application of new braced systems (steel panels, buckling restrained braces) to design of new buildings
  - Application of new braced systems (steel panels, buckling restrained braces) for refurbishing existing buildings.
- Durability of structures under climate change effects
  - Evaluation of the reliability and durability of structures along the designed lifetime
  - Methodologies for Performance Based Evaluation / Design of construction for progressive climate action exposures;
  - Intervention strategies and adaptive building technologies

A short description of each topic is given in Chapter (b-ii): *Scientific, professional and academic future development plans.*

In the following figure, the development of the research and also the planned future activities are presented. It is worthwhile to mention the research activity has been continuously increasing within the last decade. There were continuous developments in the field of seismic design, with large experimental programs, theoretical and advanced numerical contributions. But in the last years, a new topic emerged from the seismic design, i.e. robustness of structures under extreme loading. There is a strong connection between seismic design principles and robustness of structures. The FEMA Report released after the Murah Building attack, revealed that "if more recently developed detailing, such as those present in special moment frames used in seismic regions had been in place, the collapsed area would have been reduced at least by 50 % and at most by 80 %". Since there is a justified interest for linking the two research topics, it will be of great importance to support these activities.

Also the research team has been enlarged within the last decade. The national and international visibility has been another key issue, and has been supported by numerous research or dissemination project. It is worthwhile to mention two Cost Actions where the candidate participated as a Romanian representative, i.e. Cost C12 (2000-2005) and Cost C26 (2006-2010) Actions. These Actions benefited from a large and representative European Research Network and helped the interconnection between CEMSIG activities and similar European activities. Last, the national funded Partnership research project CODEC (2012-2016), where the candidate is the project director, is very important in continuing the activities within the next years, of course with the logistic and personnel contribution from the CEMSIG Centre.

Main PhD activity

Factors affecting local ductility
- *Strain rate effects*
- *Welding detail*
- *Low cycle fatigue effects*

Performance based seismic design and evaluation
- *Partial q factors for seismic design of frame structures*
- *Multi-level design methodology*

Activities post PhD

Models and methods for the control, design and evaluation of structural performance of building frames:
- *Factors affecting local ductility of beam-to-column connections*
- *Collapse control design approach for prevention of collapse in case of extreme loading*
- *Tools for practical design evaluation of dissipation capacity*

Improved structural systems and detailing for increasing the robustness under extreme loading:
- *Dual steel structural systems*
- *Dual steel frame connections*
- *Systems with removable dissipative members*

The applications for buildings

Future activities post Habilitation

- Robustness based design of buildings
  - *Experimental program on beam-to-column joints under column loss scenario*
  - *Experimental program on 3D assemblies under column loss scenario*
  - *Experimental program on macro-components and welding details under extreme loading*
  - *Validation of numerical models for members and connections to evaluate the progressive collapse resistance of framed buildings*
  - *Improved details for progressive collapse resistance*
  - *Guidelines for the collapse control performance based design of multi-story frame buildings against accidental actions*
- Improved structural systems and application to buildings
  - *New structural systems based on removable disipative members*
  - *New hysteretic devices with improved damping characteristics (eg. visco-elastic dampers)*
  - *Application of new braced systems (steel panels, buckling restrained braces) to design of new buildings*
  - *Application of new braced systems (steel panels, buckling restrained braces) for refurbishing existing buildings.*
- Durability of structures under climate change effects
  - *Evaluation of the reliability and durability of structures along the designed lifetime*
  - *Methodologies for Performance Based Evaluation/Design of construction for progressive climate action exposures;*
  - *Intervention strategies and adaptive building technologies*

Presentations within national and international Conferences

- Meeting within COST, Action C12 "Improving Building Quality by New Technologies", Rzeszow, Poland, 23-24 April, 2004.
- Meeting within COST, Action C12 "Improving Building Quality by New Technologies", Biel, Switzerland, 10-11 September, 2004.
- Final Conference Cost C12 "Improving Buildings Quality by New Technologies", 20-22 January 2005, Innsbruck, Austria.
- XVth National Conference AICPS, Bucharest, 20 May 2005.
- IVth European Conference Eurosteel 2005, 8-10 June 2005, Maastricht, Netherlands.
- The International Conference in Metal Structures: Steel – A New and Traditional Material for Building. Poiana Brașov, Romania, 20 - 22 September 2006.
- COST Action C26 "Urban Habitat Constructions Under Catastrophic Events", Management Committee Meeting, Bruxelles, Belgium, 21 June 2006.
- COST Action C26 "Urban Habitat Constructions Under Catastrophic Events", Management Committee Meeting, Napoli, Italy, 21 October 2006
- COST Action C26 "Urban Habitat Constructions Under Catastrophic Events", Working Group Meeting, Delft, Netherlands, 17 - 18 November 2006
- XVth National Conference AICPS, Bucharest, 18 May 2006.
- Workshop COST Action C26 "Urban Habitat Constructions Under Catastrophic Events", Prague, Czech Republic, 30-31 March, 2007.
- 6th International Conference on Steel and Aluminium Structures ICSAS'07, 24-27 July 2007, Oxford, UK.
- International Conference on Steel and Composite Structures, ICSCS'07, 30 July – 01 August 2007, Manchester, UK.
- 5th International Conference on Advances in Steel Structures, Singapore, 5 – 7 December 2007.
- COST Action C26 "Urban Habitat Constructions Under Catastrophic Events", Working Group Meeting, Vilnius, Lithuania, 11 - 12 April, 2008.
- Meeting within ECCS TC13 "Seismic Resistant Structures", Napoli, Italy, 16-17 May, 2008.
- 5th European Conference on Steel and Composite Structures, Eurosteel 2008, 3-5 September 2008, Graz, Austria.
- International Seminar Cost C26, "Urban Habitat Constructions under Catastrofic Events", ESF, Malta, 22-23 October 2008.
- COST Action C26 "Urban Habitat Constructions Under Catastrophic Events", Working Group Meeting, 27 - 28 March, 2009, Southampton, UK.
- COST Action C26 "Urban Habitat Constructions Under Catastrophic Events", Working Group Meeting, 24 - 25 November, 2009, Aveiro, Portugal.
- Meeting within ECCS TC13 "Seismic Resistant Structures", Ispra, Italy, 6 November, 2009.
- COST Action C26 "Urban Habitat Constructions Under Catastrophic Events", Working Group Meeting, 19 - 20 March, 2010, Nicosia, Cyprus.
- Meeting within ECCS TC13 "Seismic Resistant Structures", 7 May 2010, Aachen, Germany.
- SDSS'Rio 2010, International Colloquium Stability and Ductility of Steel Structures, 08-10 September 2010, Rio de Janeiro, Brazil.
- COST Action C26 Final Conference – Urban Habitat Constructions under Catastrophic Events, 16-18 September 2010, Naples, Italy.

- International Conference "Steel Structures: Culture & Sustainability 2010", 21-23 September 2010, Istanbul, Turkey.
- International Conference on Engineering Research University of Pécs, Pollack Mihály Faculty of Engineering, October 25-26, 2010, Pécs, Hungary.
- Meeting within ECCS TC13 "Seismic Resistant Structures", Salerno, Italy, 19 November 2010.
- 3rd International Workshop on Performance, Protection and Strengthening of Structures under Extreme Loading – PROTECT2011, 30.08-01.09.2011, Lugano, Switzerland.
- Meeting within ECCS TC13 "Seismic Resistant Structures", November 2011, Ljubljana, Slovenia.
- XVIIth National Conference AICPS, Bucharest, 20 May 2011.
- International Conference IRF 2013, Funchal, Madeira, Portugal, 22/06/2013-29/06/2013.
- International Conference Protect 2013, Mysore, India, 26-28.08.2013
- International Conference CTA 2013, Torino, Italy, 30 sept – 2 oct, 2013.

Articles constituting the habilitation thesis

This is a survey of the results constituting my habilitation thesis. It is based on the following articles.

1. Daniel Grecea, Dinu Florea, Dan Dubina, Performance criteria for MR steel frames in seismic zones, Journal of Constructional Steel Research, 2004, 01/2004; 60(3)
2. Dubina Dan, Stratan Aurel, Dinu Florea, Dual high-strength steel eccentrically braced frames with removable links, Earthquake Engineering and Structural Dynamics, 2008, vol. 37, no. 15
3. Dinu Florea, Neagu C, Dubina D, A comparative analysis of performances of high strength steel dual frames of buckling restrained braces vs. dissipative shear walls, 6th International Conference on Behaviour of Steel Structures in Seismic Areas, Philadelphia, PA, 2009, 16-20.08, ISBN978-0-415-56326
4. Dubina D., Dinu Florea, Stratan A., Design and performance based evaluation of Tower Centre International building in Bucharest. Part II: Performance based evaluation, Steel Construction, Steel Construction, 2010, ISSN 1867-0520.
5. Dinu Florea, Dubina D., Ciutina Adrian, Robustness performance of seismic resistant building frames under abnormal loads, Structures and Architecture, Guimaraes, Portugal, 2010, ISBN 978-0-415-49249-2.
6. Dubina D., Dinu Florea, Robustness based structural design: an integrated approach for multi-hazard risk mitigation, 3rd International Workshop on Performance, Protection and Strengthening of Structures Under Extreme Loading Location: Lugano, SWITZERLAND, 2011, 30.08-01.09, ISBN-13: 978-3-03785-217-0
7. Dubina D., Stratan A., Dinu Florea, Re-centring capacity of dual-steel frames Steel Construction, Steel Construction, 2011, ISSN 1867-0520.
8. Dinu Florea, D. Dubina, C. Neagu, I. Both, C. Vulcu, S. Herban, Experimental and numerical evaluation of a RBS coupling beam for moment steel frames in seismic areas, Steel Constructions, 2012, ISSN 1867-0520.
9. Dubina Dan, Dinu Florea, Experimental evaluation of dual frame structures with thin-walled, steel panels, Thin walled structures, 78, 2014.
10. Dinu Florea, Dubina Dan, Ioan Marginean, Improving the structural robustness of multi-story steel-frame buildings, Structure and Infrastructure Engineering, 2014.

2 MODELS AND METHODS FOR THE CONTROL, DESIGN AND EVALUATION OF STRUCTURAL PERFORMANCE OF BUILDING FRAMES

**National and international experience of the candidate related to the topic
"Models and methods for the control, design and evaluation of structural performance
of building frames"
(Post-PhD Thesis period)**

Member of technical boards:
- Member of Technical Committee TC13 "Seismic Design" of the European Convention for Constructional Steelwork (ECCS);
- Member of AICPS – Romanian Association of Structural Engineers;
- Member of APCMR – Romanian Association for Constructional Steelwork;
- Member of AGIR – Romanian Association of Engineers.

Conference committees:
- Organization Committee of the International Conference on Thin-Walled Structures: Recent research advances and trends, Timisoara, Romania, 5-7 September 2011;
- Organization Committee of the International Conference in Metal Structures: Steel – A New and Traditional Material for Building, Poiana Braşov, Romania, 20-22.09.2006;
- Chairman of Technical Session: 5th European Conference on Steel and Composite Structures, Eurosteel 2008, 3-5 september 2008, Graz, Austria.
- Chairman of Technical Session: International Symposium "Steel Structures:Culture & Sustainability 2010", 21-23 September 2010, Istanbul, Turkey.

Supporting projects:
- COST C26, Urban habitat constructions under catastrophic events, 2005-2010
- Structural conception and collapse control performance based design of multistory structures under aacidental actions (CODEC), PNII-PT-PCCA, 2012-2016
- Factori de comportare a structurilor metalice in zone seismice pentru implementarea criteriilor de proiectare bazate pe performanta, MEC   Grant 33047/2004, cod CNCSIS 219, 2004-2005.
- Criterii de precalificare a îmbinărilor ductile ale cadrelor metalice necontravantuite, MEC – CNCSIS, Grant CNCSIS cod 728, tema nr.2
- Sisteme constructive si tehnologii avansate pentru structuri din oteluri cu performante ridicate destinate clădirilor amplasate în zone cu risc seismic", Acronim „STOPRISC", Proiect de cercetare de excelenta Program CEEX – MATNANTECH, PC-D04-PT23-346, 2005-2007
- Simulari numerice cu MEF si incercari experimentale pe subansamble din structura de rezistenta a unei cladirii de birouri 4S+P+17+E, contract 76/2011, 2011, DMA.
- Requirements for multi-storey buildings in seismic areas, RUUKKI/2009, 2009, Rautaruukki Corporation, Finland.

Invited papers and courses:
- Invited lecturer at TUCSA (Turkish Association for Constructional Steelwork), 02.03.2009 (Lecture: Multi storey steel frame buildings in seismic areas. Authors: Dan Dubina, Florea Dinu).

- Invited course Cost C25/C26: Sustainability in Structures and Structural Interventions. Improving the contemporary and historical urban habitat constructions within a sustainability and risk assessment framework, Early stage researchers training school, 17-24 May 2009, Thessaloniki, Greece.

Reviewer in ISI journals:
Journal of Structural Engineering – ASCE (http://ascelibrary.org/sto/)

Books:
- Vulnerability and damageability of constructions under impact and explosion", COST Action Final Report – Urban Habitat Constructions under Catastrophic Events, CRC Press, A Balkema Book, ISBN 978-0-415-60686-8, 2010.

Member in PhD Juries related to the topic
- Member in the PhD Jury of Adrian Grigore MARCHIŞ Andrei Crişan: "Progressive collapse vulnerability of seismic resistant multi storey concrete frame structures", Technical University of Cluj-Napoca, October 2013.

Scientific articles with international partnership
- Robust design of steel framed buildings against extreme loading, Autori: M.P. Byfield, G. De Matteis, F. Dinu, in Proc. of COST C26 Workshop "Urban Habitat Constructions Under Catastrophic Events, Praga 30-31 martie 2007, Ed. Wald F, Mazzolani M, Byfield M, Dubina D, Faber M, ISBN 978-80-01-03583-2, p. 295-302.
- F. Dinu, D. Dubina, G. De Matteis: Direct design approach for seismic resistant steel frame buildings under extreme loading, COST Action Final Conference – Urban Habitat Constructions under Catastrophic Events, CRC Press, A Balkema Book, 16-18 September 2010, Naples, Italy, Ed. F. Mazzolani, ISBN 978-0-415-60685-1, pg. 349-354.
- G. De Matteis, F. Dinu, Structural measures for improving progressive collapse resistance of multi-storey buildings under accidental actions, Italian conference on Steel Structure XXIV CTA, Torino 30 sept.-2 oct. 2013.
- Dinu F., Santiago A., Dubina d., Simoes Da Silva L., Robustness demand for structural connections of multistory steel building frames under elevated temperature; in Performance, Protection & strengthening of structures under extreme loading, Protect 2013, Mysore, India, Aug., 26-27, 2013, Published by Indian concrete Journal (ICJ) p. 9. (CD paper).

2.1 Introduction

The conception, design and execution of structures for building, but in general for all constructions, should ensure the structure can be used for its intended purpose with anticipated maintenance but without major repair being necessary. The structural systems, materials, design methods but also the erection and maintenance works should all be selected so that this demand is fulfilled. However, during its design working life, a structure may be subjected to some extreme events, like earthquakes, impact or collisions, and this may endanger the stability and the load bearing capacity of the structure. Therefore, several design situations should be considered, i.e. (EN 1990, 2002) persistent or transient design situations, accidental design situations and seismic design situations (if the location is in a seismic zone). Thus, for permanent and transient design situations, the actions are foreseeable and the verifications are done following several limit states, like Ultimate Limit States or Serviceability Limit States. There are, however, unforeseeable hazards or actions with a

higher than expected intensity and therefore, it is also necessary to consider accidental and seismic situations (if approapriate).

In case of the seismic action, the system is traditionaly designed to dissipate a part of the induced energy by means of plastic deformations in the so called dissipative zones. Unfortunately, extreme loads associated with accidental situations do not fit easily within the ULS design approach because the implication of the ULS load being exceeded is not considered. Furthermore, ULS design, based on lower-bound strength calculations, has been shown to be capable of producing a mismatch between the strength of beams and their connections (Byfield, 2004). When combined with low ductility of the system, this will produce brittle buildings.

The activity developed in the last 10 years has focused on the following topics:
1) Performance based seismic design methodology based on partial q factors
2) A new methodology for evaluating the low cycle fatigue resistance of steel members
3) Factors affecting local ductility of beam-to-column connections
4) Collapse control design approach for prevention of collapse in case of extreme loading
5) Dual steel beam-to-column connections of moment resisting steel frames (evaluation of the plastic rotation capacity, details for improved ductility and strength properties, effect of tying in case of column loss)
6) Numerical modeling of membrane action of composite slabs in case of column loss events
7) New modeling techniques for extreme events on buildings (the Applied Element Method may be used for blast and explosion, and can model the initiation and propagation of cracks until complete separation).

First three topics are mostly related to seismic design which was an important research domain for many decades within the CMMC Department. The activities focused on the effect of damage cumulative process, or low cycle fatigue, factors that affect the local ductility of beam to column connections, e.g. strain rate effect and welding detail and also on developing a new methodology for the performance based seismic design and evaluation of buildings. This methodology uses partial q factors for the different limit states or performance levels. The advantage of the method is that it can be easily implemented in the actual forced based design codes.

The last four topics are of recent interest and gained an increasing attention in the last decade, mainly as a result of the increasing concern regarding the resistance against collapse under extreme loading events. Of particular interest is the collapse control design, that emerged as a new method that may be used to incorporate measures that reduce the risk of collapse in case of extreme loading. The development of design guides for collapse control of the multi-story buildings started in 1968 with the collapse of the Ronan Point high-rise building in the United Kingdom, due to a gas explosion. The failure of the building was identified as a "progressive collapse", because the extent of damage was disproportionate compared to the initial cause. Three decades later, in 2001, the attack against the twin towers of the World Trade Center caused the complete failure of the two buildings and massive loss in lives and property. The type of collapse was again identified as progressive collapse. More recently, during the winter 2005/2006, several construction halls, shopping centers or hotels have been damaged or destroyed throughout Europe due to very heavy snowfalls. For example, the roof of the Exhibition Hall in Katowice, Poland, collapsed due to heavy snowfall and caused 65 dead and more than 170 injured. The investigation found design and construction flaws, that caused a lack of robustness which, associated with large drifted snow, finally caused the collapse. Even this time was not a progressive collapse, the lack of alternate load paths when the most stressed elements failed could have been identified and proper measures adopted by considering the collapse control design. These tragic events alerted

construction engineers and public authorities and warned about the importance of preventing progressive collapse in case of extreme load events.

Several papers related to this topic have been published during the last 10 years. A selection of these papers is presented below:

1. Daniel Grecea, Dinu Florea, Dan Dubina, Performance criteria for MR steel frames in seismic zones, Journal of Constructional Steel Research, 2004, 01/2004; 60(3)
2. F. Dinu, D. Dubină, A. Stratan, Performance based design of steel frames, Cost C12 Final Conference Proceedings, A.A.Balkema Publishers, Leiden, The Nederlands, ISBN 04 1536 609 7, Ed. C. Schaur et al, 20-22 January 2005, Innsbruck, Austria, pg. 291-301.
3. F. Dinu, D. Dubină, A. Stratan, Welded Joints, Effect of Detailing and Strain Rate, Final Scientific Report, Cost C12 Action "Improvement of Buildings Structural Quality by New Technologies", A.A.Balkema Publishers, Leiden, The Nederlands, ISBN 04 1536 6100 0, 2005, pg. 313-318.
4. F. Dinu, D. Dubina. Robustness of seismic resistant multistory frame buildings in case of accidental column loss scenarios, Philadelphia, 16-20 aug. 2009, International Conference, STESSA 2009, Behaviour of Steel Structures in Seismic Areas, CRC Press 2009, Ed. F.M. Mazzolani, J.M. Ricles, R. Sause, ISBN: 978-0-415-56326-0.
5. Dinu Florea, Dubina D., Ciutina Adrian, Robustness performance of seismic resistant building frames under abnormal loads, Structures and Architecture, Guimaraes, Portugal, 2010, ISBN 978-0-415-49249-2.
6. F. Dinu, D. Dubina: Effect of column loss on the robustness of a high rise steel building, COST Action Final Conference – Urban Habitat Constructions under Catastrophic Events, CRC Press, A Balkema Book, 16-18 September 2010, Naples, Italy, Ed. F. Mazzolani, ISBN 978-0-415-60685-1, pg. 613-618.
7. F. Dinu, D. Dubina, G. De Matteis: Direct design approach for seismic resistant steel frame buildings under extreme loading, COST Action Final Conference – Urban Habitat Constructions under Catastrophic Events, CRC Press, A Balkema Book, 16-18 September 2010, Naples, Italy, Ed. F. Mazzolani, ISBN 978-0-415-60685-1, pg. 349-354.
8. F. Dinu, D. Dubina, C. Neagu: Experimental evaluation of q factor for dual steel frames with dissipative shear walls, COST Action Final Conference – Urban Habitat Constructions under Catastrophic Events, CRC Press, A Balkema Book, 16-18 September 2010, Naples, Italy, Ed. F. Mazzolani, ISBN 978-0-415-60685-1, pg. 975-980.
9. F. Dinu: Capitol 3 „Vulnerability and damageability of constructions under impact and explosion", COST Action Final Report – Urban Habitat Constructions under Catastrophic Events, Ed. F. Mazzolani, CRC Press, A Balkema Book, 16-18 September 2010, Naples, Italy, ISBN 978-0-415-60686-8, pg. 247-270.
10. F. Dinu, D. Dubina: Ductility vs overstrength in robustness based design of multi-story steel building frames under abnormal loadings, Proc. of the International Symposium "Steel Structures:Culture & Sustainability 2010", 21-23 September 2010, Istanbul, Turkey, Ed. N. Yardimci, A. Aydoner, Y. Gur'es, C. Yorgun, ISBN: 978-975-92461-2-9, pg. 171-178.
11. Ciutina A., Ungureanu V., Dubina D., Dinu F.: "Integrated design of buildings". Proceedings of the International Conference: Sustainability of Constructions – Towards a better built environment. 3-5 February 2011, Innsbruck, Austria, ISBN: 978-999957-816-0-6, pp. 235-246.
12. Dubina D., Dinu F.: "Robustness based structural design: an integrated approach for multi-hazard risk mitigation". 3rd International Workshop on Performance, Protection and Strengthening of Structures under Extreme Loading – PROTECT2011, 30.08-01.09.2011,

Lugano, Switzerland, Trans Tech Publications, Applied Mechanics and Materials. ISSN: 1660-9336, Vol. 82(2011), pp. 770-777.

13. Dinu F., Dubina D.: "Robustness of multi-storey steel building frames-Demands for beam to column joints". Proceedings of the 6th European Conference on Steel and Composite Structures. August 31 – September 2, 2011, Budapest, Hungary, ISBN 978-92-9147-103-4, pp. 2487-2492.

14. Dinu Florea, Dubina Dan, Ioan Marginean, Improving the structural robustness of multi-story steel-frame buildings, Structure and Infrastructure Engineering, 2014.

15. M.P. Byfield, G. De Matteis, F. Dinu, Robust design of steel framed buildings against extreme loading, in Proc. of COST C26 Workshop "Urban Habitat Constructions Under Catastrophic Events, Prague 30-31 March 2007, Ed. Wald F, Mazzolani M, Byfield M, Dubina D, Faber M, ISBN 978-80-01-03583-2, p. 295-302.

16. Dinu F., Santiago A., Dubina D., Simoes Da Silva L., Robustness demand for structural connections of multistory steel building frames under elevated temperature; in Performance, Protection & strengthening od structures under Extreme Loading - Protect 2013, Mysore, India, Aug. 26-27, 2013, Published by Indian concrete Journal (ICJ) p. 9.(CD paper).

17. Dinu F., Dubina, D., Marginean, I., Effect of connection between reinforced concrete slab and steel beams in multistory frames subjected to different column loss scenarios. Proc. 4th int. Conf on Integrity, Reliability and Failure –IRF,2013, 23-27 June, Funchal, Portugal, p 215-16, (CD paper ref 3882), ED. INEGI, Porto, Portugal, ISBN 978-9772-8826-27-7.

18. Dubina D., Dinu F., Margineani I., Collapse prevention design criteria for moment connections in multi-story steel frames under extreme actions. Proc. 4th int. Conf on Integrity, Reliability and Failure –IRF,2013, 23-27 June, Funchal, Portugal, p 41-42 (CD paper ref. 388) Porto, Portugal, ISBN 978-9772-8826-27-7

In the following, will be presented the most important results obtained by the candidate and some discussions, and comparisons and references to similar activities developed worldwide will be made. To note that the topics covered by the candidate are of large interest for the scientific community, authorities and codification bodies. It is also important to underline the continuity of the research activities throughout this period, the important international component, participation to large and important conferences and participation or coordination of important research projects.

2.2   Performance based seismic design methodology based on partial q factors

2.2.1   Introduction

During the last years, a large number of devastating earthquakes have occurred throughout the world. A large number of structures designed and built in accordance with current building codes have been subjected to strong ground-motions, exceeding the levels for which they have been designed. Damage assessments during these events have enabled engineers to learn and improve building code design provisions, as well as construction techniques for buildings located in regions of high seismic hazard. For example, steel moment resisting frames (MRF), which are widely used as lateral load resisting systems for low- to medium-rise buildings, suffered a surprising amount of damage during the 1994 M6.7 Northridge and 1995 M7.2 Hanshin-Awaji (Kobe) earthquakes.

In several countries, seismic design is in the process of fundamental change. One important reason for the need for change is that although buildings designed to current codes performed well during recent earthquakes from a life safety perspective, the economic loss was unexpectedly high. After Ghobarah [1], conventional methods of seismic design are providing

for life safety (strength and ductility) and damage control (serviceability drift limits). The design criteria are defined by limits on stresses and member forces calculated from prescribed levels of applied lateral shear force. The actual codes are presenting some uncertainties between the seismic demand and the seismic capacity of the structure. Performance based design is a more general design philosophy in which the design criteria are expressed in terms of performance objectives, like lateral deflections, interstorey drifts, element ductility, and element damage indices, when the structure is subjected to different levels of seismic hazard. To reduce high costs, due to loss of use and repair of heavily damaged structures, different levels of performance objectives need to be taken into account.

2.2.2 Performance based design and evaluation

The concept of performance based design and evaluation procedures for building is not new, but is in continuous development in the field of seismic design. For many years, the seismic design provisions contained in the building codes have been implicitly based on multiple performance objectives. However, most of the codes consider explicitly only one limit state, defined as protection of occupants lives in case of a major earthquakes.

Performance based seismic design is defined as a selection of design criteria and structural systems such that at the specified levels of ground motion and with defined levels of reliability, the structure will not be damaged beyond certain limit states or other useful limits [4,5].

2.2.2.1 Performance objectives and levels

The basic specification of performance that is used as a basis for performance based design is the performance objective. It comprises two parts, a design hazard level and a design performance level. The design hazard level is a quantification of the severity and character of ground shaking that a structure has to resist. The design performance level is a quantification of the permissible types and distribution of damage to the structure, given that design hazard level shaking is experienced. This concept is not new because for many years, the seismic design provisions contained in the building codes have been implicitly based on multiple performance objectives:

– resist to minor earth quakes without damage;

– resist to moderate earthquakes without structural damage but with some nonstructural damage;

– resist to major earthquakes with significant structural and non-structural damage and resist to the most severe earthquakes ever likely to affect the building without collapse.

Unfortunately, these performance specifications are quite vague with regard to definition of both the hazard and anticipated performance, making the attainment of the desired performance difficult.

The coupling of a performance level with a specific level of ground motion provides a performance design objective [2,6]. In the United States, the most important provisions, referring to performance based design were offered by FEMA [3] and SEAOC [2]. In this perspective, the SEAOC Vision 2000 Committee proposes four performance levels: fully operational, operational, life safe and near collapse. Fully operational is a state in which the facility continues in operation with negligible damage to non-structural elements only. In the operational state, the facility continues in operation with minor damage to both structural and non-structural elements and minor disruption in non-essential services. Structures in the life safety condition are significantly damaged, but are expected to be repairable, although perhaps not economically. Structures in the near collapse condition still guarantee the safeguard of the human lives, but corresponding to potential complete economic losses [6]. In

Figure 1, these four performance levels as a function of building destination and earthquake frequency are presented.

It can be observed in Figure 1 that for buildings belonging to category, under a frequent earthquake, structure will not suffer any damage, and under a rare or very rare earthquake, the level of damages will be extended, but life protection and prevention of collapse to be assured. However, it seems more reasonable not to ask design engineers to perform many verifications and to introduce only three levels: serviceability (verification of rigidity), damageability (strength verification) and ultimate (verification for ductility) limit states.
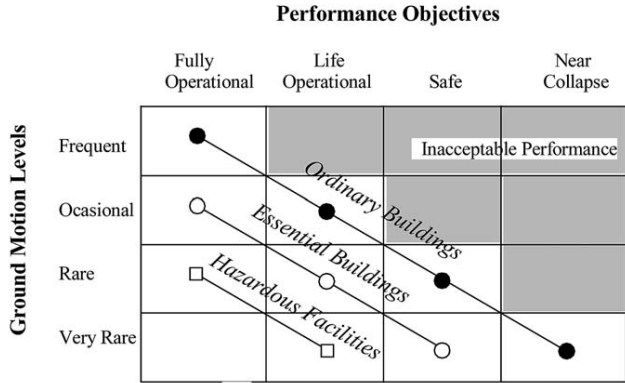
Figure 1. Performance objectives according to Vision 2000 provisions

2.2.2.2 Design methods based on performance

Structures designed against earthquakes have to comply with specific criteria such as stiffness, strength and ductility [9]. However, the majority of modern codes consider explicitly only one performance objective, defined as protection of occupants against injury or loss of life in case of major earthquakes. In the present paper, three limit states, which are referring to conditions of drift, residual drift and rotation capacity of elements, are introduced.

2.2.2.2.1 Serviceability limit state—SLS (stiffness criterion)

In case of frequent earthquakes (return period of 20 years), the building can be used without interruption, the non-structural elements present minor damages and the structure remains in elastic range. The limit state is defined as the situation where the interstorey drift exceeds 0.6% of the relevant storey height.

2.2.2.2.2 Damageability limit state—DLS (strength criterion)

In case of rare earthquakes (returning period of 475 years), the building presents important damages of non-structural elements and moderate damages of structural elements, which may be although repaired after earthquake without high costs or special technical difficulties. Structure is responding to the seismic motion in elastoplastic range and the determinant criterion is the resistance of member sections. This criterion may be considered as a state index of the building after a strong seismic motion. The limit state is defined as the situation where the residual nonrecoverable part of the interstorey drift exceeds 1% of the relevant storey height.

2.2.2.2.3 Damageability limit state—DLS (strength criterion)

18

In case of rare earthquakes (returning period of 475 years), the building presents important damages of non-structural elements and moderate damages of structural elements, which may be although repaired after earthquake without high costs or special technical difficulties. Structure is responding to the seismic motion in elastoplastic range and the determinant criterion is the resistance of member sections. This criterion may be considered as a state index of the building after a strong seismic motion. The limit state is defined as the situation where the residual non-recoverable part of the interstorey drift exceeds 1% of the relevant storey height.

2.2.2.2.4 Ultimate limit state—ULS (ductility criterion)

In case of very rare (the strongest possible ground motion—returning period of 970 years), the building presents major damages (of both non-structural and structural elements) but safety of people is guaranteed. Damages are extended so that structure cannot be repaired and demolition is unavoidable. Structure is in the elasto-plastic range and the determinant criterion is the local ductility (rotation capacity of elements and connections). The development of cracks in the beam-to-column joint regions may be associated to the exhaustion of the low-cycle fatigue strength. This strength may be expressed in terms of plastic rotation. The low-cycle fatigue resistance curve is expressed in terms of the plastic rotation according to [12]:

$$\log N = \log a - m \log \Delta\varphi \tag{1}$$

where $\Delta\varphi$ is the fatigue deformability (plastic rotation), N the number of plastic rotation range cycles, m the slope of the fatigue plastic rotation range curves and $\log a$ a constant.

Reference values for the damage evaluation may be provided from the results of monotonic tests. Monotonic loading corresponds to one-half of a cycle of a specimen deformed to $\Delta\varphi = \varphi_{mon}$ and unloaded to zero plastic deformation. That means that monotonic loading corresponds to a pair $N_{mon} = 1/2$ and $\Delta\varphi = \varphi_{mon}$. Accordingly, if the rotation capacity under monotonic loading φ_{mon} is known, the number of cycles for a certain range of plastic rotation may be determined from:

$$N = \frac{1}{2}\left(\frac{\varphi_{mon}}{\Delta\varphi_p}\right)^m \tag{2}$$

Studies from experimental investigations reveal that the value of the slope m is approximately equal to 2. Accordingly a value m Ľ 2 was adopted for the fatigue curve. For the rotation capacity under monotonic loading u_{mon}, a value equal to 0.04 radians was adopted for the fatigue curve. For variable ranges of plastic rotation, the damage assessment is performed in accordance to the linear Palmgren– Miner cumulative law in accordance with:

$$D = \sum \frac{n_i}{N_i} \tag{3}$$

where n_i is the number of cycles of deformation range $\Delta\varphi_i$ and N_i the number of cycles of the same deformation range that cause failure.
For the determination of the design spectrum in the fatigue assessment, the rainflow or reservoir method for counting the cycles for a certain deformation history has been employed. The limit state is defined as the situation where the damage index becomes equal to 1. In Table 1 the performance levels, together with the description of damage state and maximum

characteristic values (interstorey drifts, residual interstorey drift, plastic rotations) are described.

Table 1. Characteristic value limits associated to the performance levels

Performance level/limit state	Description of damage state	Limit drift (%)	Limit residual drift (%)	Plastic rotations (rad)
SLS	Light damages in structure and non-structural elements Continuity in building occupancy	0.6	-	-
DLS	Damages are moderate but structure is stable Building can be evacuated after earthquake because repairs are necessary Repairs are possible	-	1%	-
ULS	Severe damages but the collapse of structure is prevented Building repair is no longer possible	-	-	0.04[a]

[a] The corresponding drift is 3% approximately.

2.2.2.2.5 *Simplified methods of evaluation for global and local seismic performances of MR frames*

The most suitable approach for seismic design based on performance appears to be deformation-controlled design. However, today codes are based on force controlled design, using the base shear concept. The most important parameter in this approach is the behaviour q-factor [13], which is based on the maximum capacity of structure to dissipate energy during the plastic deformations corresponding to ULS criterion, without possibility to verify other performance levels.

Aribert and Grecea [7,8] have introduced a new definition of the q-factor based on the reduction of the base shear force of a structure (Eq. (4)). Values for the new q-factor have been established for different types of steel structure with rigid and full strength joints or with semirigid and/or partial strength joints.

$$q = \frac{V^{(e,th)}}{V^{(inel)}} = \frac{V^{(e)}}{V^{(inel)}} \frac{\lambda_u}{\lambda_e} \tag{4}$$

It is very important to be underlined that this new definition may be applied to any level of performance mentioned above and settled by Fig. 1, such as as strength, drift and rotation capacity. Today codes give a maximum q-factor of constant value, including both effects of ductility and overstrength. The ULS corresponding ductility cannot be attained, if higher levels of performance are required. In that case, a reduced ductility corresponding to a partial q-factor is attained by structure. This partial q-factor may be computed in any case, at any level of performance wished by design engineer, applying this new method. Thus, the use of

this partial q-factor gives the possibility to implement the multiple performance design in the actual code methodology.

Table 2. Geometric properties of the frames under consideration
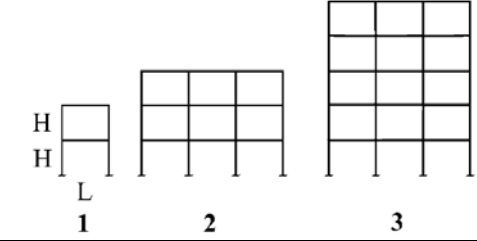
Type of frame						
Frame	L (m)	H (m)	Structure period (sec)		Beams	Columns
			Semirigid	Rigid		
1	5	3	0.73	0.67	IPE300	HEB180
2	4	4	1,27	1,16	IPE330	HEB180
3	4	3	1,39	1,25	IPE360	HEB280

2.2.3 Parametric study

The parametric study refers to frames with different geometric conditions (see Table 2). Two types of behaviour for the beam-to-column joints were examined, rigid and semirigid, with an amount of semirigidity of 0.4K (according to the definitions of Eurocode 3 [11]), where $K=25EI_b/L_b$ expresses the stiffness of the beam. The joints were considered as full resistant. If the column web is slender, it is possible to obtain beam-to-column joints with properties approaching of the parameters considered in this study. The frames were subjected to Kobe (1995) seismic record. The response spectrum of Kobe record is shown in Figure 2.

To be used in design, performance levels must be translated into seismic action, represented by magnitudes or accelerations. In case of using the recurrence period, the level of acceleration depends on it. The selection of ground motion acceleration for the three limit states was determined as a function of the return periods. For DLS and ULS, respectively, there are no contradictions concerning the return periods (475 and 970 years, respectively). Contrary to this, for SLS there are different proposals (ranging from 10 to 75 years), due to the difficulties in choosing a rational criterion for non-damage limit states. If the acceleration for damageability limit state ad is considered as a basic value for ground motion acceleration, for the other periods the corresponding accelerations are determined from the equation [10,15]:

$$\frac{a}{a_d} = \left(\frac{p_r}{p_{rd}}\right)^{0.28}$$

(5)

based on ATC 40 [16] proposal. For the SLS and ULS, the corresponding accelerations are as follows (see Figure 3):

$$a_s = 0.412a_d$$

(6.a)

$$a_u = 1.22a_d$$

(6.b)

The analysis was performed using the general purpose DRAIN-2DX software package [14]. In the first step, the maximal accelerations a, for which the structures meet the specified performance criteria, were determined by appropriate scaling (see Table 3) if the additional rigidity brought by interaction between structural and non-structural elements is considered (structure is in elastic range and non-structural elements are undamaged), this difference could

21

be reduced). In Figure 4, the variation of acceleration multipliers for the limit states considered in the analysis is presented. One of the most important problems that must be fulfilled in case of multi-level design is the optimisation of solutions. It may be observed that in case of DLS and ULS, the input accelerations are very close, which means the both requirements are simultaneously satisfied. If the additional rigidity brought by interaction between structural and non-structural elements is considered (structure is in elastic range and non-structural elements are undamaged), this difference could be reduced.

In the second step, in order to evaluate the global ductility of the frames under consideration, the q-factor was calculated using the new approach described by Eq. (4) (see Table 4). In case of SLS, a value of q-factor of 1.0 was imposed, considering the structure in elastic range. Inelastic base shear forces were evaluated at a level of acceleration specified in the first step (see Table 5).
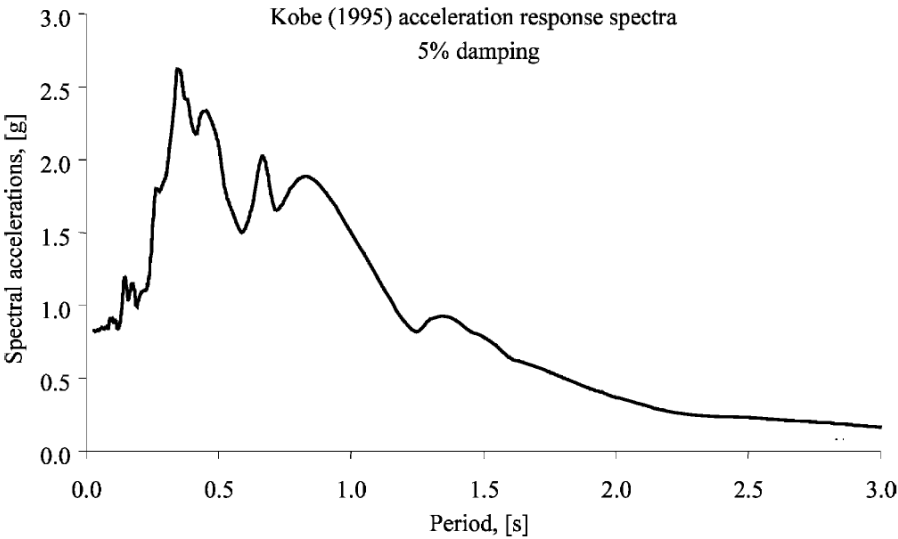
Figure 2. Acceleration response spectra of Kobe (1995) record
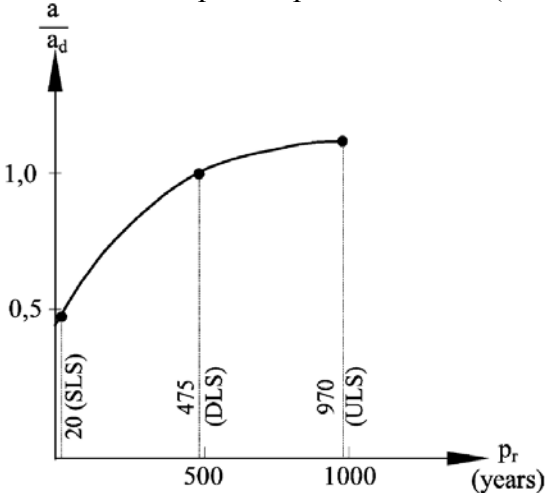
Figure 3. Characteristic of ground motion: acceleration vs. return period [11].

Table 3. Acceleration multipliers for the three limit states

	Frame 1		Frame 2		Frame 3	
	Rigid	Semirigid	Rigid	Semirigid	Rigid	Semirigid
SLS	0,31	0,29	0,36	0,30	0,32	0,29
DLS	0,46	0,44	0,53	0,62	0,74	0,77

| ULS | 0,46 | 0,43 | 0,53 | 0,63 | 0,57 | 0,62 |
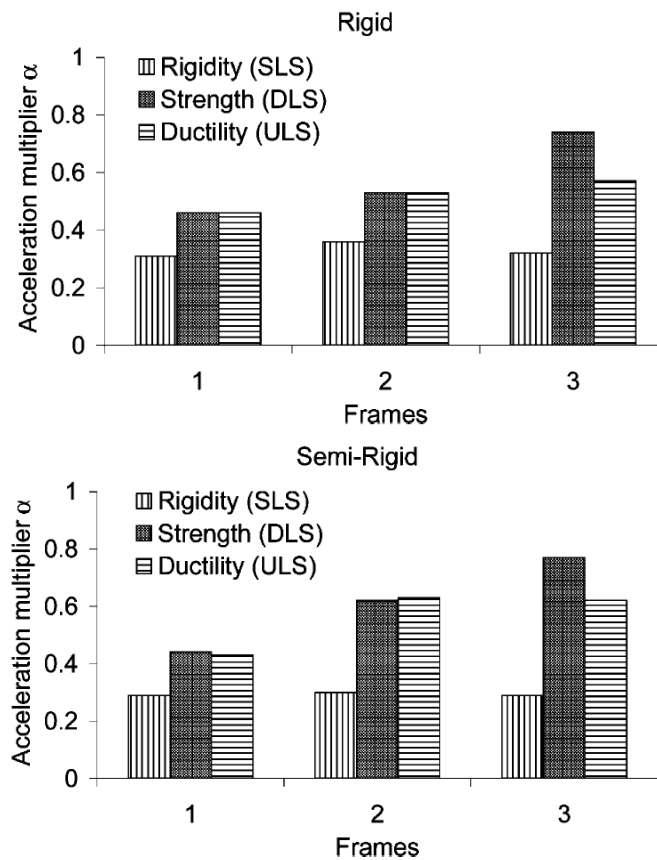


Figure 4. Limit acceleration multipliers au for rigid and semirigid frames.

Table 4. q factors for the three limit states

	Frame 1		Frame 2		Frame 3	
	Rigid	Semirigid	Rigid	Semirigid	Rigid	Semirigid
SLS	1,00	1,00	1,00	1,00	1,00	1,00
DLS	2,30	1,80	2,20	1,60	3,80	3,30
ULS	2,70	2,10	2,60	3,20	3,60	3,20

Table 5. Base shear force for the three limit states, in kN

	Frame 1		Frame 2		Frame 3	
	Rigid	Semirigid	Rigid	Semirigid	Rigid	Semirigid
SLS	81,0	96,8	160,7	176,5	304,4	348,4
DLS	131,2	131,3	271,8	278,2	583,1	613,0
ULS	131,1	131,1	270,7	277,9	583,9	617,9

In Figure 5, the variation of acceleration multipliers for the limit states considered in the analysis is presented. Analysing values of q-factor presented in Table 5, it is observed again that in case of DLS and ULS the base shear forces are quite equal, both for rigid and semirigid frames. However, q-factors are increasing from SLS to ULS, mainly due to different levels of base shear force V(e) associated with SLS.
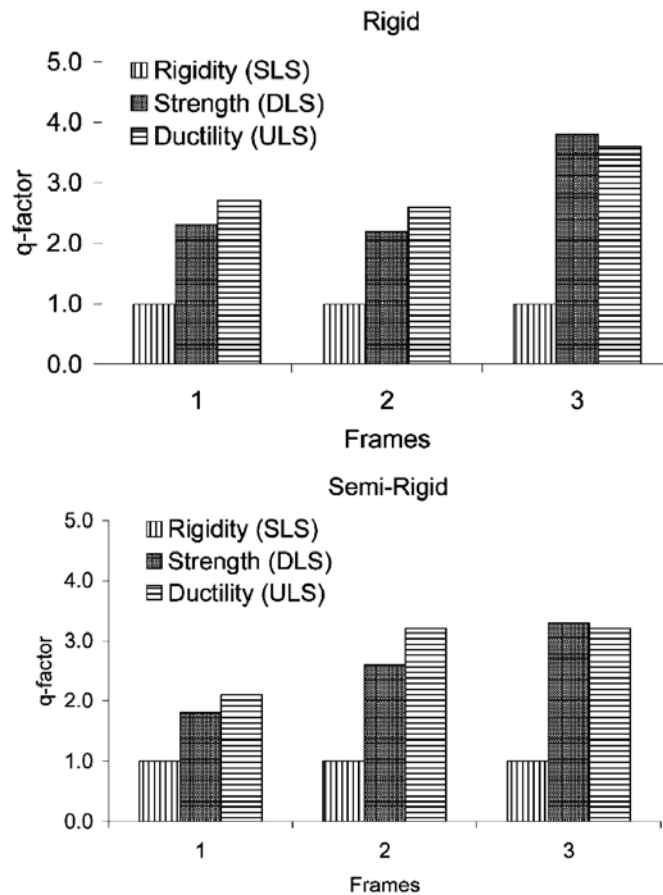
Figure 5. q factors for the three limit states

2.2.4   References

[1] Ghobarah A. Performance-based design in earthquake engineering: state of development. Eng Struct 2001;23:878–84.

[2] Structural Engineers Association of California (SEAOC). Vision 2000 a framework for performance-based engineering. Sacramento (CA): Structural Engineers Association of California; 1995.

[3] Applied Technology Council (ATC). NEHRP guidelines for seismic rehabilitation of buildings. Report No. FEMA-273. Washington (DC): Federal Emergency Management Agency; 1997.

[4] Bertero RD, Bertero VV. Application of a comprehensive approach for the performance-based earthquake resistant design buildings. 12th World Conference on Earthquake Engineering, Auckland, 30 January–4 February. 2000 [CD-ROM 0847].

[5] Bertero RD, Bertero VV. Redundancy in earthquake-resistant design. J Struct Eng 1999;125(1): 81–88.

[6] Mazzolani FM, Montuori R, Piluso V. Performance based design of seismic-resistant MR frames. In: Mazzolani FM, Tremblay R, editors. Proceedings of the Third International Conference STESSA 2000, Behaviour of Steel Structures in Seismic Areas, 21–24 August, Montreal, Canada. Rotterdam: A.A. Balkema; 2000, p. 611–8.

[7] Aribert JM, Grecea D. A new method to evaluate the q-factor from elastic-plastic dynamic analysis and its application to steel frames. In: Mazzolani FM, Akiyama H, editors. Proceedings of the Second International Conference STESSA 1997, Behaviour of Steel

Structures in Seismic Areas, 3– 8 August, Kyoto, Japan. Napoli: Edizioni 10/17, 1997. p. 382–93.

[8] Aribert JM, Grecea D. Numerical investigation of the q-factor for steel frames with semi-rigid and partial-strength joints. In: Mazzolani FM, Tremblay R, editors. Proceedings of the Third International Conference STESSA 2000. Behaviour of steel structures in seismic areas, 21–24 August 2000, Montreal, Canada. Rotterdam: A.A. Balkema; 2000, p. 455–62.

[9] Vayas I, Dinu F. Influence of joint flexibility in the seismic performance of moment resisting steel frames. NATO Advanced Research Workshop ''The Paramount Role of Joints into the Reliable Response of Structures, From the Rigid and Pinned Joints to the Notion of Semi-rigidity'', Ouranoupolis, Greece, 21–23 May. p. 240–248.

[10] Lee LH, Lee HH, Han SW. Method of selecting design earthquake ground motions for tall buildings. Struct Des Tall Build 2000;9:201–13.

[11] Eurocode 3 Part 1.1. Design of steel structures, general rules and rules for buildings. CEN, European Committee for Standardisation. pr. EN 1993-1-1. 1992.

[12] Eurocode 3 Part 1.9. Fatigue strength of steel structures. CEN, European Committee for Standardisation. pr. EN 1993-1-9. 2000.

[13] Eurocode 8 Part 1.1. Design provisions for earthquake resistance of structures. CEN, European Committee for Standardisation. ENV 1998-1-1. 1994.

[14] Kannan, A, Powel, G, DRAIN-2D. A general purpose computer program for dynamic analysis of inelastic plane structures. EERC 73-6 and EERC 73-22 reports. Berkeley, USA. 1975.

[15] Gioncu V, Mazzolani FM. Ductility of seismic-resistant steel structures. London: SPON Press; 2002.

[16] ATC. Seismic evaluation and retrofit of concrete buildings, vol. 1. ATC-40. Redwood City: Applied Technology Council; 1996.

2.3 Collapse control design approach for prevention of collapse in case of extreme loading

2.3.1 Introduction

The development of design guidelines for collapse control of the multi-story buildings started in 1968 with the collapse of the Ronan Point high-rise building in the United Kingdom, due to a gas explosion. The failure of the building was identified as a "progressive collapse", because the extent of damage was disproportionate compared to the initial cause. Three decades later, in 2001, the attack against the twin towers of the World Trade Center caused the complete failure of the two buildings and massive loss in lives and property. The type of collapse was again identified as progressive collapse. More recently, during the winter 2005/2006, several construction halls, shopping centers or hotels have been damaged or destroyed throughout Europe due to very heavy snowfalls. For example, the roof of the Exhibition Hall in Katowice, Poland, collapsed due to heavy snowfall and caused 65 dead and more than 170 injured. The investigation found design and construction flaws, that caused a lack of robustness which, associated with large drifted snow, finally caused the collapse. Even this time was not a progressive collapse, the lack of alternate load paths when the most stressed elements failed could have been identified and proper measures adopted by considering the collapse control design. These tragic events alerted construction engineers and public authorities and warned about the importance of preventing progressive collapse in case of extreme load events.

Figure 6. Ronan Point Collapse, 1968, London, UK: a) view after the collapse; b) failure of a primary structural element due to gas explosion; c) chain reaction of failure

The concept of collapse control design can be considered the most appropriate approach for preventing the progressive collapse in case of extreme load events. In principle, the collapse control design method assesses and improves the redundancy of buildings by assuming the loss of structural members such as columns and beams due to extreme accidental loads and assessing how many members might be lost until the entire collapse of the building.
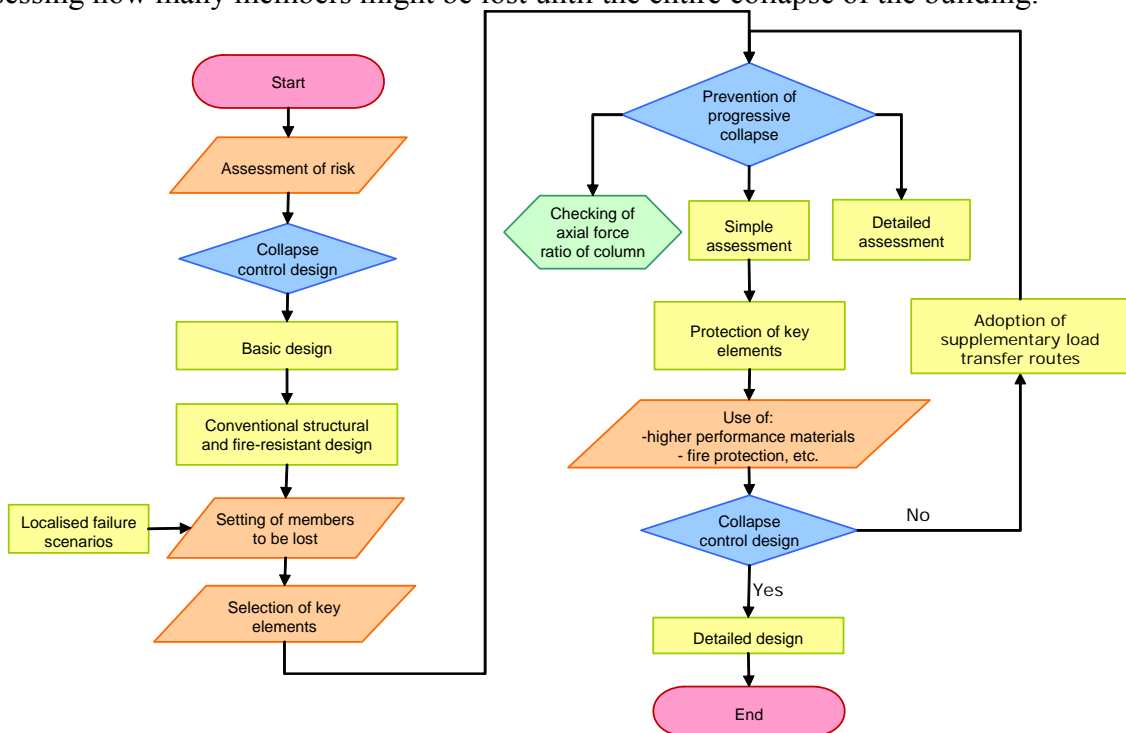
Figure 7. Collapse control design flowchart

In line with this definition, there are several measures for increasing progressive collapse resistance:
- Supplementary load transfer routes: beneficial effects like Vierendeel, Catenary, Arch or Suspension effects. For example braces installed at intermediate levels or on top of the structure, associated with vertical bracings for increasing the wind and seismic resistance are also effective in redistributing gravity loads in case some critical members are lost. This feature is especially important in case of frames with simple connections on one or two directions.
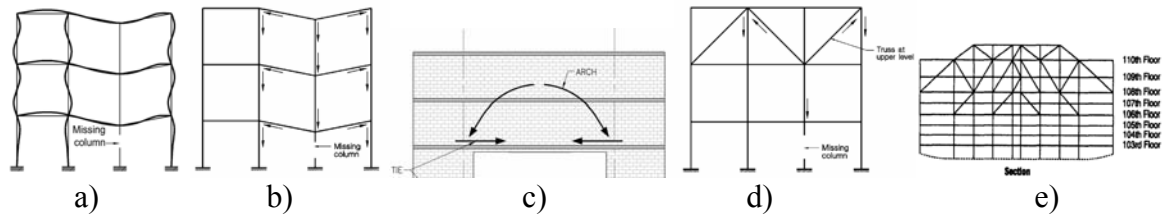
Figure 8. Examples of supplementary load transfer routes: a) Vierendeel action; b) Catenary action; c) Arch effect; d) Suspension effect; e) Hat trusses on top of WTC (suspension effect)

- Increase of load redistribution capacity: e.g. the continuity of beams at the intersection with columns allows the redistribution of loads after the column is lost.
- Increase of connection strength: e.g. frames with full strength connections joints as in case of seismic design can bridge over the missing column and can secure the resistance against progressive collapse.
- Increase of connection ductility: when some critical members are lost, e.g. columns, the vertical displacements in the affected area are large, and this requires large deformation capacity of members and their connections. For beam-to-column connections, the demand can be several order of magnitude larger than in case of earthquake.
- Proper design of fire resistance of members: this can be done by adoption of fire protection materials (e.g. concrete-filled steel tubes CFT or partially/fully encased columns) or of fire resistant materials (eg. fire resistant steel, with similar material characteristics at room temperature and elevated temperatures).

One example is the Taipei 101, a 508 m tall building, many years ranked as the world tallest building. The engineers used a combination of strong floors, outrigger and belt truss systems to prevent the probability of collapse in case of extreme load events. There are numerous hazards that could trigger the progressive collapse, each with different probability of occurrence: intentional or accidental explosion (eg. bomb detonation, gas explosion), aircraft, vehicular or debris impact, fire, natural hazard (earthquakes, extreme snow, extreme wind, extreme rain - flood), design/construction error. The different nature of the actions makes difficult to give a general model to interpret their effects on the structural behavior. Excepting the snow, which is a static load and the fire, which modifies the mechanical properties of the material, all other actions specified before are dynamic.
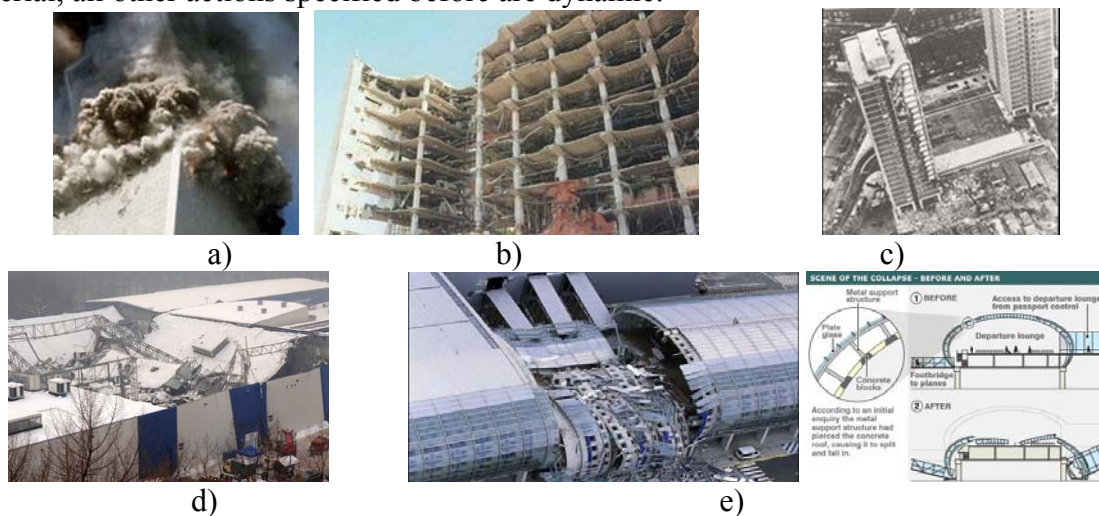

Figure 9. Progressive collapse: a) aircraft impact at WTC, 2001; b) Oklahoma City bombing, 1995; c) gas explosion at Ronan Point building, 1968; d) snow accumulation at Katowice/Poland, 2006; e) wrong steel-concrete connection details at Charles-de-Gaulle Airport new terminal, 2004

The dynamic features of the loads are different and, therefore, the consequences can be very different. Floods and landslides are characterized by the flow of a moving mass. Impacts, blasts and explosions are dynamic, and release a big amount of energy in a very short time. Figure 10 shows a typical time history of the pressure resulting from a gas explosion.
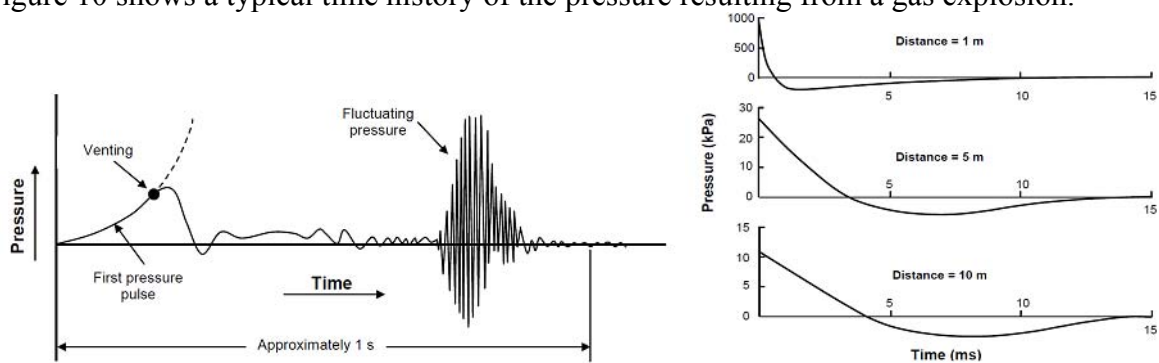

Figure 10. Typical time history of the pressure resulting from a gas explosion (left) and from detonation of explosives (right)

Venting limits the pressure intensity of the first pulse, while the high-frequency fluctuations in pressure in the second phase are of little significance to structural response. The bomb detonation creates a shock wave pressure that can be approximated by a triangular impulse load. The features of the loads are important when the design is of concern. Thus, in case of a gas explosion, the venting is important and can drastically limit the overpressure. On the other hand, the pressure released by a bomb blast decays very rapidly with the distance from the source of blast, and therefore the most efficient way to reduce the risk is creating a large safe perimeter or a large "standoff" distance. Considering the features of different loads, one can say the design of a building structure for a specific load can be ineffective for other loads. However, the seismic design or the adoption of the seismic design principles can prepare the structure for many other hazards. For example, the FEMA 277 report (1996) concluded that if the Murah Building (see Oklahoma City bombing, 1995,) would have been designed to seismic action, the progressive collapse would have been precluded. Past experience have demonstrated the resistance to progressive collapse is a multi-hazard issue (see WTC 2001 collapse, combination of impact, explosion and fire). Therefore, the mitigation of collapse is rather difficult to implement because the interaction between a particular hazard and a construction component can lead to conflicts. Some structural aspects are beneficial for the behavior under several hazards, some are undesirable or increase the vulnerability to a given hazard, and some pose little or no significant interaction. In the following, a multi-hazard design matrix is presented (FEMA 577) but adapted and restricted to site and building characteristics. A new type of hazard, i.e. explosion (including bomb and gas explosion) was also added. One can say there are some structural characteristics that can efficiently improve the expected performance of the building and mitigate the risks of collapse associated with several hazards: type of structural system, avoidance of indirect supports (column on beam), ductile connections.

Table 6. Multi-hazard design matrix

Site and building characteristics			Hazard					Interaction
			Seismic	Flood	Wind	Fire	Explosion	
1	Elevated building site		-	+	0	0	+	Highly beneficial for floods and external bomb explosion, not significant for wind or fire
2	Re-entrant corner plan forms		-	0	-	0	-	Stress concentration at corners, irregular behavior in case of earthquakes; localized wind pressures, amplification of shock wave in case of external blast
3	Very irregular buildings		-	0	-	-	-	Indirect load paths, stress concentrations in earthquakes, explosions. Localized high wind pressure, aggravates evacuation in case of fire
4	Large roof overhangs		-	0	-	-	-	Vulnerable to earthquakes (vertical motion), wind and also adjacent external blast. Mai pose risk also in case of fire evacuation
5	Steel structural frame		+	+	+	-	+	When properly detailed, is recommended in seismic and high-wind zones. Good in flood with proper detailing. Vulnerable to fire if is not protected or well detailed and designed. Low vulnerability in case of blast and explosion, offers multiple paths.
6	Indirect load path		-	0	-	-	-	Very vulnerable for seismic, wind and explosion hazards because poor structural integrity increases likelihood of collapse. Fire may further weaken structure.
7	Ductile detailing of structure and connections		+	0	+	+	+	Provides good plastic response. The structure has large ductility and is more resistant to collapse in case of extreme loading
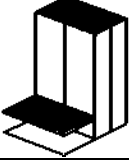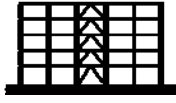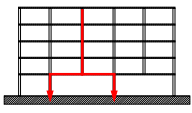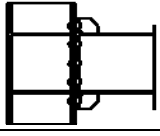
Note: The following convention has been used in the table:
+ indicates a desirable condition or beneficial interaction between the designated component/system and hazard
0 indicates little or no significant interaction between the designated component/system and hazard
- indicates an undesirable condition or the increased vulnerability of a designated component/system to a hazard

1.2.3 Design for prevention of progressive collapse

Within the Collapse Control Design Approach (Figure 7), there are two options to assess the risk of collapse. First is the protection of key elements (key element method) and the second is the adoption of supplementary load transfer routes (alternate load path method). The two methods may be used independently or complementary in design. For reduction the probability of collapse, it is advantageous to adopt the second alternative. Thus, the probability of collapse, P(C) due to the extreme load event, H, can be defined using the following equation:

$$P(C) = P(C|LD)\ P(LD|H)\ \lambda_H \qquad (1)$$

where

λ_H = rate of occurrence of the extreme load or hazard,

$P(LD|H)$ = probability of local damage given that the extreme load occurs, and

$P(C|LD)$ = probability of collapse given that local damage occurs.

One can say the basic strategies for reducing the likelihood of (progressive) collapse are based on the minimization of the terms in eq. (1). First measure refers to reducing the hazard or minimizing its intensity - λ_H. For blast event, for example, this can be done by creating a larger standoff distance. Active fire protections can put out or slow the progress of a fire. In other cases, like earthquakes, engineers can do nothing to prevent or limit the seismic hazard. If the other two terms are referred, one can say the Key Element method can be employed for reducing P(LD|H) while Alternate Load Path method for reducing P(C|LD).

Indirect Design: is a prescriptive approach and requires a minimum level of connectivity for structural members (Figure 11). This can be achieved by employing specific structural systems, the arrangement of the members, the ratio between their capacities and the capacity of connections in terms of strength and ductility. Seismic details for continuity and tying, that apply primarily lateral load resisting system, can be used as reference but extended also to gravity load resisting system.
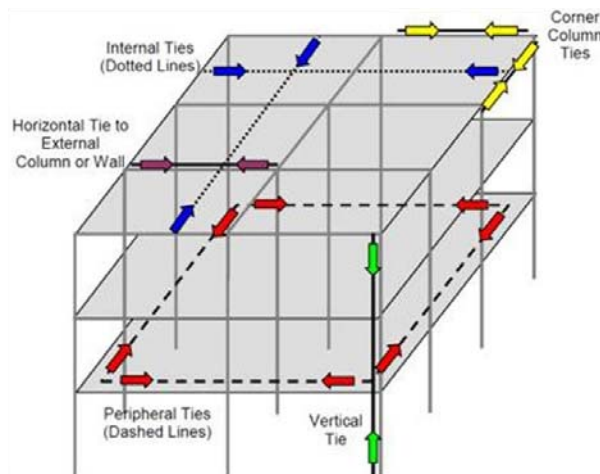

Figure 11. Different types of ties incorporated to provide structural integrity (DOD, 2005)

Direct Design explicitly considers the resistance of the structure and includes two methods:

- *Specific local resistance method*: first, critical members are identified and then their capacity to resist a specific load (such as the direct effect of an impact or explosion) is verified. This method is "threat specific method", as it does require the characterization of the hazard. This method is also referred to as *key element design*. Key elements are defined as structural elements whose notional removal would cause collapse of an unacceptable extent. They should therefore be designed for accidental loads, which are specified in several standards as 34 kPa. Such accidental design loading should be assumed to act simultaneously with 1/3 of all normal characteristic loading:

$$D + L/3 + Wn/3 \qquad (2)$$

where: D = dead load, L = live or imposed load, and W_n = wind load.

Wind load simulates the effect of overall stability and can be replaced by global imperfection. The specific local resistance design is often the only rational approach when retrofitting an

existing building. For blast and explosions but also for impact, which are dynamic load events by their nature, although the Finite Element Method (FEM) can be used in modeling the structural response (Dinu et al., 2010), a more accurate prediction of the structural performance under extreme loading may be necessary. The Applied Element Method (AEM) is a new method that can investigate the structural collapse behavior passing through all stages of the application of loads: elastic stage, crack initiation and propagation in tension-weak materials, strain hardening effect in post-elastic range, element physical discontinuity, element collision (dynamic contact), and collision with the ground and with adjacent structures. The method is very accurate compared to other simulation technologies.

- *Alternate path method*: first is assumed the loss of a structural member due to an extreme load event and then the capacity of the structure to bridge over the missing member is investigated. This is a "threat independent method", as it does not require the characterization of the hazard. This method reduces the risk of progressive collapse by ensuring structural redundancy. Another advantage of this approach is that it promotes structural systems with ductility, continuity, and energy absorbing properties that are desirable in preventing progressive collapse. Different analysis procedures can be used: Linear static (LS); Nonlinear static (NS); Linear dynamic (LD); Nonlinear dynamic (ND). There are different accidental loads, lateral loads and combinations of loads for which the building stability should be checked.

Table 7. Loads and combination of loads for alternate load path method

Standards	Load combinations after notional member removal	Accidental load
BS	$(1\pm0.5) D + L /3 + W_n /3$	34 kPa
Eurocode 2003		20 kPa
DOD UFC 4-010-01	$D + 0.5 L$ net floor uplift	
DOD UFC 4-023-03	$D +0.5 L$ net floor uplift $(0.9 \text{ or } 1.2) D + (0.5 L \text{ or } 0.2 S) + 0.2 W_n$ (nonlinear dynamic analysis) $2.0 [(0.9 \text{ or } 1.2) D + (0.5 L \text{ or } 0.2 S)] + 0.2 W$ (static analysis)	
NYC 1998, 2003	$2 D + 0.25 L + 0.2 W_n$	
GSA	$2 (D + 0.25 L)$ static analysis $D + 0.25 L$ dynamic analysis	

D, L, W_n, S = dead, live, wind and snow loads;
Q_{ak} = characteristic value of accidental action;
G_k, Q_k = characteristic dead, imposed loads per unit area of the floor or roof; Ψ is a load reduction factor which, when multiplied with Q_k, gives the frequent value of a variable action.

Because the transition from the original structural configuration to the damaged state is assumed to be instantaneous, the structure is exposed to a dynamic effect. For static analysis (LS and NS), the dynamic effect is employed by the amplification of the loads on the bays above the failed elements by means of a Dynamic Increase Factor (DIF). Previous results from the literature suggested that a DIF of two would be appropriate. However, recent results (DOD UFC, 2010; Dinu et all, 2010; Stevens et all, 2011) showed two main issues are of concern. First, the same level of DIF is used for LS and NS. However, for extreme events such as progressive collapse, it is more economical to design structures to respond in the nonlinear range. Second, DIF does not vary with level of performance and allowable ductility (plastic deformation). The results obtained so far suggests values of DIF limited to 1.5 rather than 2.0 for NS analysis. It is important to notice that much information about the mechanism of failure and stages of structural behavior during progressive collapse can be gathered from real building controlled demolitions. In the project, there will be a specific task that will deal with the evaluation of dynamic increase factors for LS and NS analysis that can be used in design, depending on the type of structural system, available ductility and level of performance.

2.3.2 Improving the structural robustness of multi-story steel-frame buildings

We investigated the behavior of multi-story steel-frame buildings by considering different local damage scenarios. The study is part of a research program devoted to the design of structures to sustain extreme load events without collapse ("Structural conception and COllapse control performance based DEsign of multistory structures under aCcidental actions", 2012-2016). Two issues are considered responsible for improving the redistribution capacity, first is the continuity between members (degree of connectivity between beams and columns) and second is the interaction with the floor system (Dubina and Dinu, 2012). For this purpose, a set of moment frames of different beam-to-column connections were designed using seismic design criteria for dissipative structures to provide for resistance to seismic actions. The interaction between concrete slabs and steel beams were modeled in detail. The behavior of beam-to-column connections, which is critical to the overall behavior of different types of connections, was also considered in the study.

Both nonlinear static and dynamic analysis were employed, and the dynamic increase factor (DIF) was computed as the ratio of the ultimate load obtained by static analysis to that obtained by dynamic analysis. The robustness criteria were obtained using as reference the ratio of the failure load to the nominal gravity load (Khandelwala & El-Tawil, 2011). It should be noted that, in our study, the robustness is viewed only in regard to column loss events, where the gravity load is the main factor contributing to the progression of collapse.

2.3.3 Case study buildings

The case study buildings were three-bay, four-span, and six-story steel structures with moment frames in both directions (Figure 12.a). The bays and spans each measured 8.0 m and the stories were each 4.0 m high. Structures were calculated for the effect of gravity loads (permanent and variable actions) and lateral loads (wind and seismic actions), using the Eurocodes. The dead and live loads were each 4.0 kN/m^2 and the reference wind pressure was 0.5 kN/m^2. The structures were located in a low-seismicity area, characterized by a design ground acceleration a_g of 0.08 g, and a control period T_C of 0.7 s. It should be noted that, the seismic intensity and the response spectrum used in design were those given in the Romanian Seismic Code, P100-1 (2006). High dissipative structural behavior was considered using a behavior factor q of 6.5. An inter-story drift limitation of 0.008 of the story height was used for the seismic design for the serviceability limit state. Persistent and seismic design situations were used for the structural design of members, connections and details, using the relevant Eurocode parts. No particular accidental design situation was considered in design.

The first structure, identified as *(S)* in Figure 12.b, had no interaction between the main or secondary steel beams and the concrete slab. Therefore, beams were calculated as pure steel elements. The second structure, identified as *(C)* in Figure 12.c-d, was designed with the secondary beams acting as composite sections using headed stud shear connectors along the entire length. The main beams had also shear connectors but only within the middle zone, and were missing within the beam ends (Figure 12.d). As the bending moment under gravity loads reaches maximum value at beam ends and it is a hogging moment, the main steel beam can be considered to work as pure steel section and not as composite. Therefore, the dimensions of the main steel beams were set taking only the steel section into consideration and disregarding the interaction with the concrete slab. This solution with shear studs in place within the beam length but missing within the end zones is typically used for dissipative beams of moment frames. The main reason is that, when plastic hinges develop in the beams in case of an earthquake (EN1998-1, 2004), structures are not meant to take advantage of composite behavior in dissipative zones; the application of the dissipative concept is conditioned by a strict compliance to measures that prevent involvement of the

32

concrete in the resistance of dissipative zones. Experimental tests performed by Ciutina et al. (2013), showed that this requirement (i.e. separation of the two elements - concrete slab and steel beam) is not very easy to accomplish, and the simple lack of connectors might not solve completely the problem.

The columns had cruciform sections made from two HEB 450 hot-rolled profiles. The main beams were made from IPE 400 hot-rolled profiles. The secondary beams of the noncomposite-floor structure *(S)* were made from IPE 330 and those of the composite-floor structure *(C)* from IPE 270. For both *(S)* and *(C)* structures, a reinforced concrete C20/25 floor slab of thickness 12 cm and span 2.67 m was employed between the floor beams. The slab reinforcement included a welded wire mesh measuring $\phi6/166$ mm $\times$ $\phi6/166$ mm. Headed studs of steel S235J2+C450 and diameter 16 mm were welded to the top flange of the secondary beams at 200 mm intervals on one row. The reason for selecting C20/25 is that it refers also to older practice, where the concrete class was lower than it is now, and, secondly, it might be interesting to find out that even with this concrete class, the benefit is considerable in what concerns the residual capacity of the structure after a column loss event.
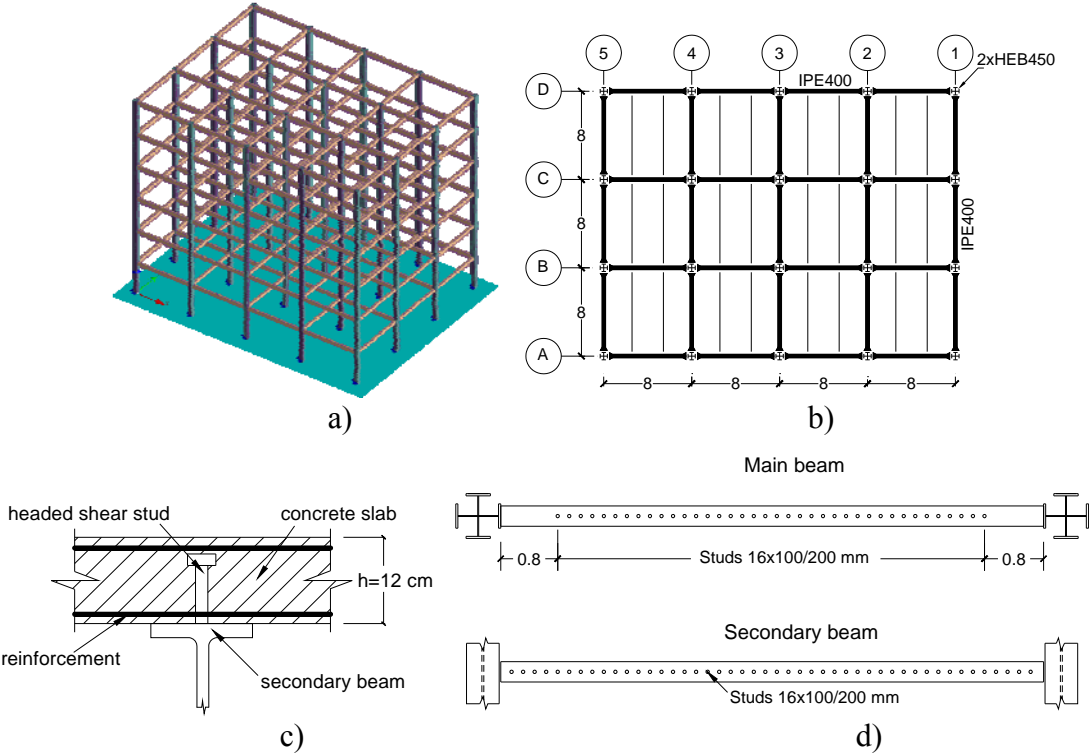
Figure 12. Details of the structure: a) Isometric view of the structural model; b) Plan layout; c) Cross section of the composite secondary beam; d) Distribution of connectors for main beam and secondary beam

To evaluate the contribution of the beam-to-column connections to the resistance to progressive collapse, the main beams were connected to the columns using two different extended end-plate bolted connections of differing end plate thickness and bolt diameters, respectively (Figure 13.a). Type 1 connection had a beam strength ratio of 1.0 and Mode 2 failure, whereas Type 2 had a beam strength ratio of 0.8 and Mode 1 failure. According to EN1993-1-8 (2005), the first connection is classified as full strength and full rigid whereas the second one is classified as partial strength and semi-rigid (Figure 13. b). It should be noted that, according to the same code, there are three possible failure modes for bolted end-plate connections. Mode 1 is characterized by complete yielding of the flange, Mode 2 is

characterized by bolt failure with yielding of the flange, and Mode 3 is characterized by connection failure due to bolt failure. The secondary beams were connected to the main beams by bolted shear-plate connections. The properties of the concrete, reinforcement, and steel materials adopted for the analysis are given in Table 8.
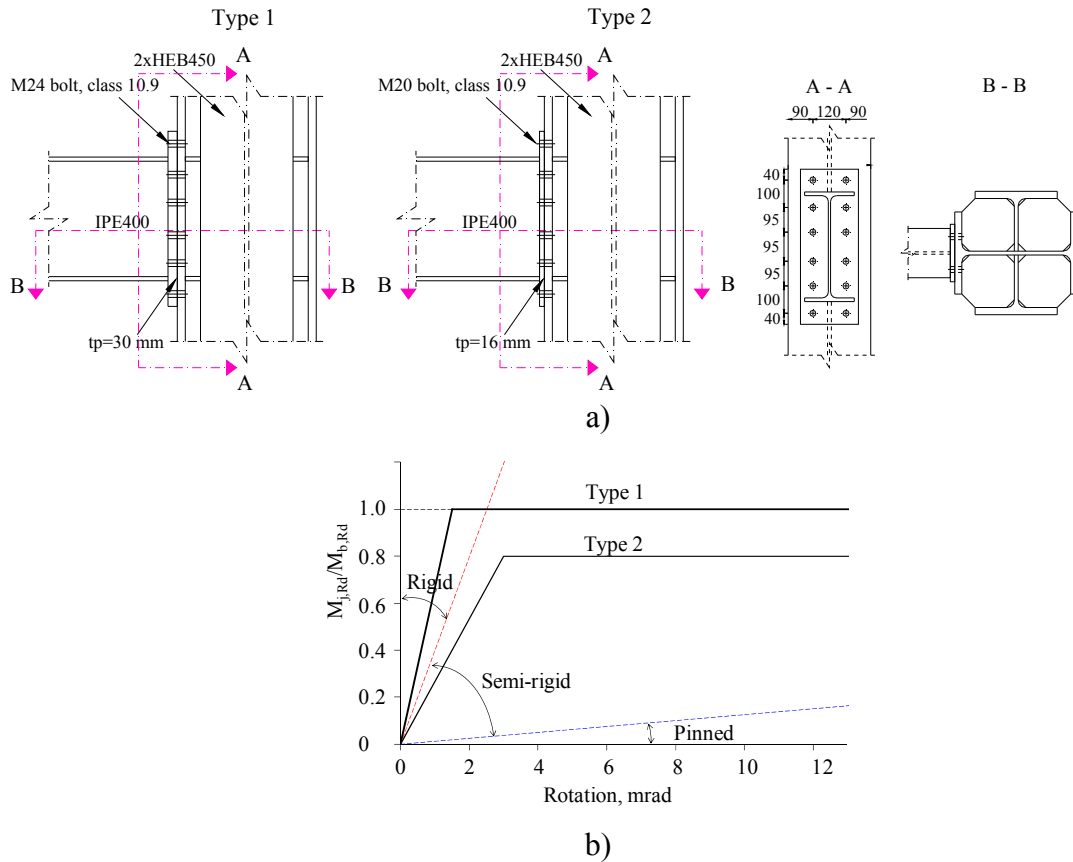

Figure 13. a) Details of the beam-to-column joint; b) Joint moment rotation characteristic.

Table 8. Material properties of the structural components

Material	Type	Material strength (MPa)		Young's Modulus (MPa)
Concrete	C20/25	Axial tensile strength	$F_{ctm}=2.2$	30 000
		Compressive strength	$F_{ck}=20$	
Reinforcement	S420	Yield strength	$f_{yk} = 420$	210 000
Headed stud	S235J2+C450	Yield strength Tensile strength	$f_y = 355$ $f_u = 500$	210 000
Steel framing	S355	Yield strength	$f_y = 355$	210 000

2.3.4 Progressive collapse assessment

The assessment of progressive collapse using the AP method is in accordance with the UFC 4-023-03 guidelines (DoD, 2009). For nonlinear static analysis, the gravity load on the bays immediately adjacent to the lost element and on all floors above it is given by

$$G_N = DIF \times [D + 0.5L] \tag{3}$$

34

where G_N is the increased gravity load for nonlinear static analysis, D is the dead load, L is the live load, and DIF is the dynamic increase factor for accounting for the dynamic effects of the column loss.

The combined load on the areas of the floor away from the lost column is given by

$$G = [D + 0.5L] \tag{4}$$

where G is the gravity load.

The lateral loads must be taken into consideration using

$$L_{LAT} = 0.002 \times [\text{sum of the gravity loads } (D + L)] \tag{5}$$

where L_{LAT} is the lateral load.

For nonlinear dynamic analysis, the gravity load on the entire structure can also be calculated using eq. (4), whereas the lateral loads are taken into consideration using eq. (5).

Although the finite element method (FEM) is accurate and reliable for analyzing continuum structures, the onset of element separation is difficult to automate and the modeling of debris collision is time consuming. A more accurate prediction of the structural performance under extreme loading may be obtained by the applied element method (AEM) (Tagel-Din & Meguro, 2000). The AEM can be used to investigate structural collapse behavior through all the stages of the application of the loads, namely, the elastic stage, crack initiation, during propagation in tension-weak materials, during the strain hardening effect in the post-elastic range, the element physical discontinuity stage, the element collision (dynamic contact) stage, and at collision with the ground and adjacent structures. The progressive collapse analysis of the structure can be used to determine how many columns may be lost before the collapse of the structure. It may also be of interest to evaluate the reserve capacity for supporting the gravity loads for a specific column loss scenario, which may be expressed as the ratio of the failure load to the nominal gravity load. This can be calculated using the combinations described earlier. For this type of analysis, the overload factor Ω may be defined as the ratio of the failure load to the nominal gravity load:

$$\Omega = \frac{\text{Failure load}}{\text{Nominal gravity load}} \tag{6}$$

2.3.5 *Applied element modeling of the structure*

The progressive collapse of multi-story steel-frame buildings was investigated using the advanced nonlinear structural analysis software ELS (2010). An overview of the model is shown in Figure 14.a. The detailed view, including the steel elements, connections, concrete slab, steel reinforcement, and studs, is shown in Figure 14.b. In ELS, the structure is modeled as an assembly of mesh elements, which are assumed to be connected by one normal and two shear springs located at contact points and distributed around the edges of the elements. The fully nonlinear path-dependent constitutive models shown in Figure 15 are adopted. The compressed concrete is modeled by the elastoplastic fracture model shown in Figure 15a. A linear stress-strain relationship is adopted for tensioned concrete until cracking of the concrete springs, at which point the stresses drop to zero. The residual stresses are then redistributed in the next loading step by applying the redistributed force values in the reverse direction. The relationship between the shear stress and shear strain for concrete springs is assumed to remain linear until cracking of the concrete, after which the shear stresses drop as shown in Figure 15b. The magnitude of the shear stress drop depends on the aggregate interlock and

friction on the crack surface. The model of the reinforcement, shear studs, and steel-element springs is shown in Figure 15c. Simulation of the complex behavior of the beam-to-column connections and the interaction between the concrete slabs and the steel beams under large deformation is difficult and requires experimental validation of the parameters of the constitutive models in Figure 15 This validation is discussed in the next section.


a)   b)
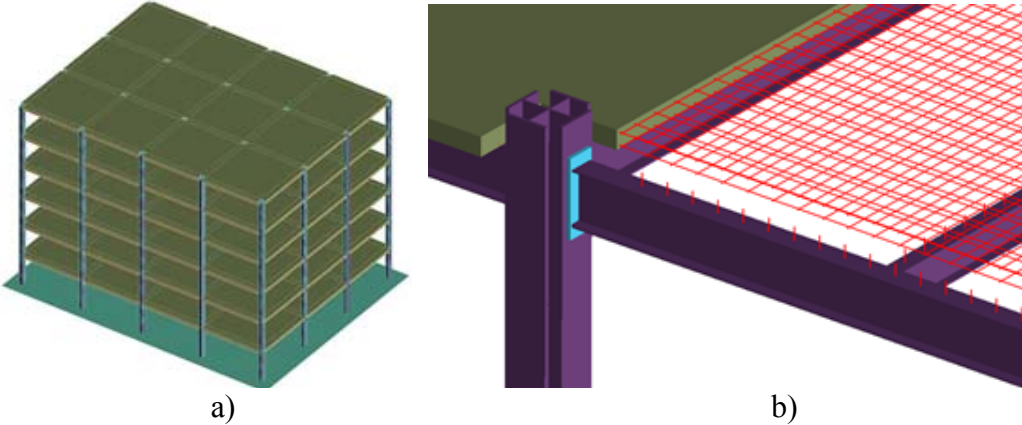
Figure 14. Applied element model of the structure: a) Overview of the model; b) Detailed views of the beams, columns, connections, concrete slab, steel reinforcement, and studs

a)   b)   c)
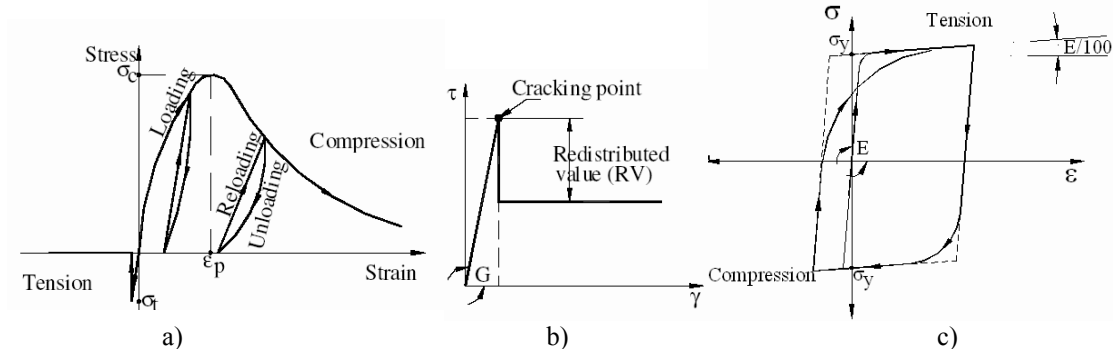
Figure 15. Constitutive models of the materials: a) Concrete under axial stresses; b) Concrete under shear stresses; c) Reinforcement and steel elements under axial stresses (ELS, 2010)

2.3.6   *Validation of numerical model*

To validate the numerical model, the experimental tests carried out within the framework of the "Robust structures by joint ductility" research program were used for reference (Kuhlmann et al., 2009). The test setup and the specimen are illustrated in Figure 16, and Figure 17 shows the detailed numerical model utilized by the ELS software.

The results of the numerical analysis showed that the model could be used to capture the behavior of the specimen and the failure mode. Figure 18.a shows the specimen after the test and Figure 18.b shows the numerical results. The overall relationship between the vertical force and the vertical displacement below the central column is shown in Figure 19. As may be seen, Figure 19 shows very good agreement between the experimental test data and those of the numerical simulation. All the phenomena that occurred during the test can be traced on the force-displacement curve (elastic behavior, plasticity due to crushing of concrete, initiation of catenary force, etc.), and it can be observed that they occurred at similar forces and almost identical displacements on the experimental and numerical curve.

36
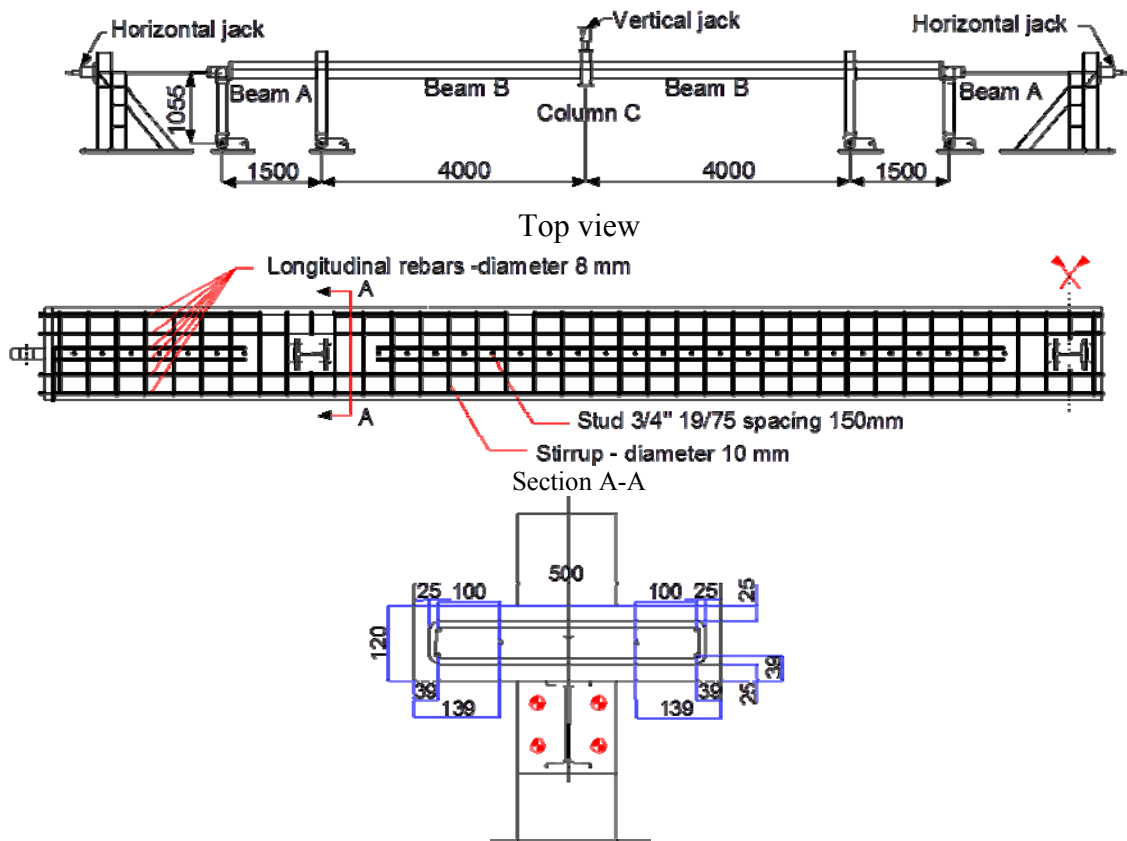
Figure 16. Detailed drawings of the test setup and the specimen.
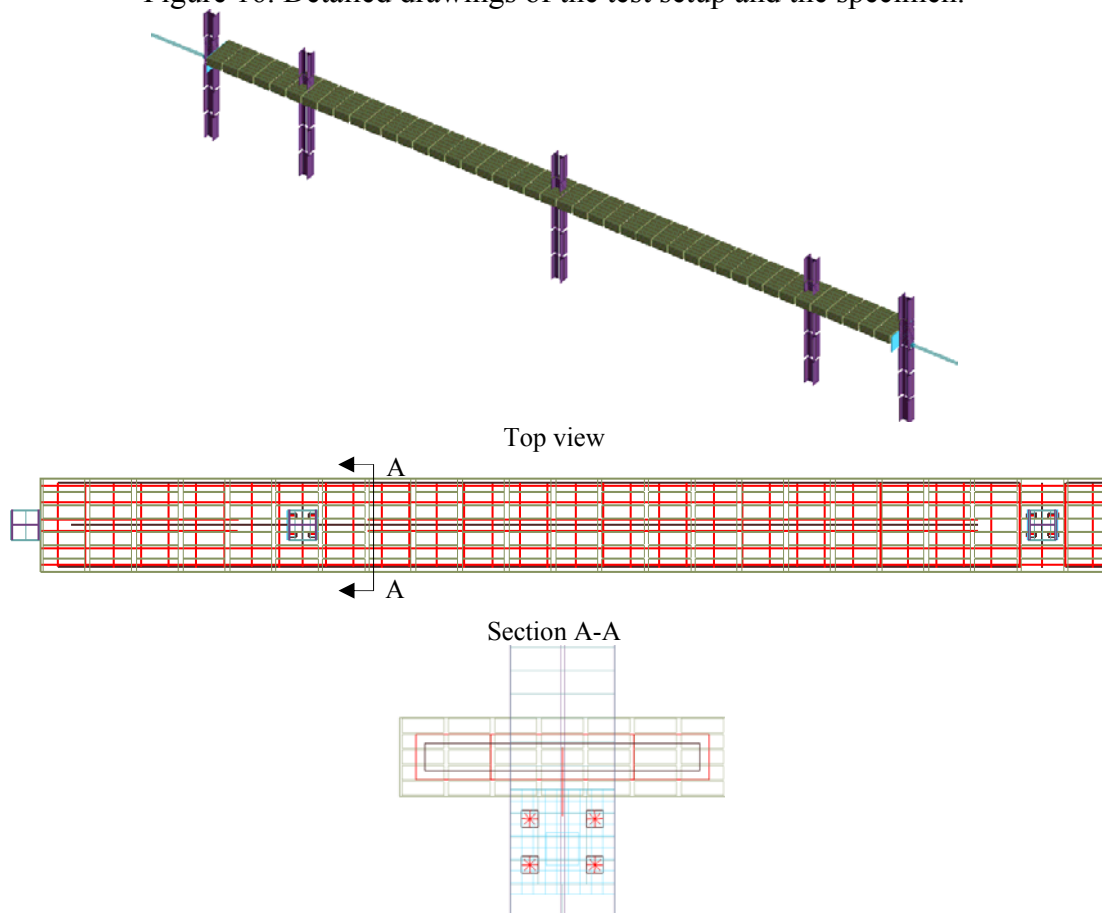

Figure 17. Numerical model
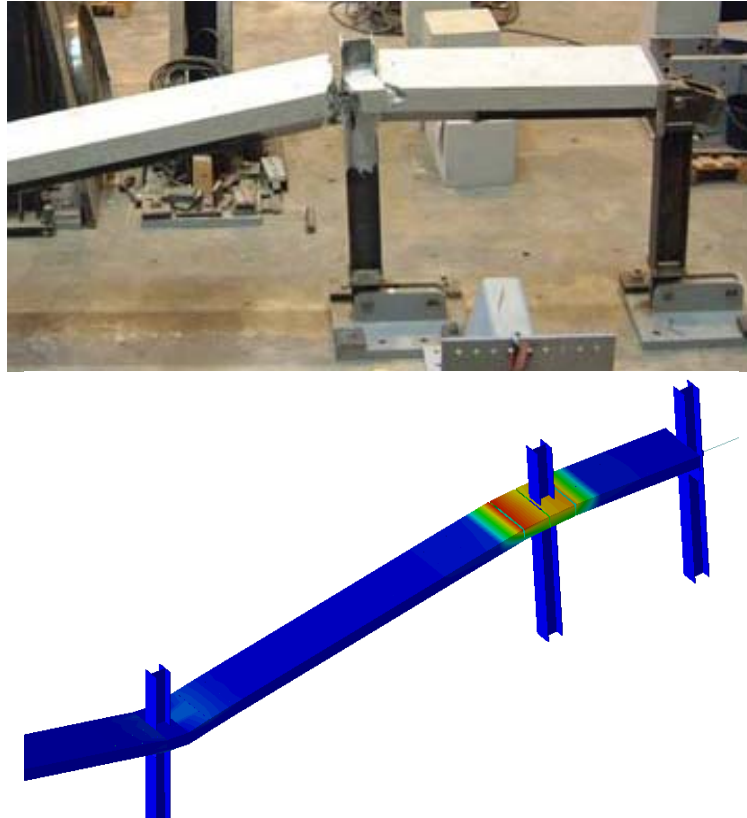
Figure 18. Specimen after the test (top), and numerical results (bottom)
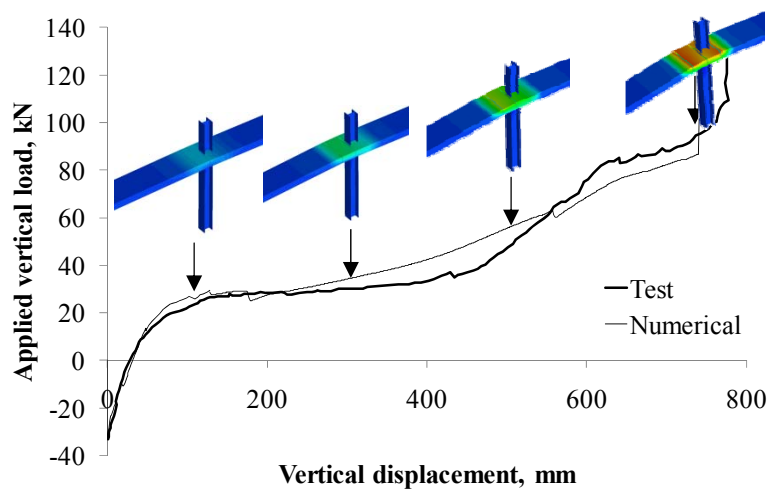
Figure 19. Vertical force–vertical displacement curve (test and numerical)

2.3.7 Analytical results

The progressive collapse analysis was carried out for five different column loss scenarios, namely, a) loss of the corner column (A1), b) loss of one edge column (A3), c) loss of one internal column (B2), d) simultaneous loss of the corner and penultimate column (A12), and e) simultaneous loss of two consecutive edge columns (A23) (see Figure 20). Table 9 summarizes the scenarios. For the first series of numerical simulations, the progressive collapse resistance was assessed using a nonlinear dynamic procedure and the load combinations specified by eqs. (4) and (5). Figure 21 shows the vertical displacements at locations above the lost columns for the pure steel structure *(S)*, composite-floor structure *(C)*,

and rigid and semi-rigid beam-to-column connections. The results show that the structures were able to survive the loss of one or two columns, with the composite beam structures and rigid connections having larger overload factors. It can be observed that the maximum vertical displacement of all the structures was greatest for scenario A12, followed by scenario A23, and then scenario B2 (Figure 22). Figure 23 is a snapshot of the deformed shape after 1.0 s for scenario A23 of Type II structure.

To observe the contribution of the connection capacity and steel-concrete interaction to the resistance to progressive collapse, the maximum vertical displacements are compared in Figure 24. For each scenario, the vertical displacement was normalized by the maximum value obtained for S-II structures (pure steel and semi-rigid beam-to-column connections). For the pure steel structure, the rigid connections reduced the vertical displacement by an average of 20% and were most effective for scenario B2 (S-II). There was no similar benefit of stronger connections for the composite structures, for which the maximum displacements were similar to those of the C-I and C-II structures (rigid and semi-rigid connections, respectively). However, greater benefit can be obtained by designing the secondary beams as composite. In that case, the steel-concrete interaction would reduce the vertical displacement by an average of 72% and would be most effective for scenario B2. The reduction of the vertical displacement reduces the plastic deformation demands on the members and connections. Table 10 and Table 11 present the maximum strain of the members and connections of the steel and composite structures with semi-rigid connections (S-II and C-II, respectively).
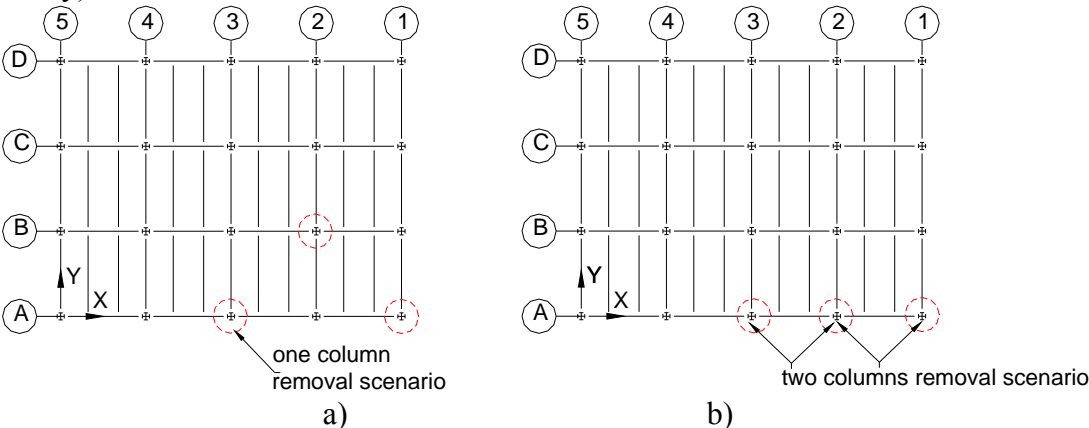

Figure 20. Column loss scenarios: a) One column; b) Two columns.

Table 9. Analyzed progressive collapse scenarios

| Scenario	Type of structure	Type of beam-to-column connection	Scenario	Type of structure	Type of beam-to-column connection
S-I-A1	Steel structure, non-composite floor beams (*S*)	Type I (rigid)	C-I-A1	Steel structure, composite floor beams (*C*)	Type I (rigid)
S-I-A3			C-I-A3		
S-I-B2			C-I-B2		
S-I-A12			C-I-A12		
S-I-A23			C-I-A23		
S-II-A1		Type II (semi-rigid)	C-II-A1		Type II (semi-rigid)
S-II-A3			C-II-A3		
S-II-B2			C-II-B2		
S-II-A12			C-II-A12		
S-II-A23			C-II-A23		

39
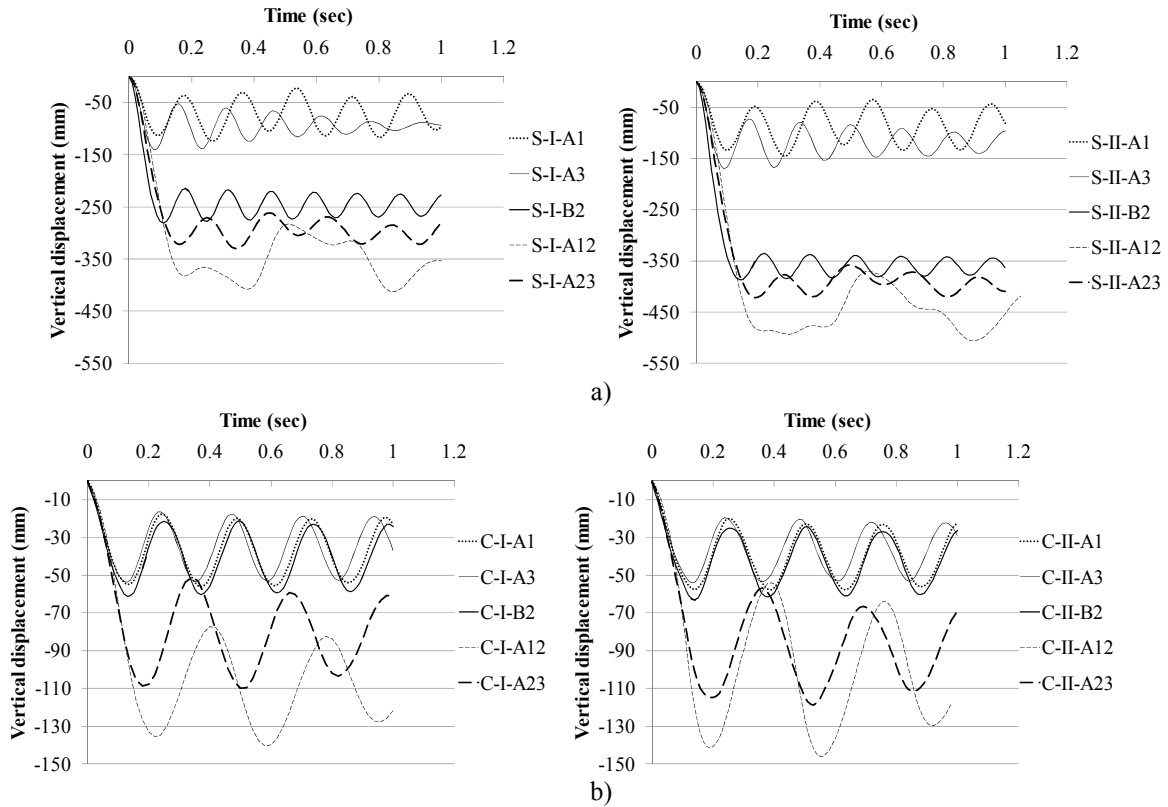
Figure 21. Structural response for nominal load combination: a) Pure steel structure, S; b) Composite-floor structure, C
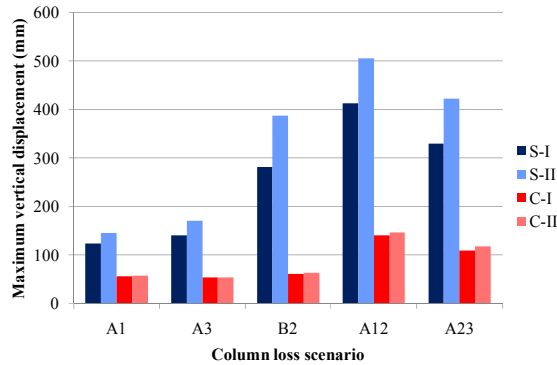

Figure 22. Maximum vertical displacement obtained by nonlinear dynamic analysis for all the structures and scenarios
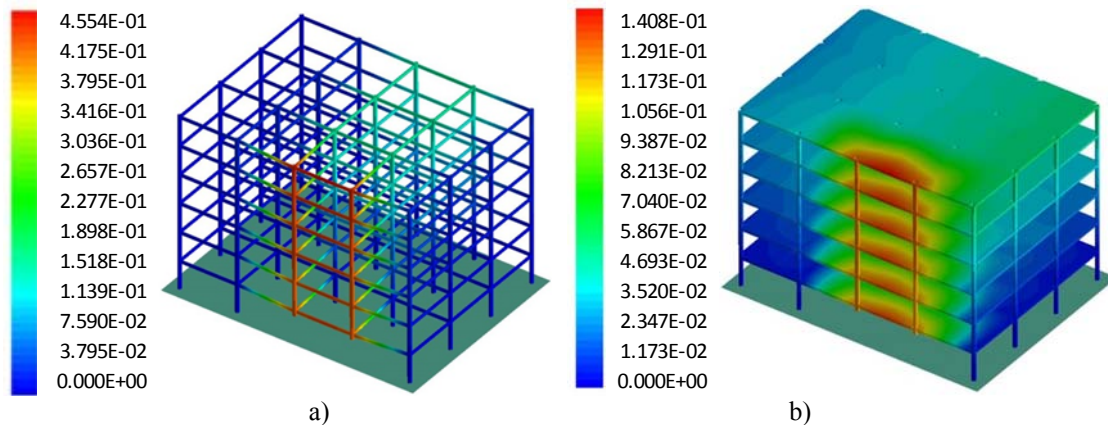

Figure 23. Deformed shape after 1.0 s for scenario A23 of Type II structure: a) Structure S; b) Structure C

As shown in Figure 21 and Table 10, if a single edge column or a corner column is lost, the pure steel structure *(S)* would undergo relatively small plastic deformation. If an internal column or two consecutive edge columns are lost, the steel structure would undergo larger deformations, and some local failure would occur in the beam-to-column connections due to fracture of the extended part of the end plates (scenarios B2 and A23). However, the connection has the capacity to resist complete separation of beam and column thereby preventing progressive collapse (Figure 23.a and Figure 25.a). The strain demands on the composite structures were significantly reduced and no local failure was observed in the connections (Table 11). Figure 25 shows the maximum strains in the steel members and concrete floor for scenarios S-II-B2 and C-II-B2.

To identify the critical components of the resistance to progressive collapse, the gravity loads were gradually scaled until collapse. The robustness criteria were to be obtained using as reference the ratio of the load at collapse to the nominal gravity load. Because the purpose included the evaluation of the DIF, both static and dynamic nonlinear analyses were conducted.

Figure 26 shows that collapse mode and propagation of damage with increasing gravity loads for scenarios S-II-B2 and C-II-B2. The failure mechanism of the pure steel structure involved fracture of the end plate in the bend above the top flange, followed by fracture of the tensioned internal bolts, and ultimately completes separation of the beam (see Figure 26.a). For the structure with composite-floor beams, progressive collapse was also initiated by fracture of the end plate in the bend and fracture of the tensioned reinforcement, followed by fracture of the tensioned internal bolts, rupture of the reinforcement near the secondary beams, and ultimately separation of the beams and concrete elements (see Figure 26.b). The DIF calculated for all the scenarios ranged between 1.25 and 1.5. Similar values were obtained in previous studies (Ruth, Marchand, & Williamson, 2006; Foley, Schneeman, & Barnes, 2008; Dinu, Dubina, & Ciutina, 2010; Khandelwala & El-Tawil, 2011). It should be noted that the DIF depends on the allowable deformation and varies with the level of performance.

Table 12 summarizes the overload factors obtained by the static (Ω_S) and dynamic (Ω_D) analyses, and the resulting DIFs. The minimum degree of robustness of the pure steel structure, Ω_D, was 1.05, which was obtained for the loss of one internal column and semi-rigid connections (S-II-B2). The most critical cases were the loss of two columns, namely, S-A12 and S-A23. The structure was much less affected by the loss of one edge column (S-A1 and S-A3), which was evident from the larger overload factors. The robustness of the structure with composite-floor beams (scenario C-II-A12) was significantly increased and the minimum Ω_D was 1.58. A comparison of the pure steel and composite structures reveals that the largest increase in capacity occurred for the loss of one internal column, for which Ω_D increases from 1.05 to 2.58. This shows that the composite action was more effective for internal spans, where the catenary action in the beams was accompanied by the development of membrane action in the concrete floor.
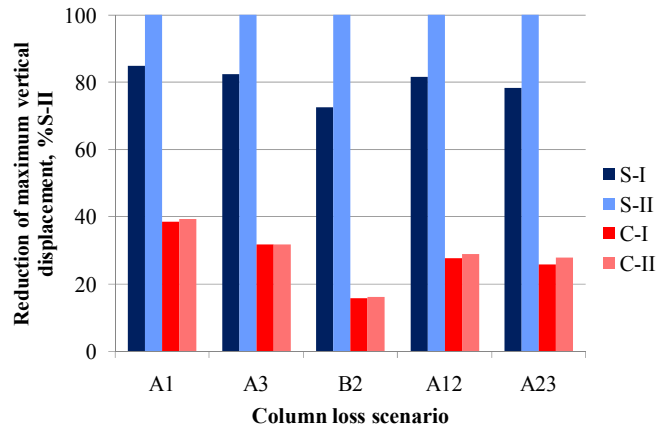
Figure 24. Vertical displacement ratios

Table 10. Maximum strain demand, S-II

Scenario	Steel beam	Beam-to-column connection
S-II-A1	0.005	0.018
S-II-A3	0.011	0.024
S-II-B2	0.029	Local failure
S-II-A12	0.028	0.053
S-II-A23	0.027	Local failure

Table 11. Maximum strain demand, C-II

Scenario	Steel beam	Beam-to-column connection	Headed stud	Concrete	Reinforcement
C-II-A1	0.0011	0.005	0.0019	-0.0001	0.011
C-II-A3	0.0051	0.005	0.0022	-0.0006	0.006
C-II-B2	0.0016	0.011	0.0020	-0.0006	0.009
C-II-A13	0.0069	0.009	0.0034	-0.0004	0.015
C-II-A23	0.0053	0.012	0.0037	-0.0004	0.018
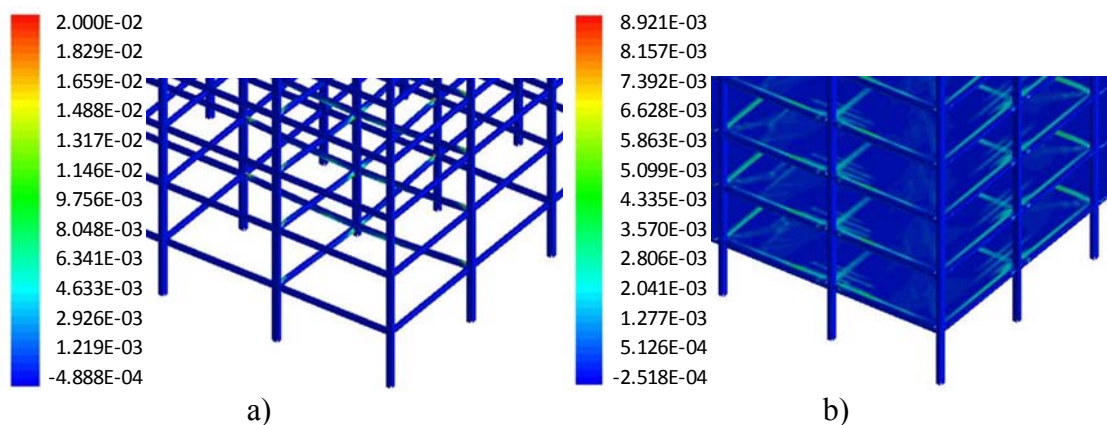
Figure 25. Maximum strains in the structures: a) S-II-B2; b) C-II-B2.

42
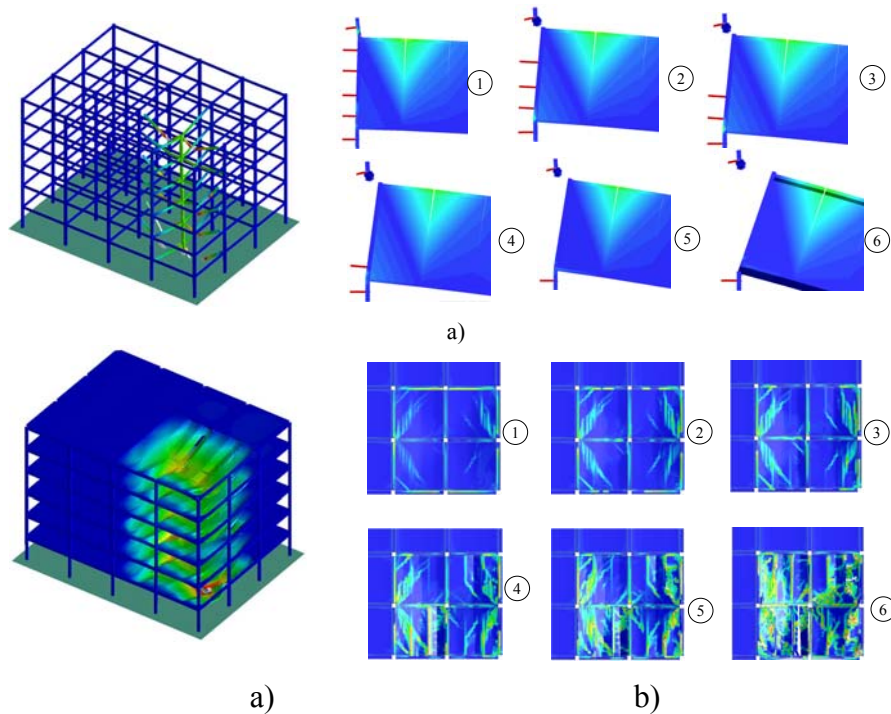
Figure 26. Failure mechanism for scenario B2: a) Global view of the pure steel structure (left) and beam-to-column connection (right) for S-II-B2; b) Global view of the composite structure (left) and concrete floor with composite beams (right) for C-II-B2.

Figure 26 shows that collapse mode and propagation of damage with increasing gravity loads for scenarios S-II-B2 and C-II-B2. The failure mechanism of the pure steel structure involved fracture of the end plate in the bend above the top flange, followed by fracture of the tensioned internal bolts, and ultimately complete separation of the beam (see Figure 26.a). For the structure with composite-floor beams, progressive collapse was also initiated by fracture of the end plate in the bend and fracture of the tensioned reinforcement, followed by fracture of the tensioned internal bolts, rupture of the reinforcement near the secondary beams, and ultimately separation of the beams and concrete elements (see Figure 26.b).

The DIF calculated for all the scenarios ranged between 1.25 and 1.5. Similar values were obtained in previous studies (Ruth, Marchand, & Williamson, 2006; Foley, Schneeman, & Barnes, 2008; Dinu, Dubina, & Ciutina, 2010; Khandelwala & El-Tawil, 2011). It should be noted that the DIF depends on the allowable deformation and varies with the level of performance.

Table 12. Values of the overload factor (Ω) obtained by static and dynamic analyses, and the dynamic increase factor (DIF)

Scenario	Overload factor, Ω		Dynamic increase factor DIF=Ω_S / Ω_D
	Static analysis, Ω_S	Dynamic analysis, Ω_D	
S-I-A1	2.88	2.3	1.25
S-I-A3	2.35	1.8	1.31
S-I-B2	1.55	1.2	1.29
S-I-A12	1.5	1.2	1.25
S-I-A23	1.58	1.15	1.37
C-I-A1	3.82	2.83	1.34

43

C-I-A3	3.95	2.83	1.39
C-I-B2	3.81	2.91	1.31
C-I-A12	2.28	1.60	1.42
C-I-A23	2.90	1.94	1.50
S-II-A1	2.7	2.05	1.32
S-II-A3	2.2	1.6	1.38
S-II-B2	1.4	1.05	1.33
S-II-A12	1.45	1.1	1.32
S-II-A23	1.5	1.15	1.3
C-II-A1	3.5	2.66	1.32
C-II-A3	3.78	2.75	1.37
C-II-B2	3.65	2.58	1.41
C-II-A12	2.11	1.58	1.34
C-II-A23	2.51	1.91	1.31

2.3.8 References

- Alashker, Y., & El-Tawil, S. (2011). A design-oriented model for collapse resistance of composite floors subjected to column loss. Journal of Constructional Steel Research, 67(1), 84–92, doi:10.1016/j.jcsr.2010.07.008.
- Alashker, Y., El-Tawil, S., & Sadek, F. (2010). Progressive collapse resistance of steel–concrete composite floors. Journal of Structural Engineering, 136(10), 1187-96, doi: 10.1061/(ASCE)ST.1943-541X.0000230.
- American Society of Civil Engineers ASCE (2006). ASCE 7-05: Minimum design loads for buildings and other structures, 424 pages, ISBN: 0784408092, Reston, USA.
- Astaneh-Asl, A., Jones, B., Zhao, Y., & Hwa, R. (2001). Floor catenary action to prevent progressive collapse of steel structures (Report No. UCB/CE-Steel-03/2001). Department of Civil and Environmental Engineering, University of California, Berkeley, USA.
- Izzuddin, B. A., Vlassis, A. G., Elghazouli, A. Y., & Nethercot, D. A. (2008). Progressive collapse of multi-storey buildings due to sudden column loss. Part I: Simplified assessment framework. Engineering Structures 30, 1308–1318, doi: 10.1016/j.engstruct.2007.07.011.
- Izzuddin, B. A., Vlassis, A. G., Elghazouli, A. Y., & Nethercot, D. A. (2008). Progressive collapse of multi-storey buildings due to sudden column loss. Part II: Simplified assessment framework, Engineering Structures, 30, 1424-38, doi:10.1016/j.engstruct.2007.08.011.
- Yang, B., & Tan, K. H. (2013). Experimental tests of different types of bolted steel beam–column joints under a central-column-removal scenario. Engineering Structures, 54, 112–130, doi: 10.1016/j.engstruct.2013.03.037.
- Ciutina, A., Dubina, D., & Danku, G. (2013). Influence of steel-concrete interaction in dissipative zones of frames: I – Experimental study. Steel and Composite Structures, 15(3), 299-322.
- Department of Defense DoD (2009). Design of buildings to resist progressive collapse. UFC 4-023-03, Washington, DC.
- Dinu, F., Dubina, D., & Ciutina, A. (2010). Robustness performance of seismic resistant building frames under abnormal loads. In Proceedings of the 1st International Conference on Structures and Architecture, ICSA 2010, Guimaraes, Portugal, 21-23 July 2010, 613-620, CRC Press, Taylor& Francis Group, ISBN: 978-0-415-49249-2.

- Dubina, D., & Dinu, F. (2012). Collapse prevention design of multistorey steel building frames under extreme action. In Proceedings of the Nordic Steel Construction Conference, 05-07 September 2012, Oslo, Norway, ISBN 978-82-91466-12-5, 1-14.
- European Committee for Standardization CEN (2002). EN 1990: Eurocode - Basis of structural design.
- European Committee for Standardization CEN (2006). EN 1991: Eurocode 1 - Actions on Structures, Part 1-7: General actions - Accidental actions.
- European Committee for Standardization CEN (2005). EN 1993: Eurocode 3 - Design of steel structures, Part 1-8: Design of joints.
- European Committee for Standardization CEN (2004). EN 1998-1: Eurocode 8 - Design of structures for earthquake resistance, Part 1: General rules, seismic actions and rules for buildings.
- Applied Science International (2010). Extreme Loading for Structures (Version 3.1). Durham, NC.
- Federal Emergency Management Agency FEMA (1996). The Oklahoma City Bombing: Improving building performance through multi-hazard mitigation, FEMA 277, ASCE.
- Foley, C. M., Schneeman, C., & Barnes, K. (2008). Quantifying and enhancing the robustness in steel structures: Part 1 - Moment-resisting frames. Engineering Journal, 45(4), 247–266.
- HMSO (1976). Statutory Instrument, No. 1676: Building and Buildings, London, UK.
- Khandelwala, K., & El-Tawil, S. (2011). Pushdown resistance as a measure of robustness in progressive collapse analysis. Engineering Structures 33, 2653–2661, doi: 10.1016/j.engstruct.2011.05.013.
- National Institute of Standards and Technology NISTIR (2007). Best Practices for Reducing the Potential for Progressive Collapse in Buildings NISTIR 7396, Technology Administration, U.S. Dep. of Commerce.
- Ministry of Transport, Construction and Tourism MTCT (2006). Seismic Design Code. Part 1: Earthquake Resistant Design of buildings P100-1/2006, Buletinul Construcţiilor, No. 12-13, INCERC, Bucharest, Romania (in Romanian).
- Final Report of COST Action TU0601 (2011). Robustness of Structures. Editor Faber Michael, Publisher: Czech Technical University in Prague, ISBN: 978-80-01-04803-0.
- Ruth, P., Marchand, K. A., & Williamson, E. B. (2006). Static equivalency in progressive collapse alternate path analysis: reducing conservatism while retaining structural integrity. Journal of Performance of Constructed Facilities, 20(4), 349–364, doi:10.1061/(ASCE)0887-3828(2006)20:4(349).
- Sadek, F., El-Tawil, S., & Lew, H. (2008). Robustness of composite floor systems with shear connections: modeling, simulation, and evaluation. Journal of Structural Engineering, 134(11), 1717–1725, doi:10.1061/(ASCE)0733-9445(2008)134:11(1717).
- El-Tawil, S., Li, H., & Kunnath, S. (2013). Computational simulation of gravity-induced progressive collapse of steel-frame buildings: current trends and future research needs. Journal of Structural Engineering, 10.1061/(ASCE)ST.1943-541X.0000897.
- Tagel-Din, H., & Meguro, K. (2000). Applied element method for simulation of nonlinear materials: theory and application for RC structures. Structural Engineering/Earthquake Engineering, International Journal of the Japan Society of Civil Engineers (JSCE), 17(2), 137-148.
- Tan, S., & Astaneh-Asl, A. (2003). Cable-based retrofit of steel building floors to prevent progressive collapse. Berkeley: University of California, 2003.

- Kuhlmann, U., Rölle, L., Jaspart, J.-P., …, Baldassino, N. (2009). Robust structures by joint ductility. Contract No RFSR-CT-2004-00046, 2004 - 2007, Final report, European Commission, RFCS, ISBN 978-92-79-10360-5.
- Mazzolani, F. M. (2010). Urban habitat constructions under catastrophic events. COST C26 Action final report, CRC Press, ISBN-13: 9780415606868.
- Yu, M., Zha X.-X, & Ye, J. (2010). The influence of joints and composite floor slabs on effective tying of steel structures in preventing progressive collapse. Journal of Constructional Steel Research, 66(3), 442-451, doi:10.1016/j.jcsr.2009.10.008.

2.4 Effect of local ductility on the progressive collapse resistance and development of catenary action (improved beam-to-column connections, membrane action of composite beams and floors)

2.4.1 Introduction

Steel moment-resisting frames have been traditionally used in seismic areas for low and middle-rise buildings, being considered advantageous from the seismic point of view, due to their inherent local and global ductility. However, the earthquakes of Northridge (1994) and Hyogoken-Nanbu (1995) revealed a series of undesirable brittle failure modes in welded beam-to-column joints that undermined the high seismic performance of steel moment-resisting frames. Extensive laboratory studies have been carried out to explain the poor performance of beam-to-column joints and to improve connection details and methodologies. Among the possible causes of brittle fractures in welded joints, have been identified the followings:
- workmanship (welding defects)
- detailing (stress concentration at the root or the toe of welds)
- materials (low-toughness weld metal), and
- unusually high seismic input (high strain rates).

The research on the causes of brittle failures of beam to column joints observed in the last earthquakes took different directions. Japanese research concentrated on dynamic testing, influence of temperature on connection performance, the material properties of base and weld metal, the development of new materials, the geometry of weld copes and other details, and the elimination of these copes. The U.S. research has attempted to better understand nonlinear and brittle performance of steel frame structures and properties of material and welding, a significant portion of the research being devoted toward developing new connection geometry. Nakashima et. al. (1998) tested 86 full scale beam-column subassemblies, with the type of connection, type of weld access holes, type of run-off tabs, and type of loading as major variables. The results of 40 specimens applied to shop-welding connection were summarized, and the primary findings indicated that the type of run-off tabs affected significantly the ductility capacity, and dynamic loading showed no detrimental effect on ductility compared to quasi-static loading.

Local ductility has also large impact on the ultimate capacity of structures to withstand the loss of critical members. Thus, alternative load paths can be improved through catenary action within members and floor slabs, see Figure 27. However, the performance requirements necessary to generate catenary action in the structure need to be properly taken into account. This is particularly important at perimeter connections where tying is believed to prevent progressive collapses by catenary action following the removal of a column. When a framed building is affected by the loss of a column, the flexural resistance of the beams or their connections to the columns ensures the transfer of the loads through alternative paths. When compared with normal load conditions or with seismic condition, the loss of a column may lead to significant differences, like the large axial forces in the beam-to-column connections

and therefore the connections must be designed for the combined effects of bending and axial load. Thus, Marchand (2005) proposed that, for connections in which catenary action may develop, the design should be done for two limit states: 1) developing beam plastic moment and 2) developing beam axial tension capacity.
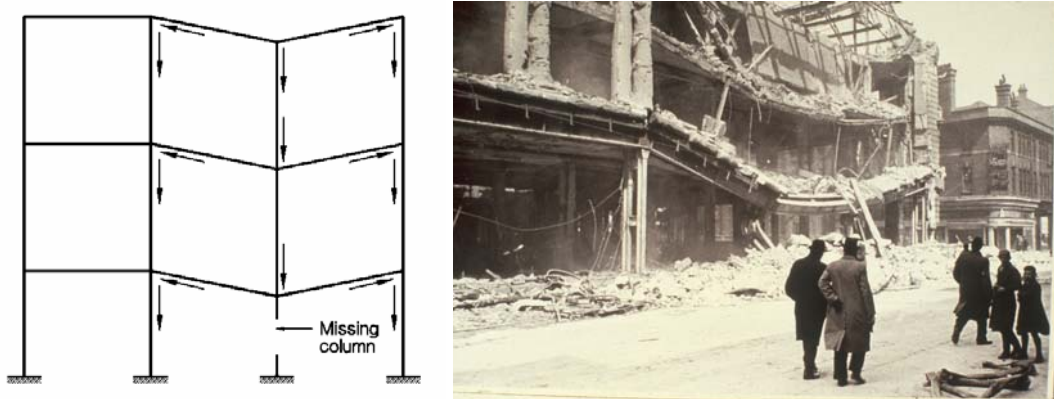

Figure 27. Development of catenary action (left) and large sagging deflections after loss of columns following a bomb attack (right)

The application of design rules from EN 1993-1-8 to beam-to-column joints in bending is limited to joints in which the axial force N_{Ed} in the connected member does not exceed 5% of the design resistance $N_{pl,Rd}$ of its cross-section. If the axial force N_{Ed} in the connected beam exceeds 5% of the design resistance, $N_{pl,Rd}$, the following conservative method may be used (see eq. 1):

$$\frac{M_{j,Ed}}{M_{j,Rd}} + \frac{N_{j,Ed}}{N_{j,Rd}} \leq 1 \qquad (1)$$

where:

$M_{j,Rd}$ is the design moment resistance of the joint, assuming no axial force;

$N_{j,Rd}$ is the axial design resistance of the joint, assuming no applied moment;

$M_{j,Ed}$, $N_{j,Ed}$ are the bending moment and axial force applied to a joint.

The method proposed in EN 1993-1-8 was considered quite questionable, and an improved design procedure, based on the component method concept, has been developed to predict the response of steel joints subjected to combined axial loads and bending moments (Cerfontaine, 2003). Demonceau (2008) extended the design procedure developed by Cerfontaine to composite joints and validated through comparisons to the experimental test results. Sokol et al. (2002) developed a design model of end plate joints loaded by combination of bending moment and normal force (Figure 28).

Da Silva et al. performed experimental work on beam-to-column joints in order to extend the philosophy of the component method to deal with the combined action of bending moment and axial force (da Silva et al. 2004). For the chosen flush end-plate joint, a reduction of the moment resistance was noted for tensile axial force below 20% of the beam plastic resistance. A generalized component-based model for semi-rigid beam-to-column connections including axial force versus bending moment interaction was developed by Del Savio et al. (2009). Liu studied the retrofitting of steel construction and improvement of their catenary ability through strengthening the beam-to-column connection (Liu, 2010). Sadek et al. investigated the

response of steel beam-column assemblies with moment connections under monotonic loading conditions simulating a column removal scenario (Sadek et al., 2013).
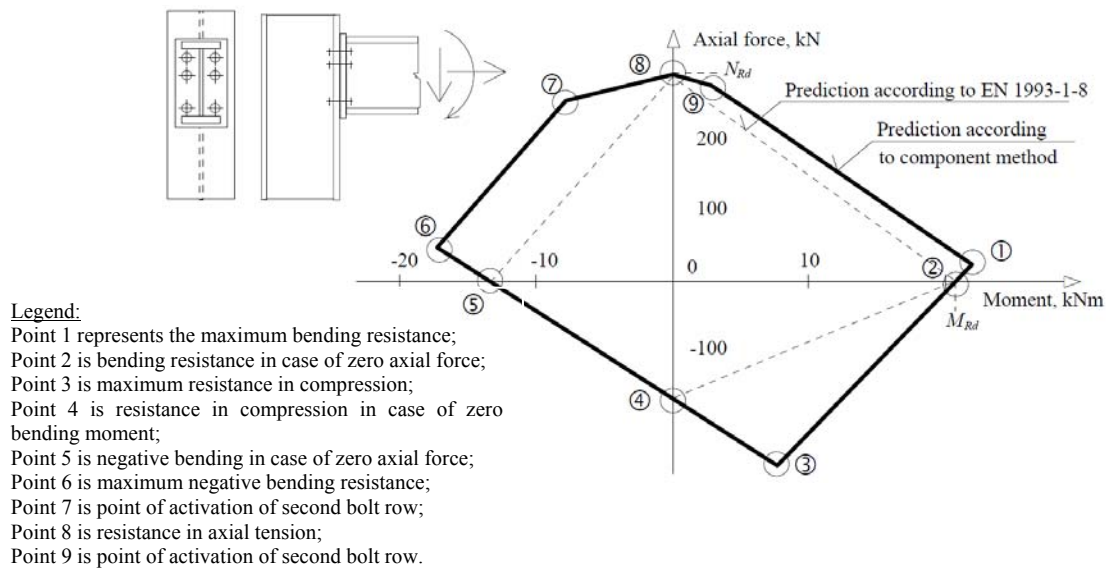
Figure 28. Moment – axial load interaction curve, prediction according to EN 1993-1-8 is marked by dotted line; the component method is marked as a solid line (Sokol et al., 2002)

In this section, two important research programs that were developed at the CEMSIG Research Center within the last 10 years are presented. First program aimed at evaluation of strain rate effect on the ultimate deformation capacity of welding details and has been justified by the unforeseen failure of weld during the earthquakes of Northridge (1994) and Hyogoken-Nanbu (1995). Three weld details have been designed, first was a filet weld, second a single bevel but weld and third a double bevel but weld. Three strain rates have been considered, and he tests were done at room temperature. Second program has been developed in the frame of Codec research project, where a large experimental program has been designed for the evaluation of connections and their component to withstand large deformations in case of column loss. The experimental program had two main components:
- Monotonic tests on bolted macrocomponents (bolted T-stubs) and welding details
- Monotonic tests on beam-to-column joints

For first testing program, T-stubs with different failure modes and weld detailing are tested until failure at room and elevated temperature and considering static and dynamic loading. In the second testing program, four beam-to-column connections are tested failure. Two of the connections are partial strength while the other two have overstrength compared to the beam.

2.4.2   *First experimental program on welded joints, 2004*

The importance of strain rate on the performance of welded joints, led to an experimental program mainly devoted to the behavior of "T" assemblies, composed of an end plate and two flanges (Figure 29). A number of 54 specimens have been prepared, that would simulate as close as possible conditions met in beam-to-column welded joints. Three types of welds were used: fillet weld, double bevel butt weld – K type, and single bevel butt weld – 1/2V type. Testing was performed on a 250kN universal testing machine UTS RSA 250 (Figure 30).

(a)   (b)
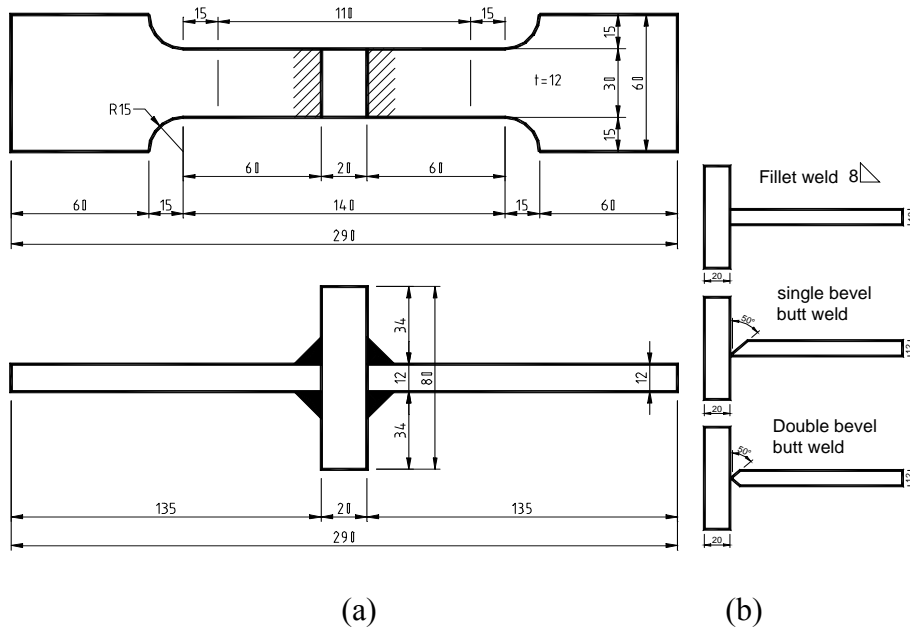
Figure 29. Welded specimens (a) and edge preparation (b)
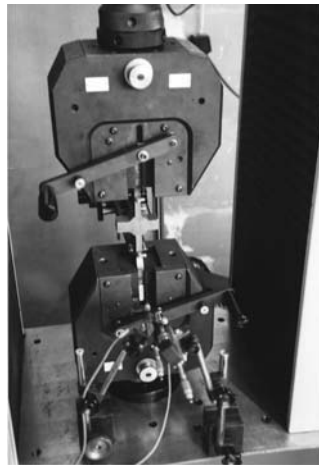
Figure 30. Test set-up

The following parameters were considered in this experimental program:

− Steel grade: S235 and S355.
− Strain rate: $\dot{\varepsilon}_1$=0.0001s^{-1}; $\dot{\varepsilon}_2$=0.03s^{-1}; $\dot{\varepsilon}_3$=0.06s^{-1}. The first value represents a quasi-statical loading, while the other two strain rates are characteristic for seismic conditions.
− Welding type: fillet weld, double bevel butt weld − K type, and single bevel butt weld − 1/2V type, see Figure 29.b.
− Type of loading (monotonic and cyclic pulsating).

It was not possible to analyze the influence of steel grade, due to delivery of different base metal grades than the required ones (S275 instead of S235 and S355 for flanges). A global view of the experimental program is presented in Table 13.

Table 13. Experimental program on welded specimens

Material/weld type	Base metal and deposited metal	Welded specimens
	t=12mm, t=20mm weld	Fillet, K, 1/2V
Strain rate [s^{-1}]	$\dot{\varepsilon}_1$=0.0001 $\dot{\varepsilon}_2$ =0.03	

49

	$\dot{\varepsilon}_3 =0.06$	
Steel grade	S235, S355	
Loading	Monotonic (1 or 2 specimens)	monotonic (1 specimen) and cyclic (2 specimens)
Total specimens	18	54

2.4.3 Tensile tests on component materials

Tensile tests have been performed on base and deposited metals in order to determine the mechanical characteristics of the materials. It was found out that the material in flanges (steel plate of nominal thickness of 12 mm) was not delivered according to the specifications (grades S235 and S355). Instead, the material showed to be S275 steel grade, according to SR EN10025. Only the end plate material (t=20 mm) was delivered as required. The deposited metal showed a resistance close to the S355 steel grade but higher yield strength.

The lower yield strength (R_{el}) increases for higher strain rates with a maximum of 27% for $\dot{\varepsilon}_3$. This maximum increase was found out for the mild steel (S235) (see Figure 31.a). On the ordinate the parameter values are normalized in respect to the quasi-static ones. It is seen that the constitutive law proposed by Soroushian fits very well the experimental results in case of mild steel (S235) but overestimates the strain-rate sensitivity for steel with higher yield strength (S275 and S355). For these steel grades, another law, proposed by Wakabayashi (1994), covers very well the experimental results. This leads to conclusion that constitutive laws must consider, as well, as significant parameter the steel grade influence.

The ultimate tensile strength (R_m) increases with increasing of strain rates but is less strain-rate sensitive than yield strength (maximum value of about 8% for $\dot{\varepsilon}_3$). The maximum influence is again observed for the mild steel (S235). The strain rate sensitivity of Rm obtained from experimental tests together with constitutive law proposed by Soroushian (1987) is presented in Figure 31.b. On the ordinate the parameter values are normalized in respect to the quasi-static ones. Typical values of the ratio between the tensile strength and the yield strength (R_m/R_{eH}) are 1.2 to 1.55, and the ratio is decreasing for higher strain rates.

The total elongation at fracture (A_t) is not influenced by strain rate, implying that strain rates of the magnitude of 0.03-0.06 s^{-1} do not reduce the ductility of the base and deposited metals.

Lower yield strength for dynamic to static ratio

a)

Ultimate tensile strength for dynamic to static ratio
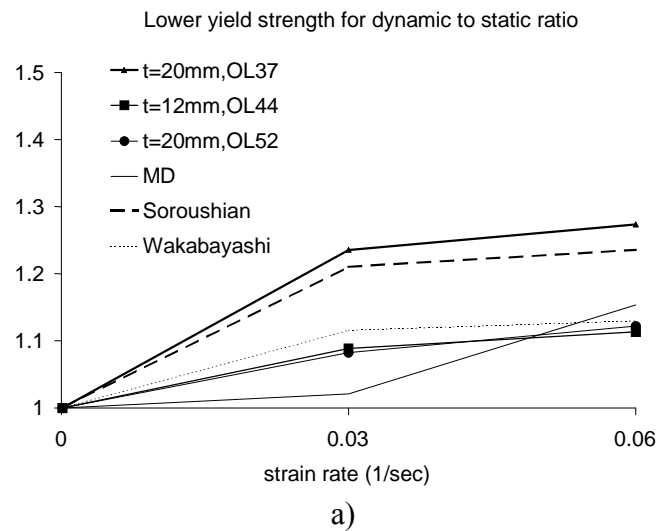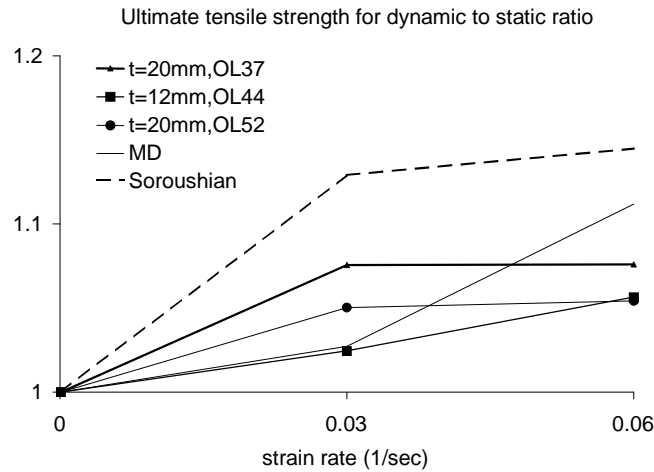
b)

Figure 31. Variations of lower yield strength (R_{el}) and ultimate tensile strength (R_m) for the component materials (theoretic and experimental) (*note: MD – deposited metal)

2.4.4   Tests on welded specimens

The parameters used to evaluate the behavior of welded specimens were basically the same used for analysis of component materials, with one exception, i.e. lower yield strength (R_{el}) has been replaced by the conventional yield strength (R_{p02}) for an offset elongation of 0.2%. Higher *strain rate* caused an increase of the conventional yield strength (R_{p02}) with about 18% for $\dot{\varepsilon}_3$ (see Figure 32). It could be observed that the yield strength of welded specimens is less sensitive to strain rate than the yield strength of component materials.

The ultimate strength of the welded specimens (R_m) increases slightly with strain rate for the monotonically loaded specimens (maximum 10% for $\dot{\varepsilon}_3$). An exception is the 5VM specimen, which failed by brittle fracture in the weld and is characterised by an important increase of R_m (40% for $\dot{\varepsilon}_3$). In case of cyclically loaded specimens, the ultimate strength is less sensitive to strain rate (a maximum of 5%). Strain rate affects the ultimate strength of welded specimens approximately in the same extent as observed in case of component materials. Contrary to component materials, a higher strain rate does imply a reduction of the ductility for monotonically loaded welded specimens. The total deformation at failure (A_t) diminishes for higher strain rates (exception 5CM).

Conventional yield strength for dynamic to static ratio

a)

b)
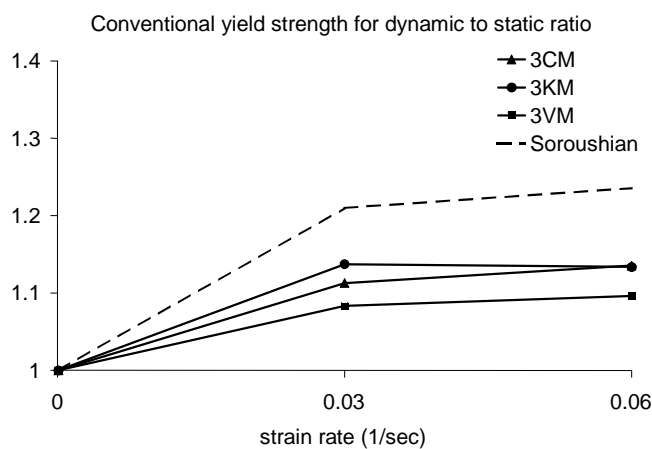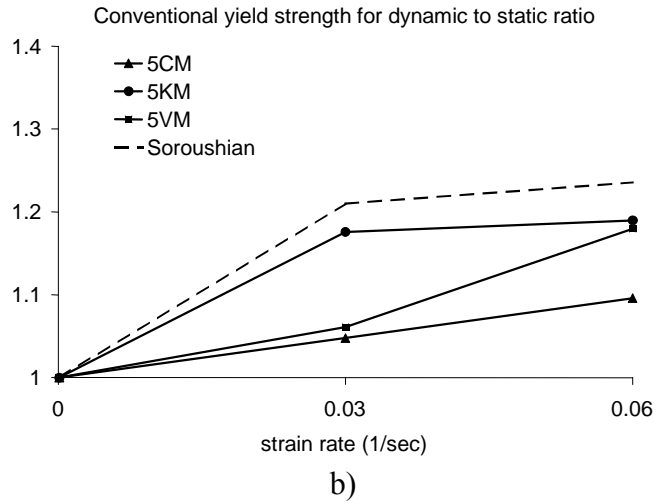
Figure 32. Variations of conventional yield strength (R_{p02}) for the monotonically loaded specimens: a) S235; b) S355. (Denomination of welded specimens is: 3 – S235, 5 – S355; C – fillet weld, V - single bevel weld, K – double bevel weld; M – monotonic loading
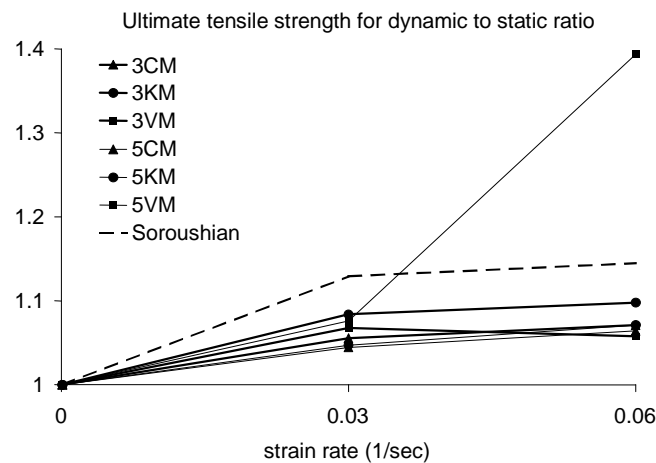

Figure 33. Influence of the weld type on the ultimate strength (R_m) of welded specimens.
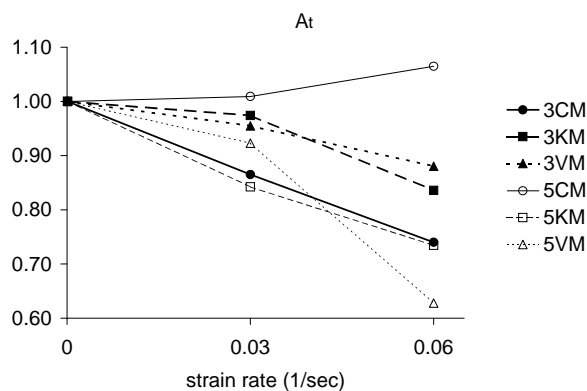
Figure 34 Ductility (elongation at fracture) vs. strain rate for monotonically loaded welded specimens

In case of cyclic loading, high strain rate leads generally to an increase in the connection ductility, a decrease of A_t being also observed in several cases, the results being rather scattered. A possible explanation for the increase in ductility under high strain rate cyclic loading may be attributed to the specimen heating, as noted elsewhere (Suita et al, 1998).

Two failure types were observed for the welded specimens: fracture in the base metal (BM) and in the weld (W). For monotonically loaded specimens, the failure occurred in the base metal. An exception was S355 single bevel butt weld specimens, caused by excessive weld defects at root of weld. Therefore, the failure mode was independent of strain rate.

a)   b)
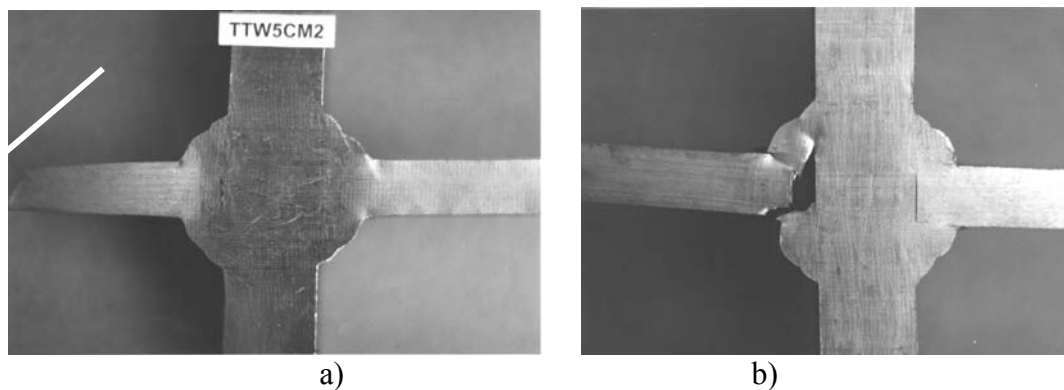
Figure 35. Failure of fillet weld specimens: in the base metal (a), and in the weld (b).

For cyclically loaded specimens, the number of failures in weld increased for fillet and single bevel butt weld specimens, only. This failure type had a higher occurrence in specimens loaded with high strain rates ($\dot{\varepsilon}_2$=0.03s^{-1} and $\dot{\varepsilon}_3$=0.06s^{-1}). The two failure modes of fillet weld specimens are presented in Figure 35 (failure in base metal under monotonic loading - a, and in the weld under cyclic loading - b). No weld failure occurred in double bevel butt weld specimens, recommending them as the most reliable for this type of loading. One of the factors that led to a poor performance of fillet welds (besides incomplete penetration) was the undersized weld throat, making them partially resistant.

Single bevel butt welds were characterized by excessive defects, among them the incomplete penetration at the weld root was the most significant.

2.4.5   Tests on connection macro-components and weld details, period 2013-2014

The T-stub configurations have been design to fail in mode 1, 2 and 3. From all possible configurations, the following typologies have been selected for the experimental program: T-10-16-100-C(T); T-10-16-120-C(T); T-10-16-140-C(T); T-12-16-100-C(T); T-12-16-120-C(T); T-12-16-140-C(T); T-15-16-100-C(T); T-15-16-120-C(T); T-15-16-140-C(T); T-15-16-120-C(T); T-18-16-140-C(T); T-10-16-90-C(T); T-15-16-90-C(T).

First letter represent the T-stub, second term repreents the end plate thickness, followed by the diameter of the bolt and then distance between the bolts, in mm. Every specimen has been tested in four different conditions:
- Cvasistatic test: imposed strain rate of 0.05mm/sec, room temperature T=20°C
- Cvasistatic test: imposed strain rate of 0.05mm/sec, elevated temperature T=542°C
- Dynamic test: imposed strain rates of 10 and 15 mm/sec, room temperature T=20°C
- Dynamic test: imposed strain rates of 10 and 15 mm/sec, elevated temperature T=542°C

Three types of welding details have been considered, i.e. fillet weld, single bevel and double bevel butt weld, respectively. Every specimen has been tested in four different conditions:
- Cvasistatic test: imposed strain rate of 0.05mm/sec, room temperature T=20°C

- Cvasistatic test: imposed strain rate of 0.05mm/sec, elevated temperature T=542°C
- Dynamic test: imposed strain rates of 10 and 15 mm/sec, room temperature T=20°C
- Dynamic test: imposed strain rates of 10 and 15 mm/sec, elevated temperature T=542°C

In order to plot the stress - strain curves, tensile tests on base materials and bolts have been performed. For each material, three specimens have been fabricated and tested. Position P19 has been ordered from S355 steel, and the actual properties indicate larger yield strength by almost 10%. Positions P20-P22 have been ordered from S235 and the actual properties indicate larger yield strength by minimum 18%. The ultimate elongation shows the steel has a good ductility.

Table 14. Design of experimental program on bolted T-stubs

Varianta S235		2	3	4	5	7	8	9	10	13	14	15	18	19	20	23	24	25	30	34	35	40	42	43	44	45	47	48	49	50	53
t	10	X	X	X	X	X	X	X	X														X	X	X	X	X	X	X	X	
	12									X	X	X	X	X	X																X
	15															X	X	X	X												
	18																			X	X	X									
c	70																														
	90	X				X														X			X								
	100		X				X			X			X			X								X			X				X
	120			X				X			X			X			X								X			X			
	140				X				X			X			X			X			X	X				X			X		
M.16	8.8	X	X	X	X					X	X	X				X	X	X		X	X										
	10.9					X	X	X	X				X	X	X				X			X									
M20	8.8																						X	X	X	X					X
	10.9																										X	X	X	X	
Mode 1		82	69	53	43	82	69	53	43	100	76	62	100	76	62	156	119	97	97	172	139	139	87	73	56	45	87	73	56	45	105
Mode 2		104	97	84	75	126	117	102	90	104	90	80	124	108	95	116	101	90	105	115	102	117	153	142	124	109	188	174	151	134	149
Mode 3		181	181	181	181	226	226	226	226	181	181	181	226	226	226	181	181	181	226	181	181	226	282	282	282	282	353	353	353	353	282
		82	69	53	43	82	69	53	43	100	76	62	100	76	62	116	101	90	97	115	102	117	87	73	56	45	87	73	56	45	105
R mode		1	1	1	1	1	1	1	1	1	1	1	1	1	1	2	2	2	1	2	2	2	1	1	1	1	1	1	1	1	1
Fx1.2		98	83	64	51	98	83	64	51	119	92	74	119	92	74	140	122	108	116	138	122	141	104	88	67	54	104	88	67	54	126

sudura cap la cap

| Varianta S235		2	3	4	5	7	8	9	10	13	14	15	18	19	20	23	24	25	30	34	35	40	42	43	44	45	47	48	49	50	53
t	10	X	X	X	X	X	X	X	X														X	X	X	X	X	X	X	X	
	12									X	X	X	X	X	X																X
	15															X	X	X	X												
	18																			X	X	X									
c	70																														
	90	X				X														X			X				X				
	100		X				X			X			X			X								X				X			X
	120			X				X			X			X			X			X					X				X		
	140				X				X			X			X			X			X	X				X				X	
M.16	8.8	X	X	X	X					X	X	X				X	X	X		X	X										
	10.9					X	X	X	X				X	X	X				X			X									
M20	8.8																						X	X	X	X					X
	10.9																										X	X	X	X	
Mode 1		64	56	45	37	64	56	45	37	80	63	54	80	64	54	125	101	84	84	145	121	121	67	58	46	39	67	58	46	39	84
Mode 2		93	86	76	68	112	105	92	83	93	82	73	111	98	87	104	92	82	96	104	93	108	136	127	112	100	166	155	137	123	133
Mode 3		181	181	181	181	226	226	226	226	181	181	181	226	226	226	181	181	181	226	181	181	226	282	282	282	282	353	353	353	353	282
		64	56	45	37	64	56	45	37	80	63	54	80	64	54	104	92	82	84	104	93	108	67	58	46	39	67	58	46	39	84
R mode		1	1	1	1	1	1	1	1	1	1	1	1	1	1	2	2	2	1	2	2	2	1	1	1	1	1	1	1	1	1
Fx1.2		76	67	54	45	76	67	54	45	96	76	64	96	77	64	125	110	99	101	125	112	129	80	70	56	47	80	70	56	47	101
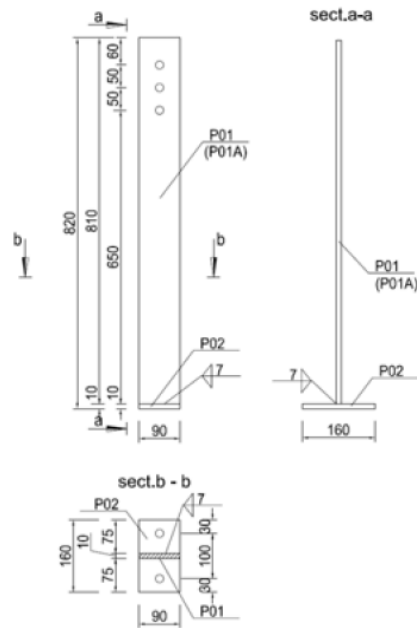
Figure 36. Bolted T-stub detail
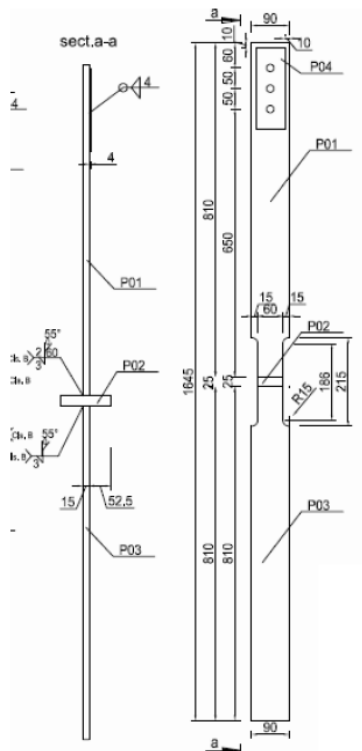
Figure 37. Welding detail

In order to plot the stress - strain curves, tensile tests on base materials and bolts have been performed. For each material, three specimens have been fabricated and tested. Position P19 has been ordered from S355 steel, and the actual properties indicate larger yield strength by

almost 10%. Positions P20-P22 have been ordered from S235 and the actual properties indicate larger yield strength by minimum 18%. The ultimate elongation shows the steel has a good ductility.
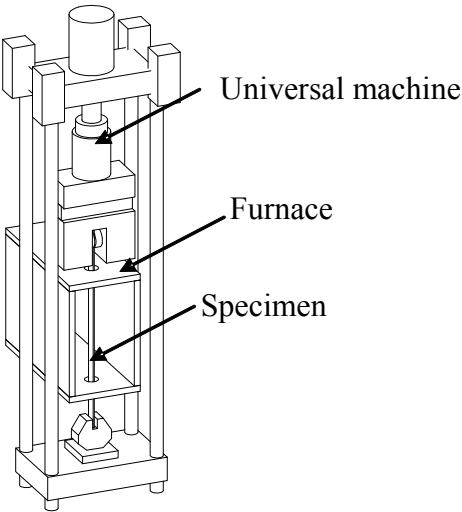
Figure 38. Test set-up for macro-component tests

Table 15. Mechanical properties of steel elements

Element	f_y	f_u	A_{gt}	A_t
	N/mm²	N/mm²	%	%
P19	390	569	18.7	26.5
P20	310	408	22.5	34.7
P21	305	445	23.3	32.7
P22	278	400	22.8	34.2
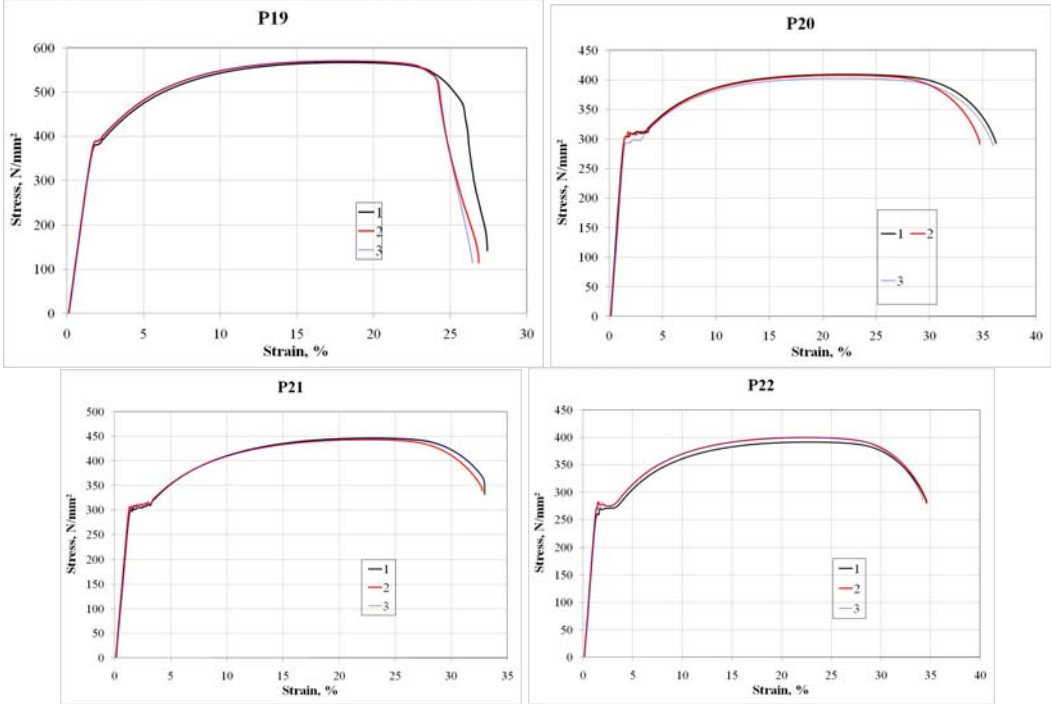
Figure 39. Mechanical properties of steel elemnets
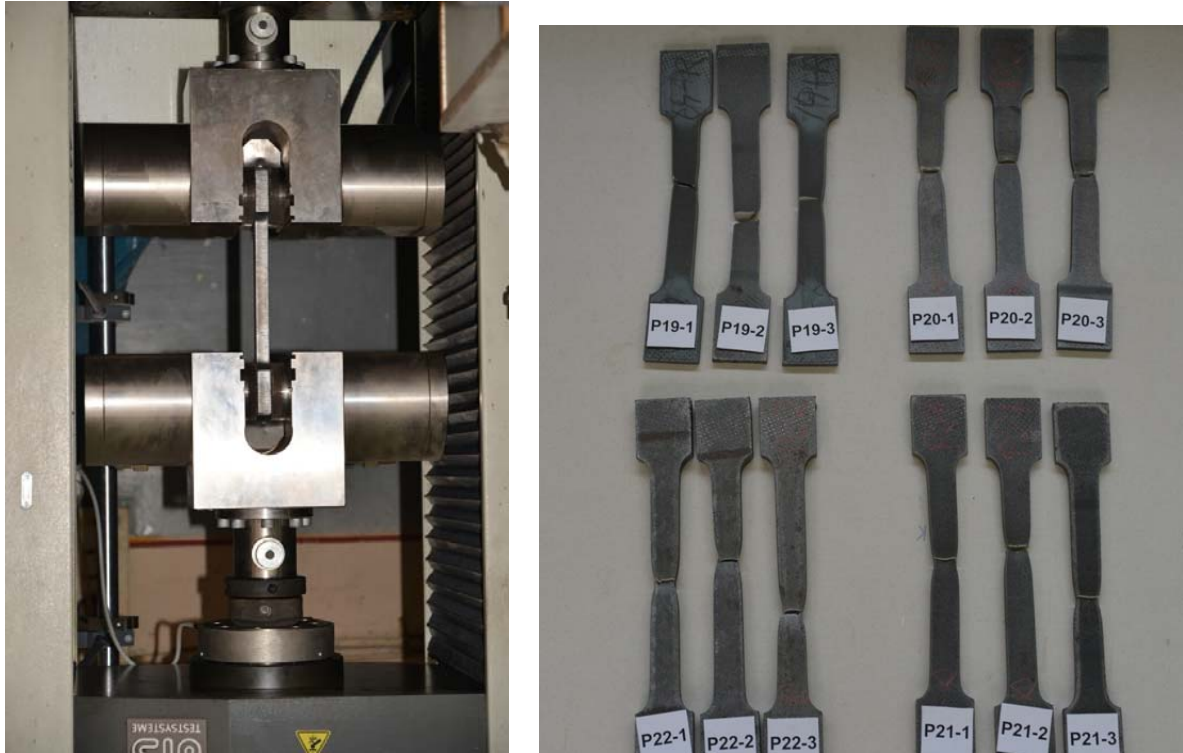
Figure 40. Coupon specimen in universal machine (left) and failure mode (right)

2.4.5.1 Tests on welding details

Three types of welding details were fillet weld, singles bevel butt weld and double bevel but weld. Specimens have been tested in four different conditions:

- Cvasistatic test: imposed strain rate of 0.05mm/sec, room temperature T=20°C
- Cvasistatic test: imposed strain rate of 0.05mm/sec, elevated temperature T=542°C
- Dynamic test: imposed strain rates of 10 and 15 mm/sec, room temperature T=20°C
- Dynamic test: imposed strain rates of 10 and 15 mm/sec, elevated temperature T=542°C

The notations are as follows:

- W-D-1-C: cvasi-static test, room temperature
- W-D-1-CS: dynamic test, room temperature (strain = 15 mm/sec)
- W-D-1-T: cvasi-static test, elevated temperature (t=542°C)
- W-D-1-TS: dynamic test, elevated temperature (t=542° C) (strain = 15 mm/sec)

Figure 41- Figure 43 plot the force-displacement curves for the three welding details at different test conditions. It may be seen for room temperature test, there is a slight increase of tensile stress and ultimate strength, accompanied by a small reduction of the ultimate elongation. For temperature test, the strain rate leads to a significant increase of ultimate strength. The ultimate elongation is not much affected. To note that all specimens failed in the base material, with no degradations in the welding (Figure 44).
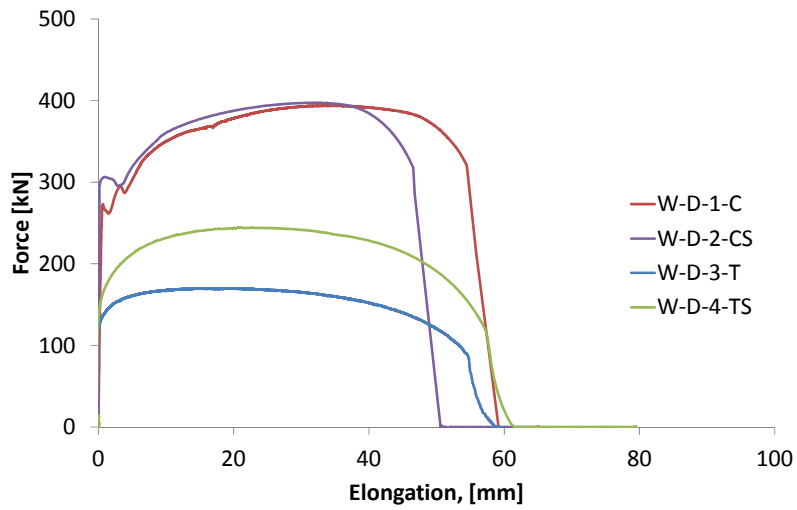
Figure 41. Force-displacement curves for filet weld specimens
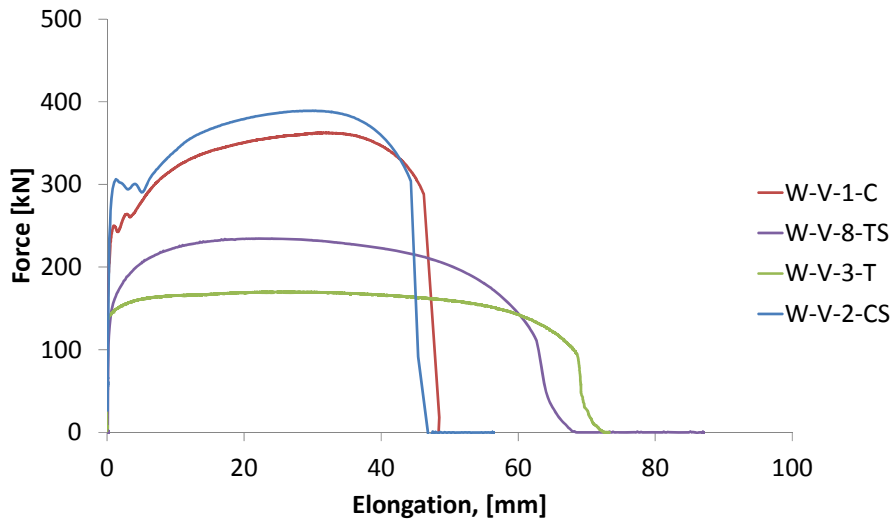
Figure 42. Force-displacement curves for single bevel butt weld specimens
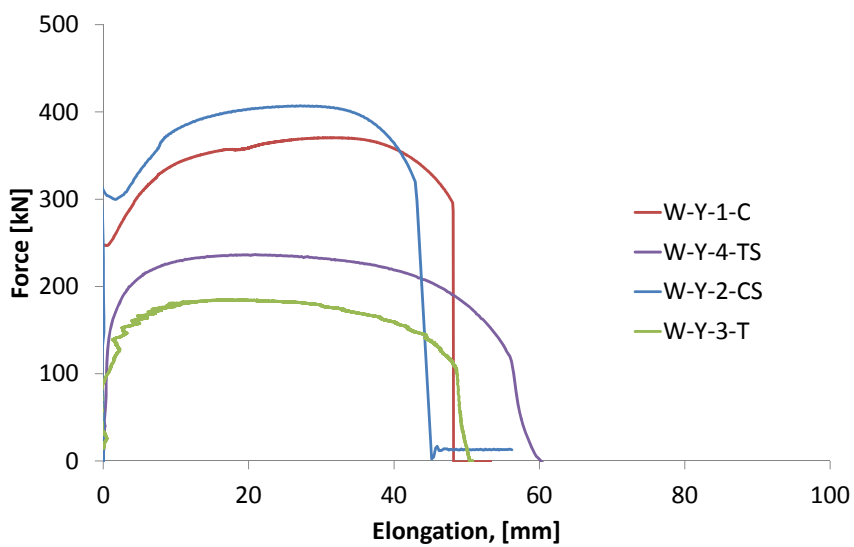
Figure 43. Force-displacement curves for double bevel butt weld specimens

58

a)

b)

c)

d)

Figure 44. Failure mode for filet weld specimen: a) Cvasistatic test, room temperature; b) Dynamic test, room temperature; c) Cvasistatic test, elevated temperature; Dynamic test, elevated temperature

2.4.5.2   Tests on connection macro-components

Specimen have been tested in four different conditions:
- Cvasistatic test: imposed strain rate of 0.05mm/sec, room temperature T=20°C
- Cvasistatic test: imposed strain rate of 0.05mm/sec, elevated temperature T=542°C
- Dynamic test: imposed strain rates of 10 and 15 mm/sec, room temperature T=20°C
- Dynamic test: imposed strain rates of 10 and 15 mm/sec, elevated temperature T=542°C

Figure 45. Test set up with the universal machine for room temperature tests
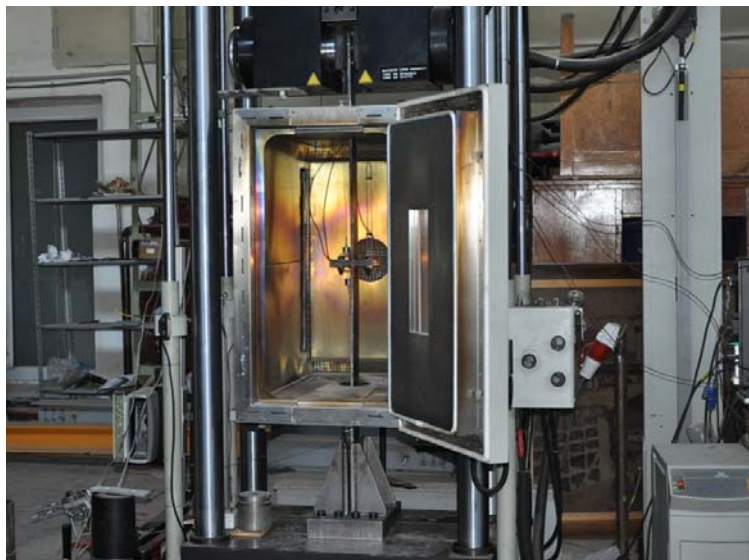
Figure 46. Test set up with the furnace for elevated temperature

In Figure 47 - Figure 52 the force-displacement curves for T-stub specimens are presented. The notations are as follows:
- T-10-16-100-C: cvasi-static test, room temperature
- T-10-16-100-CS: dynamic test, room temperature (strain = 15 mm/sec)
- T-10-16-100-T: cvasi-static test, elevated temperature (t=542° C)
- T-10-16-100-TS: dynamic test, elevated temperature (t=542° C)

From the curves plotted in Figure 47 - Figure 52 it may be seen there is an increase of yield strength and tensile stress under dynamic loading. For tests at room temperature, the larger strain rate tests do not lead to a reduction of the ductility, as expected. Contrary, for elevated temperature tests, strain rate induces an increase of the yield strength and ultimate tensile strength, and also to a considerable increase of the ultimate elongation. When distance between bolts increases from 100mm to 140mm the ultimate elongation increases dramatically and this may be explained by the tensile stage that developes at large deflection, and this may be classified as "catenary state".

The failure is always initiated by fracture of bolts, even in case of T-stubs designed for mode 1 – failure of end plate in bending – the failure begins after very large deformations of the end plate.

Figure 57 and Figure 58 show the failure mode for bolts room temperature and elevated temperature. It may be seen at elevated temperature the failure is initiated within the threaded part while at room temperature tests the failure is initiated in the net area.
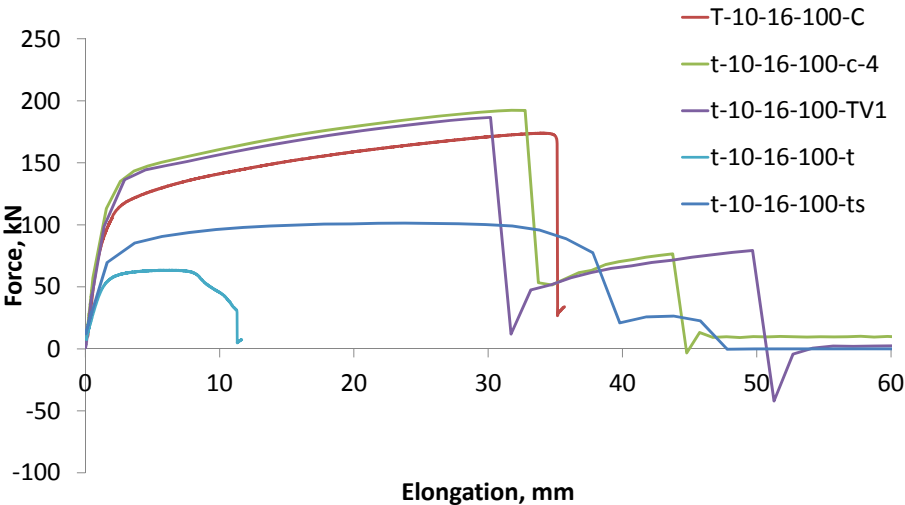
Figure 47. Force-displacement curves for T-10-16-100 specimens
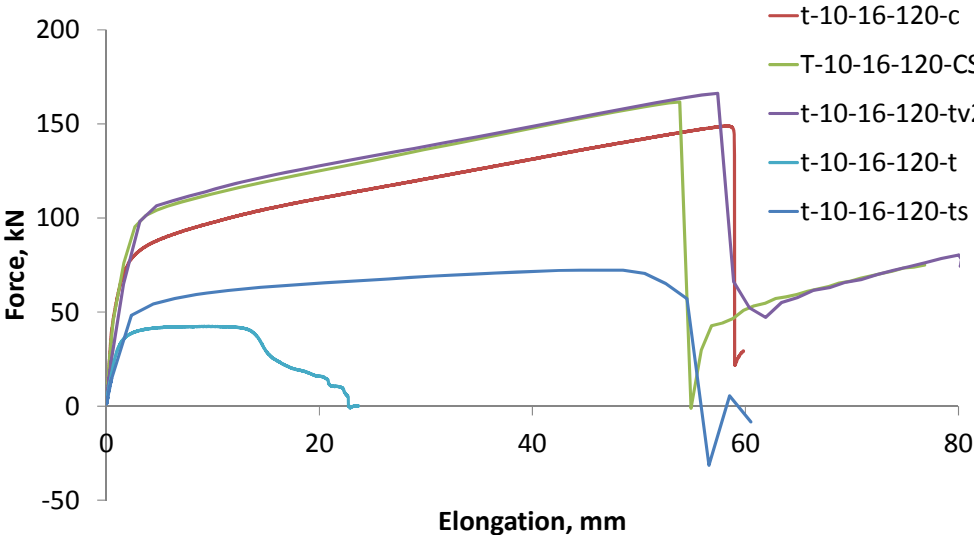
Figure 48. Force-displacement curves for T-10-16-120 specimens
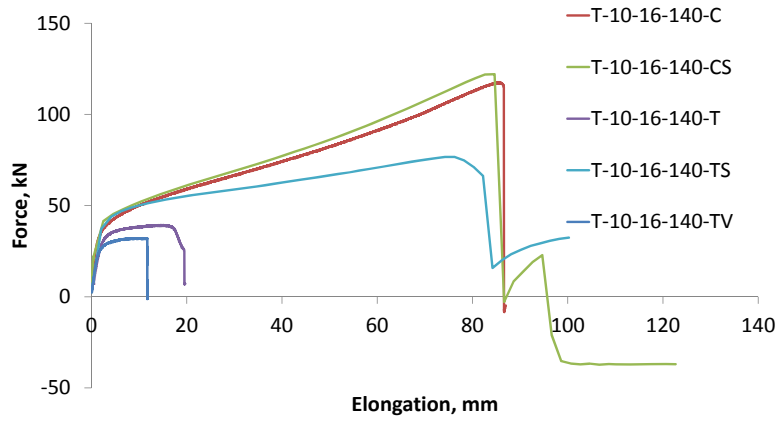
Figure 49. Force-displacement curves for T-10-16-140 specimens
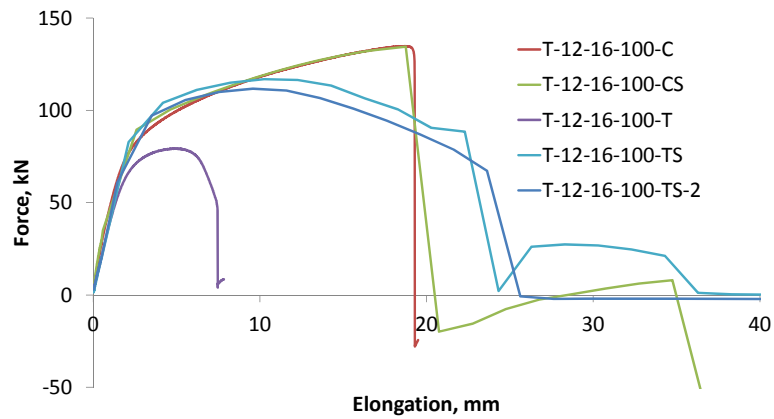
Figure 50. Force-displacement curves for T-12-16-100 specimens
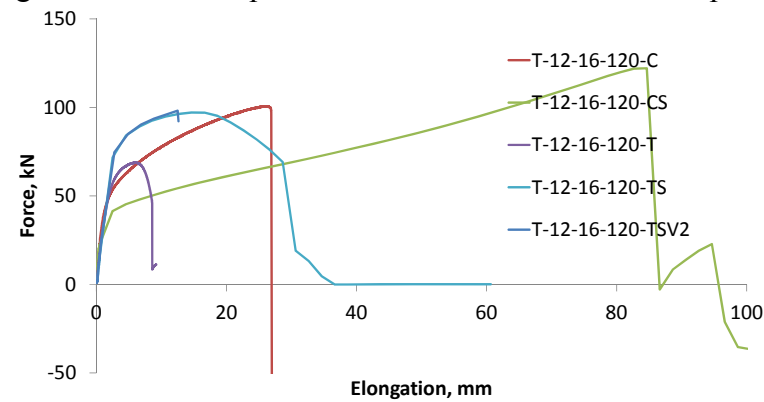
Figure 51. Force-displacement curves for T-12-16-120 specimens
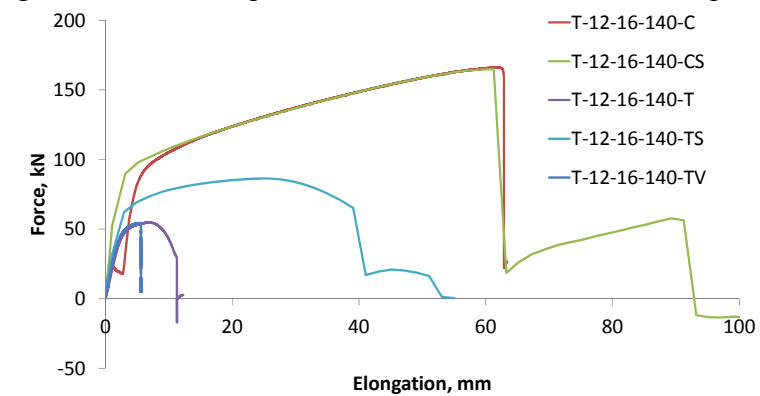
Figure 52. Force-displacement curves for T-12-16-140 specimens
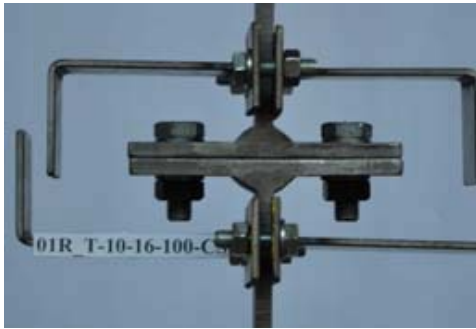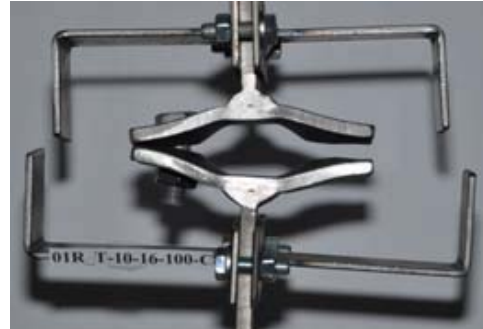
| Initial | cvasistatic, T=20°C |
| $v_1 = 10$ mm/sec. T=20°C | $v_2 = 15$ mm/sec, T=20°C |
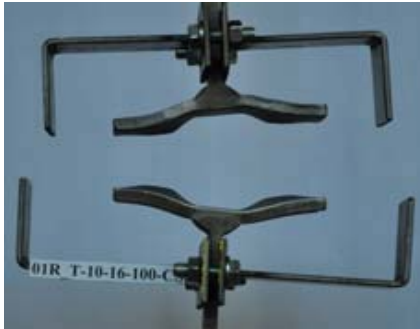
Figure 53. Failure mode for T-10-16-100 specimens
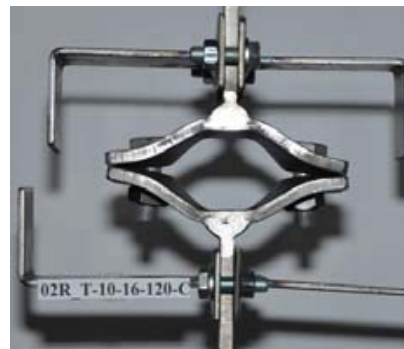
| Initial | cvasistatic |
| $v_1 = 10$ mm/sec | $v_2 = 15$ mm/sec |

Figure 54. Failure mode for T-10-16-120 specimens
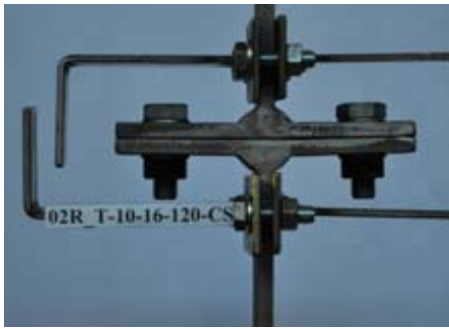
Initial
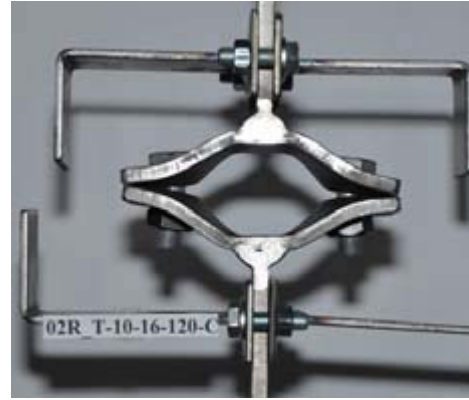
cvasistatic

$v_1 = 10$ mm/sec
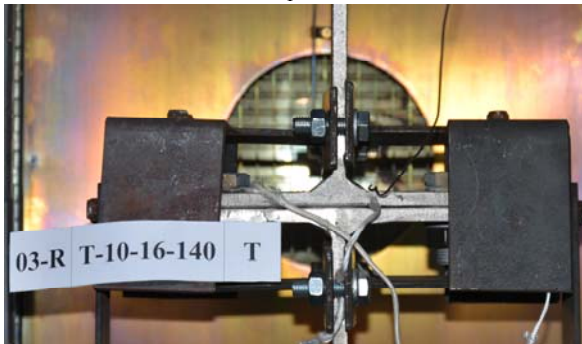
$v_2 = 15$ mm/sec

Initial, T=542°C
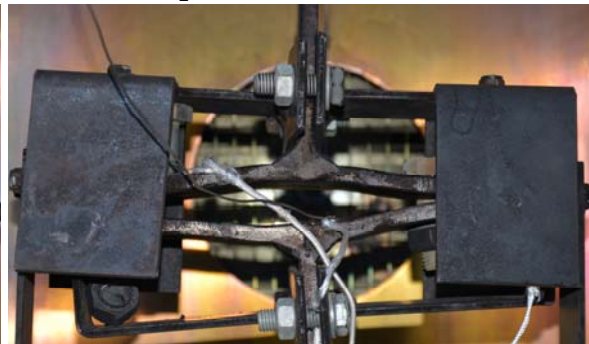
cvasistatic, T=542°C

$v_1 = 10$ mm/sec, T=542°C

$v_2 = 15$ mm/sec, T=542°C

Figure 55. Failure mode for T-10-16-140 specimens

Figure 56. Failure mode 1 (left, T-10-16-140) and failure mode 2 (right, T-10-16-100)

Figure 57. Bolt failure at room temperature tests

Numerical models have been validated based on the results obtained in the experimental program. All the numerical simulations were run in software Abaqus FEA 6.11 as nonlinear dynamic analysis in explicit solver. Figure 58 shows the very good agreement between the failure mode obtained in experimental tests and the numerical simulation. Figure 59 plots comparatively the force-displacement curves obtained in experimental tests and numerical simulations. It may be observed the two curves are closed, with almost the same ultimate deflections before failure that indicates the numerical model may approximate very well the experimental one.
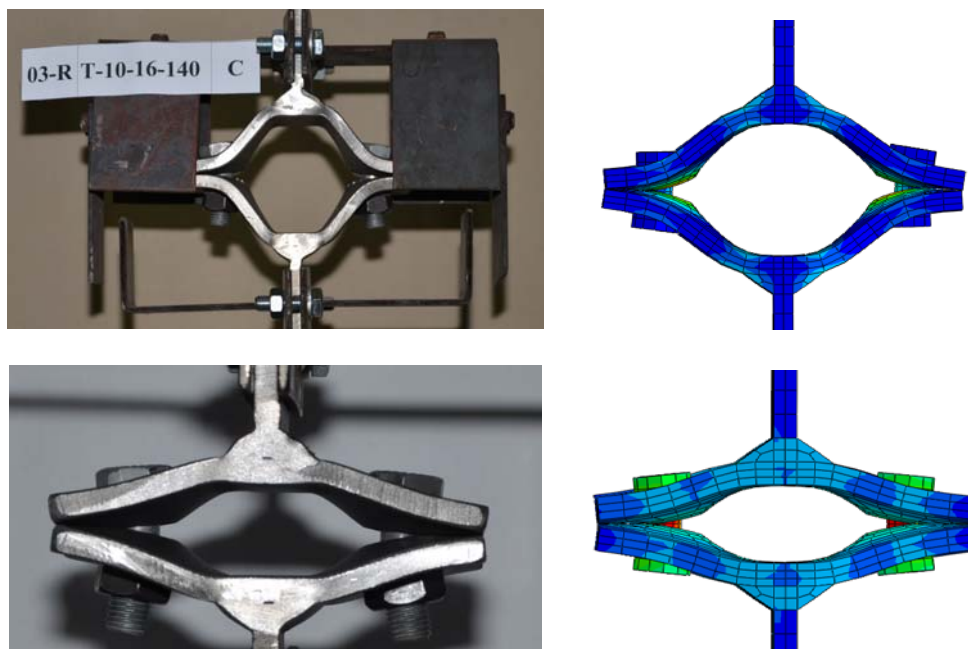
Figure 58. Failure mode: experimental (left) and numerical (right), for mode 1 (top) and mode 2 (bottom)
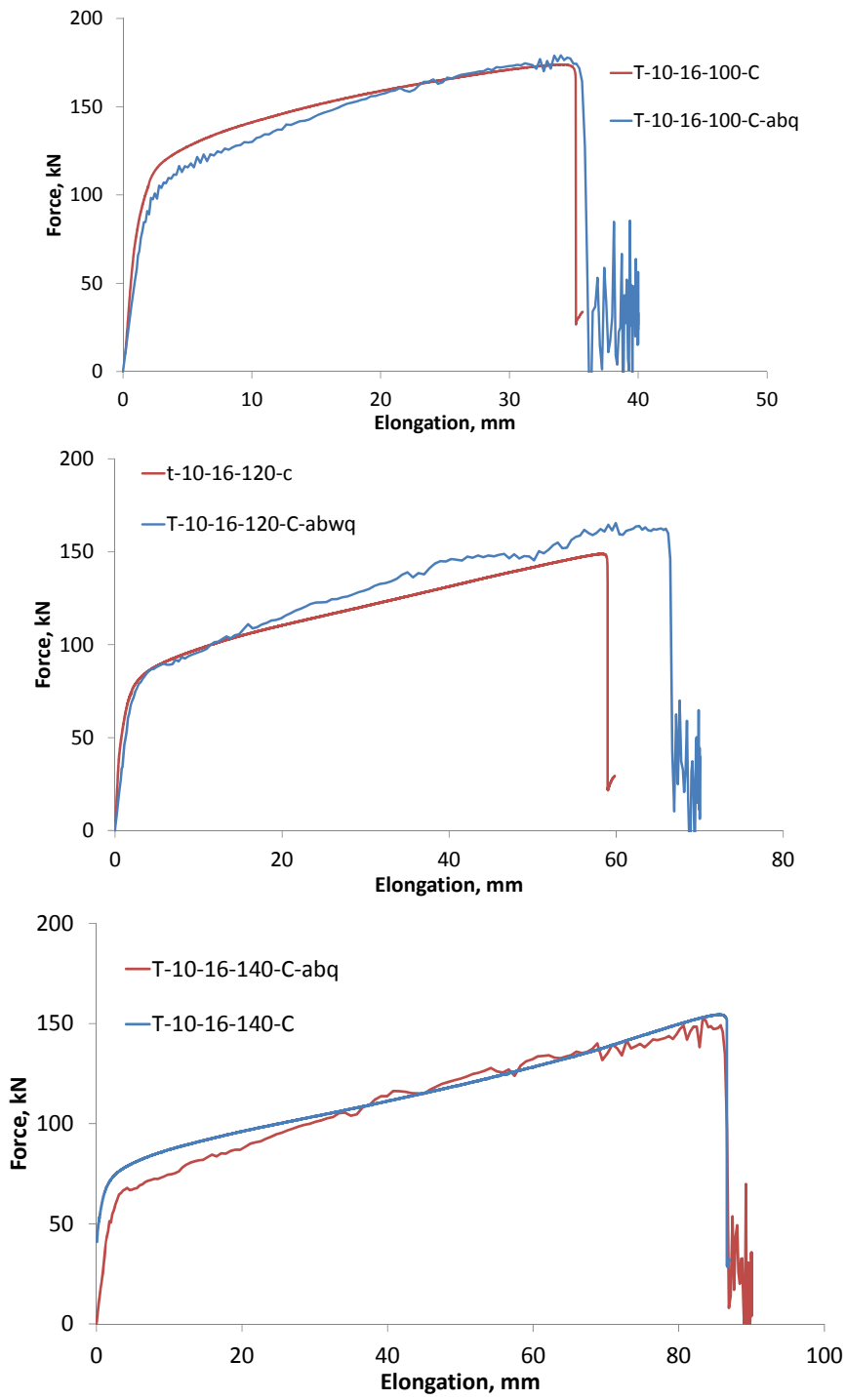
Figure 59. Force displacement curves: numerical vs. experimental

3 IMPROVED STRUCTURAL SYSTEMS FOR INCREASING THE ROBUSTNESS UNDER EXTREME LOADING

National and international experience of the candidate related to the topic
"Improved structural systems for increasing the robustness under extreme loading"
(Post-PhD Thesis period)

Member of technical boards:
- Member of Technical Committee TC13 "Seismic Design" of the European Convention for Constructional Steelwork (ECCS);
- Member of AICPS – Romanian Association of Structural Engineers;
- Member of APCMR – Romanian Association for Constructional Steelwork;
- Member of AGIR – Romanian Association of Engineers.

Conference committees:
- Organization Committee of the International Conference on Thin-Walled Structures: Recent research advances and trends, Timisoara, Romania, 5-7 September 2011;
- Organization Committee of the International Conference in Metal Structures: Steel – A New and Traditional Material for Building, Poiana Braşov, Romania, 20-22.09.2006;
- Chairman of Technical Session: 5th European Conference on Steel and Composite Structures, Eurosteel 2008, 3-5 september 2008, Graz, Austria.
- Chairman of Technical Session: International Symposium "Steel Structures:Culture & Sustainability 2010", 21-23 September 2010, Istanbul, Turkey.

Supporting projects:
- COST C26, Urban habitat constructions under catastrophic events, 2005-2010
- Structural conception and collapse control performance based design of multistory structures under aacidental actions (CODEC), PNII-PT-PCCA, 2012-2016
- Factori de comportare a structurilor metalice in zone seismice pentru implementarea criteriilor de proiectare bazate pe performanta, MEC Grant 33047/2004, cod CNCSIS 219, 2004-2005.
- Criterii de precalificare a îmbinărilor ductile ale cadrelor metalice necontravantuite, MEC – CNCSIS, Grant CNCSIS cod 728, tema nr.2
- Sisteme constructive si tehnologii avansate pentru structuri din oteluri cu performante ridicate destinate clădirilor amplasate în zone cu risc seismic", Acronim „STOPRISC", Proiect de cercetare de excelenta Program CEEX – MATNANTECH, PC-D04-PT23-346, 2005-2007
- Simulari numerice cu MEF si incercari experimentale pe subansamble din structura de rezistenta a unei cladirii de birouri 4S+P+17+E, contract 76/2011, 2011, DMA.
- Requirements for multi-storey buildings in seismic areas, RUUKKI/2009, 2009, Rautaruukki Corporation, Finland.

Invited papers and courses:
- Invited lecturer at TUCSA (Turkish Association for Constructional Steelwork), 02.03.2009 (Lecture: Multi storey steel frame buildings in seismic areas. Authors: Dan Dubina, Florea Dinu).
- Invited course Cost C25/C26: Sustainability in Structures and Structural Interventions. Improving the contemporary and historical urban habitat constructions within a

sustainability and risk assessment framework, Early stage researchers training school, 17-24 May 2009, Thessaloniki, Greece.

Reviewer in ISI journals:

Journal of Structural Engineering – ASCE (http://ascelibrary.org/sto/)

Books:

Vulnerability and damageability of constructions under impact and explosion", COST Action Final Report – Urban Habitat Constructions under Catastrophic Events, CRC Press, A Balkema Book, ISBN 978-0-415-60686-8, 2010.

Member in PhD Juries related to the topic

Member in the PhD Jury of Adrian Grigore MARCHIŞ Andrei Crişan: "Progressive collapse vulnerability of seismic resistant multi storey concrete frame structures", Technical University of Cluj-Napoca, October 2013.

3.1 Introduction

In case of steel framed buildings located in seismic areas, the selection of an appropriate structural system must satisfy three criteria: strength, stiffness and, in particular, ductility. Moment Frames (MRF) take the benefit of good ductility but they are not efficient for taller buildings, due to large deflection that may lead to large story drifts. On the other hand, Centrically Braced Frames (CBF) have good stiffness and strength, but lower ductility. Eccentrically Braced Frames (EBF) combine the strength and stiffness of a centrically brace system with the ductility of a moment frame. For these systems, there are large expertise and code provisions that generally refer to all design aspects (EN1998-1, AISC 2005). In the recent years, have been developed new structural systems, e.g. Buckling-Restrained Braced Frames (BRBF) or Steel Plate Shear Walls (SPSW). The main advantages of slender SPSW consist of economy in steel weight due to thinner walls, fast construction time and easier retrofit. Furthermore, with appropriate design and detailing, SPSW systems may be classified as ductile systems. BRBFs also show a good ductility and stable cyclic behavior, and are highly recomended for retrofitting existing buildings.

A major role in the recent developments of the later systems may be attributed to the introduction of these new systems in the code Provisions (AISC, 2005). Unfortunately, in Europe there are not significant applications, partly due to the lack of design provisions form the design codes, including EN1998-1. One major problem in such cases is the definition of reduction factor q and the overstrength factor Ω. In case of frames of inverted V braces (CBF), in EN1998 q factor is taken equal to 2.5, while for dual frames (MRF + CBF) q can be up to 4.8. However in case of BRB it is expected to obtain a better behaviour, comparable to Moment Resisting Frames (MRF). On the other hand, if Carbon Mild Steel (S235, S275) is used in the dissipative members, which are the BRB in CBF, and the beams in MRF, while High Strength Steel (S460) is used in "non-dissipative members, beams in CBF and columns, a global plastic mechanism failure can be obtained. For design purpose, according to EN1998-1, a crucial problem is to use a correct value of Ω factor, which in case of these specific structures is still a matter of research. The same MRF stiffened with dissipative steel shear walls (SW) are analyzed as an alternative to CBF systems.

The activity developed in the last 10 years has focused on the following topics:
1) Dual steel structural systems
2) Dual steel frame connections

3) Systems with removable dissipative members and improved recentring capacity: dual frames with removable steel panels, dual frames with removable buckling restrained braces, frames with coupling beams

These topics are related to seismic design and may be seen as an attempt to develop new systems or adapt the existing ones, such that the seismic behavior is improved while reducing the cost, the technical difficulties in application or the time of intervention in the aftermath of an earthquake.

Several papers related to this topic have been published during the last 10 years. A selection of these papers is presented below:

1. Dubina Dan, Stratan Aurel, Dinu Florea, Dual high-strength steel eccentrically braced frames with removable links, Earthquake Engineering and Structural Dynamics, 2008, vol. 37, no. 15.
2. Dubina Dan, Dinu Florea Experimental evaluation of dual frame structures with thin-walled steel panels, Thin walled structures, 2014.
3. Dubina D., Dinu Florea, Neagu Calin, Global performance of steel frames of shear walls, 7th International Conference on Behaviour of Steel Structures in Seismic Areas (STESSA), Santiago, CHILE, 2012, 9-11.01, ISBN: 978-0-415-62105.
4. Dinu Florea, Bordea S., Dubina D., Strengthening of non-seismic reinforced concrete frames of buckling restrained steel braces ,7th International Conference on Behaviour of Steel Structures in Seismic Areas (STESSA), Santiago, CHILE, 2012, 9-11.01, ISBN: 978-0-415-62105-2.
5. Dinu Florea, Neagu C, Dubina D, A comparative analysis of performances of high strength steel dual frames of buckling restrained braces vs. dissipative shear walls, 6th International Conference on Behaviour of Steel Structures in Seismic Areas, Philadelphia, PA, 2009, 16-20.08, ISBN978-0-415-56326-0.
6. Dubina D., Stratan A., Dinu Florea, Re-centring capacity of dual-steel frames Steel Construction, Steel Construction, willey ,2011, ISSN 1867-0520
7. Dinu Florea, D. Dubina, C. Neagu, I. Both, C. Vulcu, S. Herban, Experimental and numerical evaluation of a rbs coupling beam for moment steel frames in seismic areas, Steel Construction, Willey, 2012, ISSN 1867-0520.
8. Dubina D., Stratan A., Dinu Florea, High Strength Steel EB frames with low strength bolted links, 5th International Conference on Advances in Steel Structures, ICASS 2007, Scopus, 2007, 978-981059371-1.

3.2 Dual steel structural systems

3.2.1 *Frames design*

The buildings considered in the investigation have eight and sixteen story, respectively. The four lateral load resisting systems are: Eccentrically Braced Frames (EBF), Centrically V Braced Frames (CBF), Buckling Restrained Braced Frames (BRB) and Shear Walls (SW). They are made by European H-shaped profiles. EBF, CBF and BRB systems have three bays of 6m. SW system has exterior moment frames bays of 5.0m, interior moment frame bay of 3.0m and shear wall bays of 2.5m. All structures have equal storey heights of 3.5m. Each building structure use different combinations of mild carbon steel S235 and high strength steel S460. The design was carried out according to EN1993-1 (EN1993-1, 2003), EN1998-1 and P100-1/2006 (Romanian seismic design code, aligned to EN1998-1) (P100-1/2004, 2006). A 4 kN/m2 dead load on the typical floor and 3.5kN/m2 for the roof were considered, while the live load amounts 2.0kN/m2.

The buildings are located in a high seismic area (i.e. the Romanian capital, Bucharest), which is characterized by a design peak ground acceleration for a returning period of 100 years equal to 0.24g and soft soil conditions, with Tc=1.6sec. It is noteworthy the long corner period of the soil, which in this case may affect flexible structures. For serviceability check, the returning period is 30 years (peak ground acceleration equal to 0.12g), while for collapse prevention it is 475 years (peak ground acceleration equal to 0.36g) (P100-1, 2006). Interstorey drift limitation of 0.008 of the storey height was considered for the serviceability verifications.

According to EN1998-1, the maximum value of the reduction factor q for dual frame systems of moment frames and eccentrically braced frames (MRF+EBF) is equal to 6. For dual frame systems made from moment frames and centrically braced frames (MRF+CBF), q factor amounts 4.8. For dual frame systems of moment frames and buckling restrained braces (MRF+BRB) and moment frames and shear walls (MRF+SW), EN1998-1 does not provide any recommendations regarding the q factor. For these structural systems, AISC 2005 provisions were taken as guidance. According to the later code, the reduction factor for MRF+BRB systems and MRF+SW is similar to that of special moment frames. Concluding, the design was based on a q factor equal to 6, excepting the MRF+CBF, which was designed for q equal to 4.8.

For designing the non-dissipative members, EN1998-1 and P100-1/2006 amplifies the design seismic action by a multiplicative factor 1.1 $\gamma_{ov}\Omega$, where γ_{ov} is equal to 1.25. Unlike EN1998-1, which considers Ω as the minimum value of Ωi among all dissipative members, Romanian code P100-1/2006 suggests the use of maximum value. A similar approach is also employed in AISC 2005, where the multiplicative factor $1.1\gamma_{ov}\Omega$ is replaced by a unique factor $\Omega 0$, called the overstrength factor. AISC 2005 and P100-1/2006 also contain values of multiplicative factors to be used in design, which ranges between 2.0 and 2.5. Table 1 presents the multiplicative factors for each structural system obtained by calculation. factors ranges between 1.90 and 2.90 for eight story structures and between 1.70 and 2.90 for sixteen story structures.

For the eight-story building, two exterior bays of braces or shear walls on each exterior frames were necessary. For sixteen story building, the larger demand in lateral resisting capacity leads to braces or shear walls in all for bays. Figure 1 shows the eight and sixteen story frame systems.

The four structural systems were designed for similar base shear force capacities, with the exception of EBF, which were designed for lower capacities. The first mode periods for eight and sixteen story structures are presented in Figure 60. It may be seen the four structural systems amount almost identical the first-mode periods.

Table 16. First mode periods and multiplicative factors for the structures

| Structure	EBF8	CBF8	BRB8	SW8
$1.1\gamma_{ov}\ \Omega$	2.2	2.2	1.9	2.9
Period, [sec]	0.92	0.97	0.97	1.00
Structure	EBF16	CBF16	BRB16	SW16
$1.1\gamma_{ov}\ \Omega$	2.9	1.7	2.1	2.5
Period, [sec]	1.79	1.53	1.61	1.61
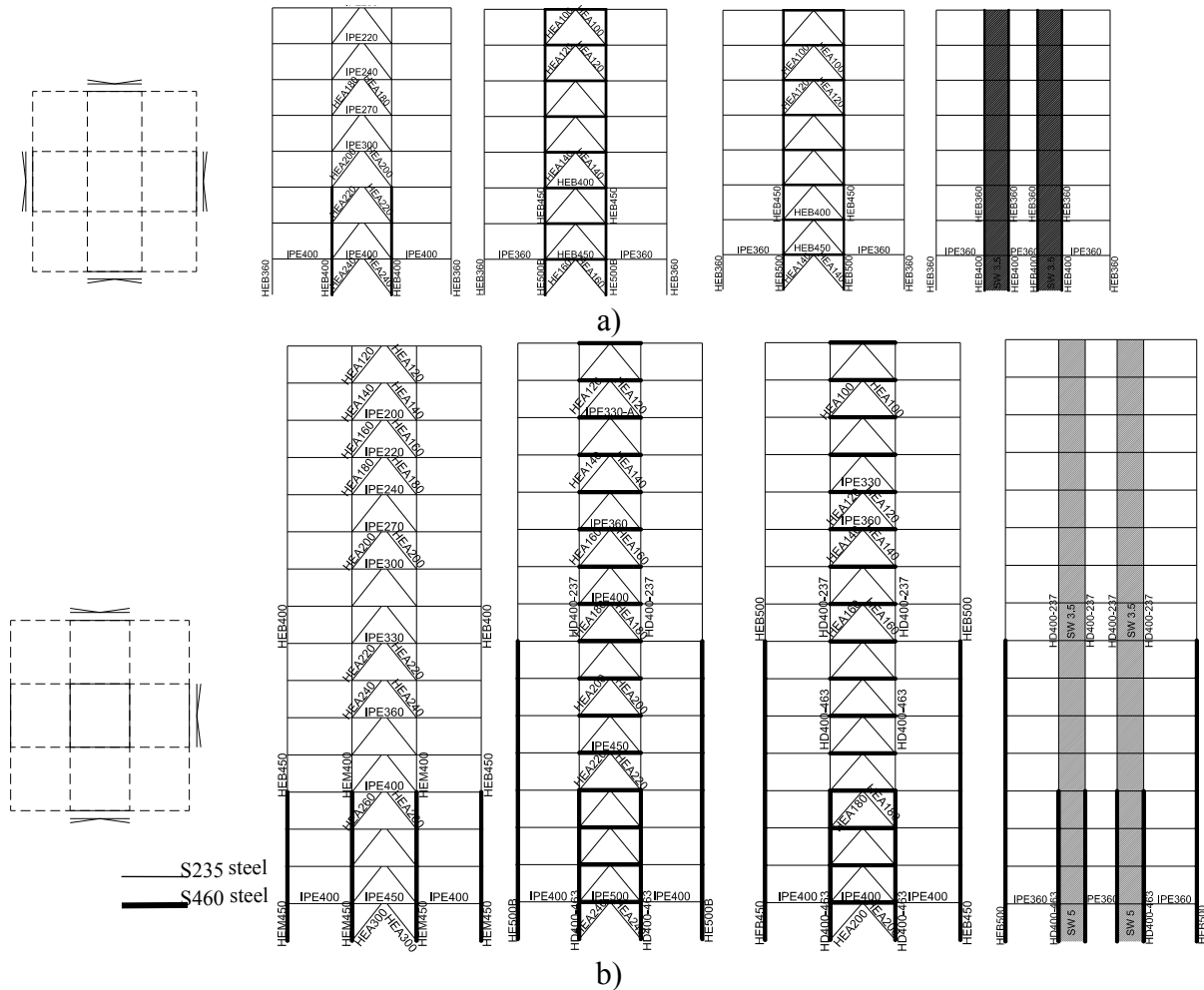
Figure 60. Frame systems: (a) plan view and elevation of EBF8, CBF8, BRB8 and SW8 structures; (b) plan view and elevation of EBF16, CBF16, BRB16 and SW16 structures

3.2.2 Frames modelling

Beams and columns were modelled with plastic hinges located at both ends. In order to take into account the buckling of the diagonals in compression, the post buckling resistance of the brace in compression was set $0.2N_{b,Rd}$ (Figure 61.a), where Af_y is the tensile yield resistance and $N_{b,Rd}$ is the buckling resistance for compression (FEMA 356, 2000). For the braces of the BRB systems, similar behaviour in tension and compression was adopted, as the buckling in compression is prevented (Figure 61.b).
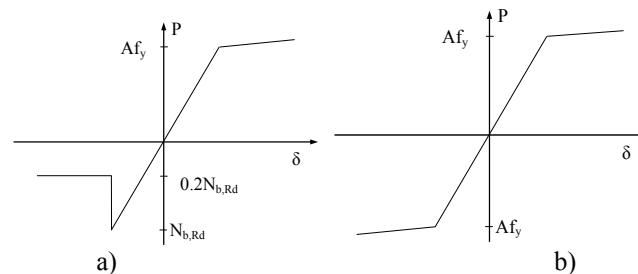
Figure 61. Response of bracing members: a) conventional brace; b) buckling restrained brace

The inelastic shear link element model used for the EBF systems was based on the proposal of Ricles and Popov (1994). As the original model consisted in four linear branches, it was adapted to the trilinear envelope curve available in SAP2000 (2005). A rigid plastic behaviour was adopted till the attainment of the shear plastic capacity.

71
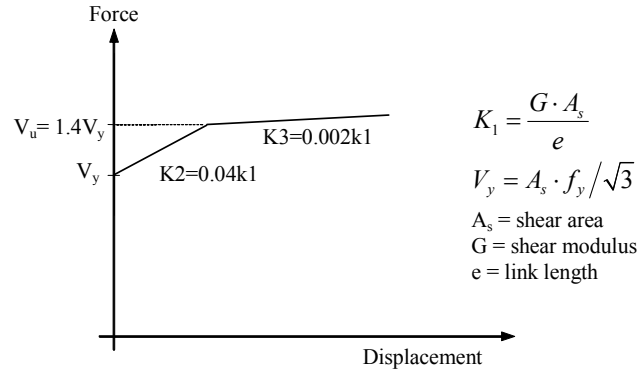
Figure 62. Force – displacement relationships for shear link element

For shear wall structures (SW), non-compact shear walls, with the slenderness ratio h/tw larger than λ_p but smaller than λ_r were selected (Figure 63) (AISC 1999), where k_v is given by:

$$kv = 5 + \frac{5}{(a/h)^2}$$ (1)

$$= 5 \ when \ a/h > 3.0 \ or \ a/h > \left[260/(h/t_w) \right]^2$$

where:
a=distance between tension fields
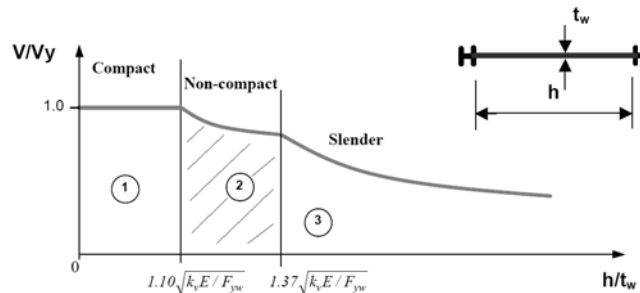
Figure 63. The regions of behaviour of the steel shear walls

The walls framed within this category are expected to buckle, while some shear yielding has already taken place. In this case, the story shear is resisted by the horizontal components of the tension and compression diagonal forces. In order to model the steel shear walls, Thorburn et al. (1983), replaced the steel plates by a series of truss members (strips), parallel to tension fields (Figure 64). In this model, the infill steel plate is modelled as a series of tension–only strips oriented at the same angle of inclination, α, as the tension field. Studies have shown that ten strips per panel adequately represent the tension field action developed in the plate. Driver *et al.* (1997) noted that there were certain phenomena present in steel plate shear wall behaviour that are not captured by the strip model. In their study, a compression strut oriented in the opposite diagonal direction to that of the tension strips was introduced. Moreover, a discrete axial hinge that includes the effects of deterioration was provided only for the two tension strips that intersect the frame closest to the opposite corners of the steel plate shear wall panel, as shown in Figure 64. The equation for the area of the compression strut is as follows:

$$A = \frac{tL \sin^2 2\alpha}{2 \sin \phi \sin 2\phi}$$ (1)

72

where

-ϕ is the acute angle of the brace with respect to the column;

- L is the centre-to-centre distance of columns;

-α is the angle of inclination of the average principle tensile stresses in the infill plate with respect to the boundary column;

- t is the infill plate thickness.

The equation for ϕ is as follows:

$$\tan\phi = \sqrt[4]{\frac{1+tL/2A_c}{1+th\left(1/A_b + h^3/360I_cL\right)}} \tag{2}$$
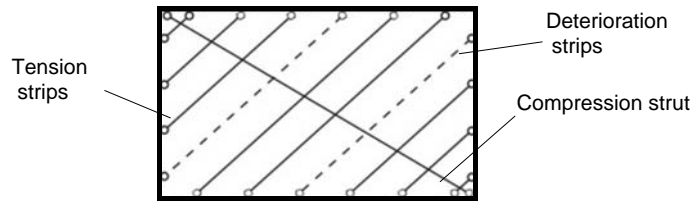

Figure 64. Strip model

a)

b)

c)
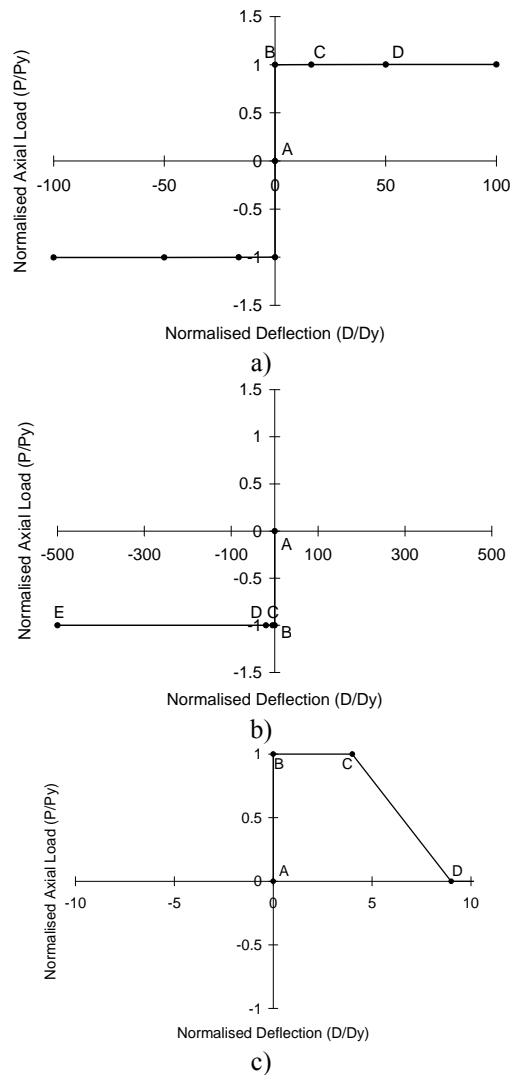
Figure 65. Axial hinge definitions: a) tension strip (infill plate); b) compression strut; c) deterioration hinge

The width and spacing of the pin-ended tension and deterioration strips for each panel, based on ten strips per panel, were calculated to determine the area of each strip. The area calculated for the compression strut is equally distributed among the tension strips. Figure 6 presents the typical behaviour for axial tension strip hinge, compression strut hinge and deterioration strip hinge.

3.2.3 Analysis procedure and results

The nonlinear response of the structures was analysed using the N2 method (Fajfar, 2000). This method combines the push-over analysis of a multi-degree of freedom model (MDOF) with the response spectrum analysis of a single degree of freedom system (SDOF). The elastic acceleration response spectrum was determined according to new Romanian seismic code P100-1/2006, for a peak ground acceleration of 0.24g. The lateral force, used in the push-over analysis, has a "uniform" pattern and is proportional to mass, regardless of elevation (uniform response acceleration). The non-linear analysis was performed with SAP2000 computer program. Table 17 gives the values of target displacement, D_t, for the studied frames, calculated using N2 method.

Table 17. Target displacement, D_t, for the MDOF systems for ULS

Structure	EBF8	CBF8	BRB8	SW8
D_t, m	0.34	0.29	0.31	0.32
Structure	EBF16	CBF16	BRB16	SW16
D_t, m	0.64	0.49	0.53	0.62

Three performance levels were considered: serviceability limit state (SLS), ultimate limit state (ULS) and collapse prevention (CPLS) limit state. Intensity of earthquake action at the ULS is equal to the design one (intensity factor $\lambda = 1.0$). Ground motion intensity at the SLS is reduced to $\lambda = 0.5$ (similar to $\nu = 0.5$ in EN 1998-1), while for the CPLS limit state was increased to $\lambda = 1.5$ (FEMA 356, 2000). Based on FEMA 356, the following acceptance criteria were considered in the study:
- link deformations at SLS, ULS and CPLS are γ_u=0.005rad, γ_u=0.11rad and γ_u=0.14rad.
- for conventional braces in compression (except EBF braces), plastic deformations at SLS, ULS and CPLS are $0.25\Delta_c$, $5\Delta_c$ and $7\Delta_c$, where Δ_c is the axial deformation at expected buckling load.
- for conventional braces in tension (except EBF braces), plastic deformations at SLS, ULS and CPLS are $0.25\Delta_t$, $7\Delta_t$ and $9\Delta_t$, where Δ_t is the axial deformation at expected tensile yielding load.
- for beams in flexure, the plastic rotation at ULS and CPLS are $6\theta_y$ and $8\theta_y$, where θ_y is the yield rotation
- for columns in flexure, the plastic rotation at ULS and CPLS are $5\theta_y$ and $6.5\theta_y$, where θ_y is the yield rotation

The performance is assessed by comparing the capacity of the structure, obtained from the push-over analysis, with the seismic demand expressed by the target displacement. Pushover curves for the EBF, CBF, BRB and SW structures are shown in Figure 66. The occurrence of plastic hinges up to the target point is shown in Figure 67. Table 18 presents the interstory drift demands for SLS and Table 19 presents the plastic deformations demand in members for the SLS, ULS and CPLS.
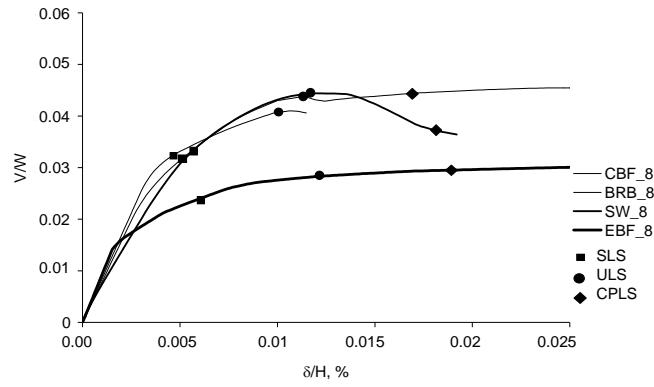
a)
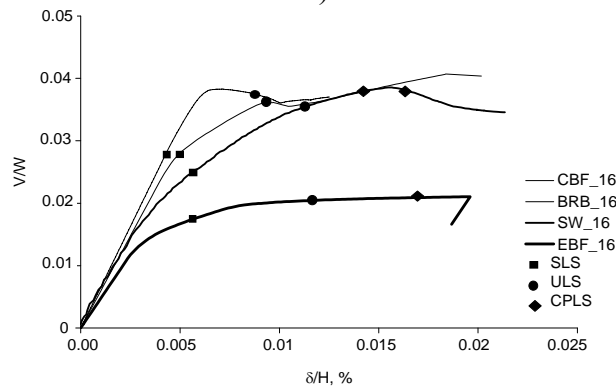
b)

Figure 66. Pushover curves (normalized base shear vs. normalzed top displacement) for: a) eight story buildings; b) sixteen story buildings
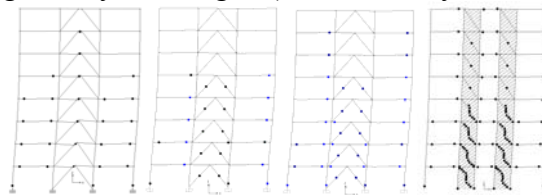
a)
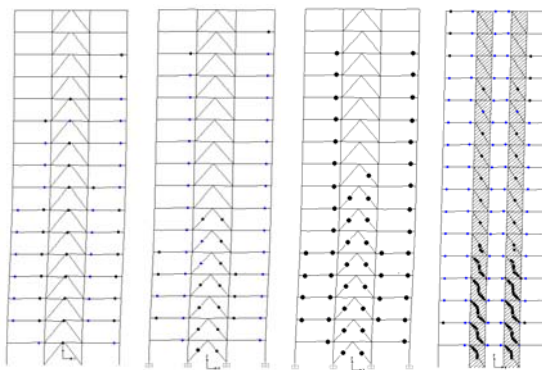
b)

Figure 67. Plastic hinges at ULS: a) EBF8, CBF8, BRB8 and SW8 structures; b) EBF16, CBF16, BRB16 and SW16 structures

In comparison with the centrically braced structures (using conventional braces CBF and buckling restrained braces BRB), the ones using eccentrically braces (EBF) and shear walls (SW) are characterized by lower stiffness. Base shear force capacity is very similar for CBF, BRB and SW structures, implying similar design strength under seismic action. Lower base shear force capacities are recorded for EBF structures. Displacements demands for SLS

75

are lower than the interstorey drift limitation of $0.008H_s$ used in design. Structures designed using the dissipative approach, may experience structural damage even under moderate (SLS) earthquake. This is clearly seen in Table 19, where plastic deformation demands in members are presented. Plastic deformations in dissipative members indicate a moderate damage to the structure at SLS.

Table 18. Interstory drift demands for SLS

Structure	EBF8	CBF8	BRB8	SW8
δ/H_s, %	0.8	0.7	0.8	0.7
Structure	EBF16	CBF16	BRB16	SW16
δ/H_s, %	0.8	0.5	0.6	0.7

All structures satisfy the criteria for ULS. Plastic deformation demands in beams are more severe for EBF and SW compared to CBF and BRB, and plastic mechanisms develop almost on entire height of the structures. Shear wall frames show a very good ductility, comparable to eccentrically braced ones, but also providing a higher stiffness. For sixteen story buildings, no plastic hinges are recorded in the columns, while for eight story buildings plastic hinges are recorded at the bottom part of the first story columns. This shows that in case of higher buildings, when the contribution of the gravity loads (i.e. dead loads, live loads) is lower, the Ω factor is more effective in design of non-dissipative members. Dissipation capacity shown by the structures confirms the reduction factors q used in design. Ductility of EBF, BRB and SW structures is similar to that of MRF, while CBF proved to be less ductile.

Structures perform well till the attainment of the target displacement at CPLS, excepting CBF systems, which fail prematurely, mainly due to the failure of the braces in compression. When conventional braces are replaced by BRBs, the performance is improved and the performance level of collapse prevention is reached. In case of EBF structures, plastic rotation demands in links exceed the rotation capacity. However, experimental tests on such elements have shown that in case of very short links, plastic rotation capacity may reach 0.17-0.20 rad (Stratan et al, 2004). The ductility demands in the buckling restrained braces are plotted in Figure 68. Experimental investigation on such type of members has shown the ductility of braces may exceed 25-30, depending on the material properties (Bordea et al, 2009).
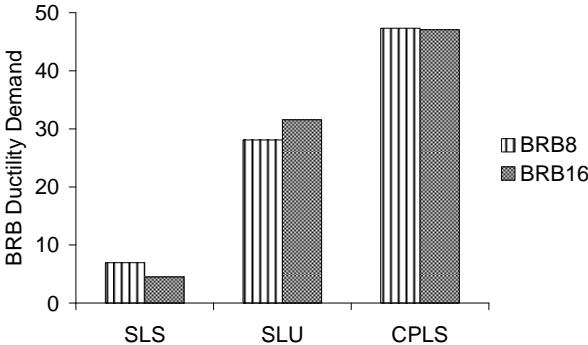

Figure 68. Ductility Demand Ratios for the buckling restrained braces

Table 19. Plastic deformation demands in members at SLS (λ= 0.5), ULS (λ = 1.0) and CPLS (λ = 1.5)

	Beams				Columns				Links	Braces	
	EBF8	CBF8	BRB8	SW8	EBF8	CBF8	BRB8	SW8	EBF8	CBF8	BRB8
SLS	0.004	0.0013	0.0012	0.005	-	-	-	-	0.04	0.0012	0.0036
ULS	0.018	0.016	0.016	0.016	0.006	0.002	0.002	0.004	0.10	0.043	0.0034
CPLS	0.027	PF*	0.035	0.038	0.01	PF*	0.03	0.033	0.15	PF*	0.094
	EBF15	CBF15	BRB15	SW15	EBF15	CBF15	BRB15	SW15	EBF15	CBF15	BRB15
SLS	0.007	0.0004	0.007	0.007	-	-	-	-	0.037	-	0.0038
ULS	0.021	0.013	0.015	0.017	-	-	-	-	0.11	0.044	0.028
CPLS	0.033	PF*	0.028	0.027	-	PF*	-	-	0.165	PF*	0.067

3.2.4 References

AISC 1999. Load and Resistance Factor Design Specification, American Institute of Steel Construction Inc., Chicago.

AISC 341-05, 2005. Seismic provisions for structural steel buildings. American Institute for Steel Construction, 2005.

Bordea, S., Stratan, A., Dubina, D. 2009. Performance based evaluation of a RC frame strengthened with BRB steel braces. *PROHITECH `09 International Conference, 21-24 June, 2009, Rome, Italy.*

Driver, R. G., Kulak, G. L., Kennedy, D. J. L. and Elwi, A. E. 1997. Seismic behavior of steel plate shear walls. *Structural Engineering Rep. No. 215,* Dept. of Civil Engineering, Univ. of Alberta, Edmonton, Alberta, Canada.

EN1993-1-1 Eurocode 3 Design of Steel Structures. Part 1-1: General rules and rules for buildings, CEN, Brussels, 2003.

EN 1998-1, 2004. Design provisions for earthquake resistance of structures - 1-1: General rules - Seismic actions and general requirements for structures, CEN, EN1998-1-1.

Fajfar, P. 2000. A nonlinear analysis method for performance based seismic design. *Earthquake Spectra, vol.16, no. 3, pp. 573-592, August 2000.*

FEMA 356, 2000. Prestandard and commentary for the seismic rehabilitation of buildings. *Federal Emergency Management Agency and American Society of Civil Engineers, Washington DC, USA.*

P100-1/2004, 2006. Seismic design code – Part 1: Rules for buildings (in Romanian) Indicativ P100-1/2004. *Buletinul Constructiilor, Vol. 5, 2005* (in Romanian).

Ricles J.M. & Popov, E.P. 1994. Inelastic link element for EBF seismic analysis, *ASCE. Journal of Structural Engineering, 1994*, Vol. 120, No. 2: 441-463.

SAP2000, Version 9, 2005. Computers and Structures Inc. University Avenue, Berkeley, California 94704, USA.

Stratan, A., Dubina, D. 2004. Bolted links for eccentrically braced steel frames. *Proc. of the Fifth Int. Workshop "Connections in Steel Structures V. Behaviour, Strength & Design", June 3-5, 2004.* Ed. F.S.K. Bijlaard, A.M. Gresnigt, G.J. van der Vegte. Delft University of Technology, Netherlands.

Thorburn, L. J., Kulak, G. L., and Montgomery, C. J., 1983. Analysis of steel plate shear walls. *Structural Engineering Rep. No. 107,* Dept. of Civil Engineering, Univ. of Alberta, Edmonton, Alberta, Canada.

3.3 Systems with removable dissipative members and improved recentring capacity: dual frames with removable steel panels

3.3.1 *Introduction*

Steel plate shear walls (SPSW) are efficient lateral load resisting systems and can act as an alternative to traditional systems. Depending on their slenderness, SPSW may yield under applied shear before they buckle or may buckle while almost elastic. Depending on the construction and design, the plate walls may be stiffened or unstiffened. Prior to 1980s, SPSW design was based on the concept of preventing the out of plane buckling of the infill panel by the use of heavily stiffened steel plates [1]. Such systems presented a good seismic behavior thanks to their dissipation capacity through the shear mechanism. However, when compared with reinforced concrete shear walls, the system was not very competitive, due to its higher cost. In order to make the SPSW more competitive, further studies focused more on slender systems, which utilize unstiffened thin walled steel panels and resist lateral forces mainly through post-buckling tension field action ([2], [3], [4], [5], [6], [7], [8]). Part of this research resulted in the development of first design guidelines for plate wall structures. Thus, the 2001 edition of the Canadian Steel Design Standard, CAN/CSA S16-01 [9] included design guidelines for SPSW structures, followed by the 2009 edition [10]. In the US, the 2005 edition of the AISC Seismic Provisions [11] incorporated first recommendations for the design of SPSW systems, followed by the 2010 edition [12].

The main advantages of slender SPSW consist of economy in steel weight due to thinner walls, fast construction time and easier retrofit [13]. Furthermore, with appropriate design and detailing, SPSW systems may be classified as ductile systems. Code designed SPSW are also capable of meeting drift limitations when subjected to ground motions that approximate the design shaking [14]. However, there are some concerns regarding the seismic response of slender steel plate shear wall systems because they buckle during the early stages of lateral loading and therefore the response of the system is characterized by a pinched cyclic behavior. The pinching effect decreases the area of the hysteresis loops and, as a result, decreases the energy absorption of SPSW. In order to reduce pinching and increase energy absorption, plate walls may be combined with frames that have rigid moment connections between boundary elements. The resulting frame action provides some stiffness around zero storey drift [8]. Another method is either to use a thicker plate, which is uneconomical, or to use stiffeners [15]. Too much stiffening leads to a loss of structural deformability and therefore, an optimum amount of stiffeners should be used to achieve both sufficient rigidity and deformability.

Two issues have recently raised interest for seismic applications of SPSW. The first issue is related with the potential of improving the seismic behavior by linking two or more plate walls. Thus, typical SPSW systems include either singular SPSW (Figure 69(a)), where the shear wall is the only element resisting storey shear, or dual SPSW systems with parallel moment frames (Figure 69(b)). A coupled shear wall system is a specific dual system, whereby a coupling beam connects two shear wall bays (Figure 69(c)). A particular system, which consists of inserting plate walls inside moment frames, aiming at providing additional lateral rigidity, has been proposed and studied by the authors (Figure 69(d)). The plate wall is bordered by additional vertical elements (stanchions) having simple connections at their ends to the beams. The beam outside the plate wall acts as a short, intermediate or long link, depending on the relative length of the plate walls and bay width. Such systems may be applied for new constructions and also for upgrading the lateral resistance of existing constructions. For large bays, the shear wall inside the moment frame (Figure 69(b)) results in a large length to height ratio (L/h) that can make the shear panel to be excessively flexible. Therefore, the system with plate walls and link beam (Figure 69(d)) may be used instead. In

comparison with the systems based on singular shear walls inside gravity frames, the dual systems shown in Figure 69(b-d) have better seismic response, higher dissipation capacity, and smaller residual drifts. Their use may also improve the overturning stiffness and reduce the axial force demand on vertical boundary elements [5]. Despite the potential benefits of such systems, there is limited research available, while current code provisions contain limited guidance for their design [16], [17].
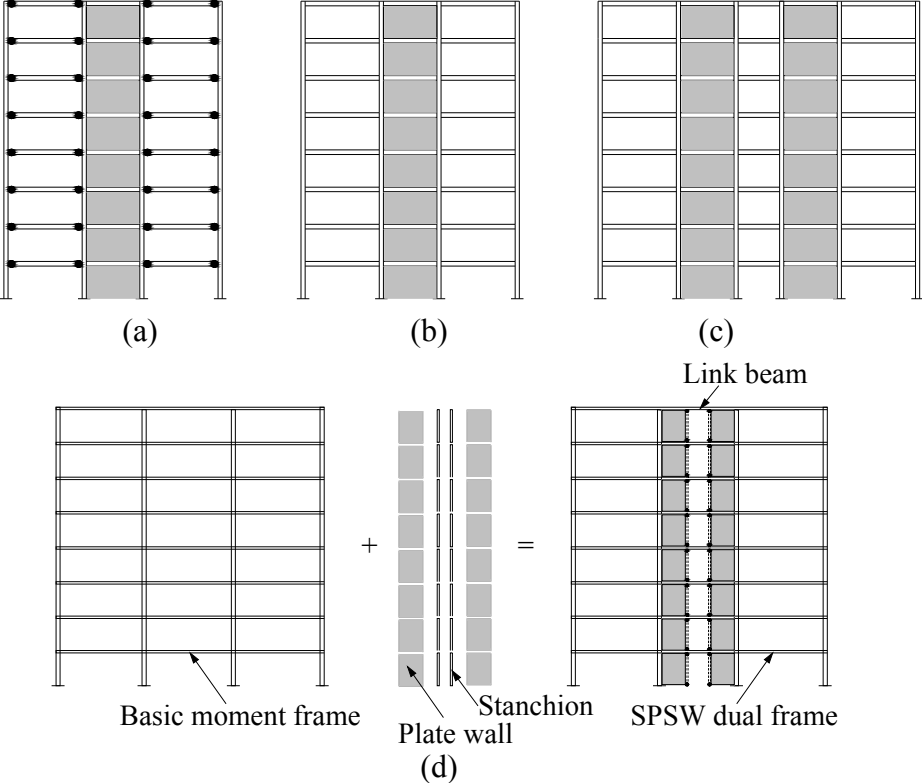

Figure 69: SPSW frame systems: a) singular shear wall inside gravity frame; b) dual system with shear wall and moment frames; c) dual system with shear wall and coupling beams; d) dual system with link beam

The second issue is related with the reduction of residual displacements after an earthquake so as to reduce to cost of intervention. Residual or permanent displacements are considered harmful because they suggest structural damage. Repairing damaged structural elements can be technically tasking if not impossible; nevertheless, the process is expensive. If the damage is localized in easily replaceable members, repairing is easier and costs less. In addition, structure recentering allows for easy replacement of damaged or "sacrificial" members. The particular behaviour of SPSW makes them appropriate for such applications [18]. The results of our previous study [19] also showed that dual structural configurations composed of a rigid subsystem with removable ductile elements and a more flexible subsystem, designed to remain elastic, are appropriate for demonstrating the "removable dissipative element" concept. The use of simple connections between boundary beams and columns reduces the recentering force; thus, rigid moment connections may prove more beneficial. When a shear wall is placed inside a moment frame, the corners of the shear wall plate act as gusset plates above and below the moment connection and impose considerably less rotation demand on rigid connections. This particular behavior suggests that connections with lower stiffness (i.e., semi-rigid connections) can be used instead of rigid ones. Moreover, semi-rigid connections reduce costs and enhance constructability. Frames of the type shown in Figure 69(b-d) may be

designed to prevent plastic deformation in the frame members for low-to-moderate seismic action, and thus to recover their initial position after the damaged panels are replaced.

This study focused on the seismic performance of thin walled SPSW with link beams. Rigid and semi-rigid moment connections between horizontal boundary elements (HBE) and vertical boundary elements (VBE) have been employed. We evaluated the effectiveness of capacity design for vertical and horizontal boundary elements, the influence of HBE–VBE connections on overall system behavior, and the behavior factor. For addressing the abovementioned issues, a research program including experimental testing and numerical analyses was developed within the Steel Structures Laboratory at the Politehnica University, Timisoara [20]. Structures were tested under monotonic and cyclic loadings. This paper presents the results of the experimental program.

3.3.2 *Experimental program*

3.3.2.1 *Design of SPSW structure*

The study building is six stories tall and is in Bucharest (Figure 70(a)). According to the Romanian Seismic Code, P100-2006 [21], the building site is characterized by a design peak ground acceleration of 0.24 g and soft soil conditions, with T_C = 1.6 s. The structure has a dual frame system made of moment frames toward the exterior and SPSW interconnected by link beams toward the interior. The exterior bays are 4.8 m long, the interior bay is 8.4 m long and has two braced spans of 2.8 m long each, and storey height is 3.5 m. For the preliminary design of the structure, the SPSW were approximated by a vertical truss with tension diagonals in line with the AISC Seismic Provisions [11] (Figure 70(b)). The equivalent structure with the vertical trusses was designed according to Eurocodes ([22], [23], [24], [25], [26]). Because the Romanian seismic Code P100-2006 and European seismic code EN1998-1 do not make any recommendations for the behavior factor q of SPSW structures, AISC Provisions [11] were used as a reference. AISC code specifies for special moment frames and dual systems with special moment frames and SPSW the same reduction factor R of 8. Because EN 1998-1 specifies a maximum value of 6.5 for the reduction factor q of moment frames, the same value was selected for the SPSW structure for maintaining consistency with the AISC code.
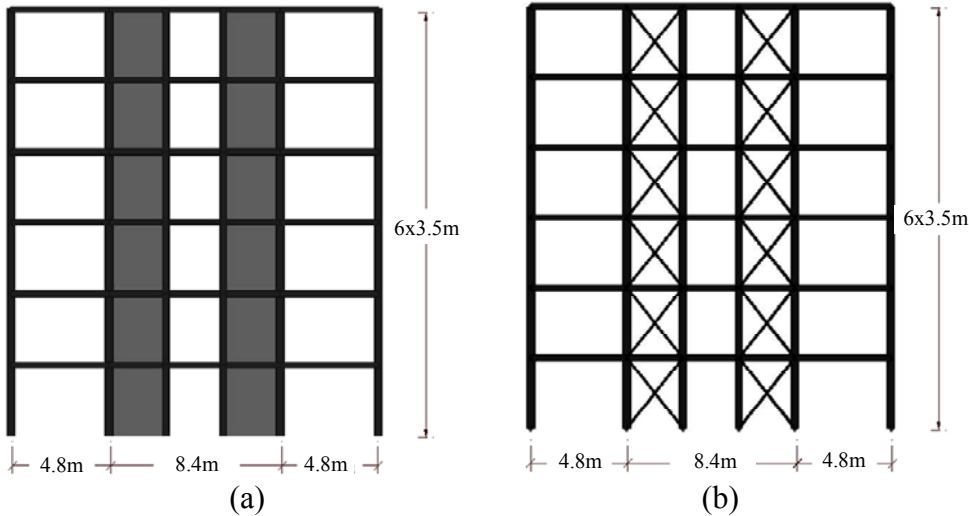
Figure 70: Case study building: a) SPSW structure and b) equivalent structure with tension diagonals

80

The beams and columns were designed using S355 steel, which has a nominal yield strength f_y of 355 N/mm^2. The braces were designed using S235 steel, which has a nominal yield strength f_y of 235 N/mm^2. The cross sections of all elements were made of hot-rolled European H profiles. The floors were considered to have dead and live loads of 4.0 kN/m^2 and 3.0 kN/m^2, respectively. The cross sections of the equivalent braces were adjusted to meet the structure's drift requirements. The required strengths of HBEs and VBEs were checked against the expected yield strength of the braces using AISC provisions.

After the equivalent structure with the vertical trusses was designed and configured, the thicknesses of the infill plates in the original structure were calculated using the area of the tension diagonals that were arrived at in the design process. For an assumed angle of inclination α of the tension field, the wall thickness t_w is given by [11]:

$$t_w = \frac{2A\Omega_s \sin\theta}{L\sin 2\alpha} \tag{1}$$

where
A = area of equivalent tension brace, in mm^2
θ = angle between vertical axis and diagonal tension brace
L = distance between VBE centerlines, in mm
α = assumed angle of inclination of tension field measured from the vertical, taken as 45°
Ω_s = system overstrength factor, taken as 1.2 for SPSW (see [5])

According to capacity design principles, the boundary elements (HBE and VBE) are designed to resist the maximum forces developed under the tension field action of the fully yielded panels. Axial forces, shear forces, and bending moments develop in the SPSW boundary elements because of the overall overturning, shear, and tension field action in the panels. According to AISC Provisions, the VBEs and HBEs should remain essentially elastic under forces generated by fully yielded plates, but flexural hinges are allowed at the ends of HBEs. To prevent excessive deformation, leading to premature buckling under the pulling action of the plates, the minimum moment of inertia of the columns was calculated.

3.3.2.2 Test specimens

Four SPSW specimens were designed and constructed. The specimens were constructed from the second and third stories of the six-storey structure described in the previous section (Figure 71(a)). Owing to actuator limitations, the specimens were built to half scale. This scaling resulted in frame specimens that were 3500-mm-tall and 4200-mm-wide between member centerlines (Figure 71(b)). The infill plate thicknesses were 2 and 3 mm, respectively. The aspect ratio of the steel plates, L/h, was 0.8, whereas the slenderness factor L/t_w was 595 for the 2-mm panels and 397 for the 3-mm panels. It can be noted that the constructional system is composed of a moment resisting frame, two infill panels that are attached to the beams and two additional stanchions that are placed as vertical boundary members. Table 20 lists the thicknesses of the infill plates, size of boundary elements, types of beam-to-column connections, and types of loading. Each specimen was installed in the reaction frame as shown in Figure 72. The reaction frame was braced to reduce the in plane deformations. At the first and second storey levels, guide beams were installed to allow in plane displacements only. A lateral bracing system was used to prevent out of plane deformations of the guide beams.

Two types of bolted end plate HBE–VBE connections were employed for investigating the influence of connection type on the overall behavior of the SPSW frame. The first type is a flush end plate bolted connection (Figure 73(a)), whereas the second is an extended end plate bolted connection (Figure 73(b)). According to the classification under EN1993-1-8 [25], the flush end plate beam-to-column connection is semi-rigid and partial strength ($M_{j,Rd}$ =

0.53$M_{b,Rd}$) (further denoted as *semi-rigid SR*), and the extended end plate connection is rigid and partial strength, but with a capacity almost equal to that of the connected beam ($M_{j,Rd}$ = 0.96$M_{b,Rd}$), (further denoted as *rigid R*) (Figure 74). Figure 73(c) shows the connection between the internal column (stanchion) and the beam. According to the classification under EN1993-1-8, this connection can be classified as a nominally pinned connection.


(a)   (b)
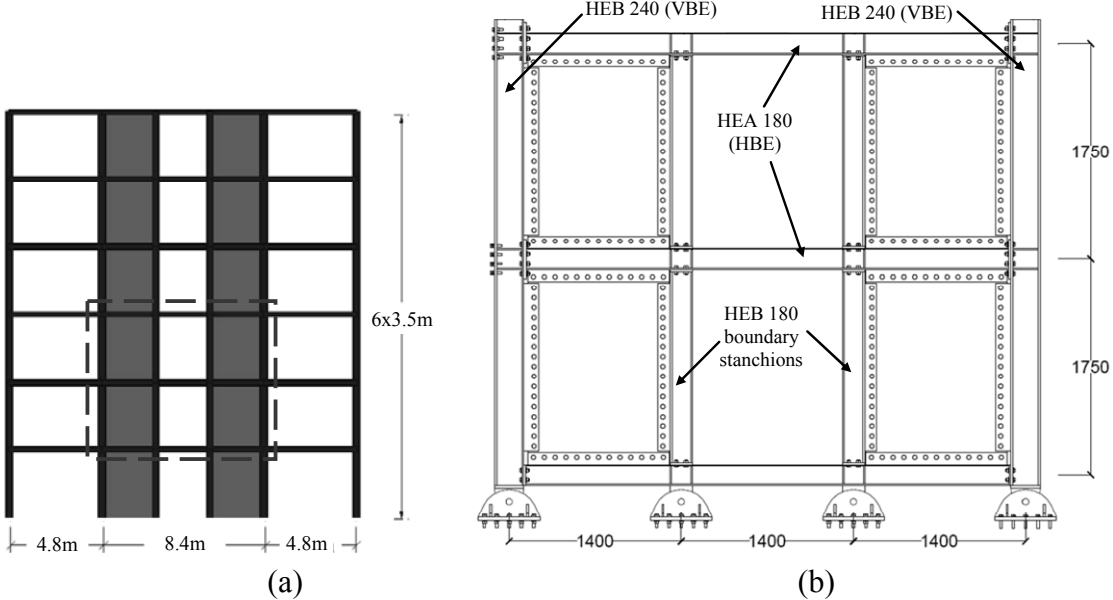
Figure 71: Construction of half-scale specimen: a) six-storey case study structure; b) half-scale specimen
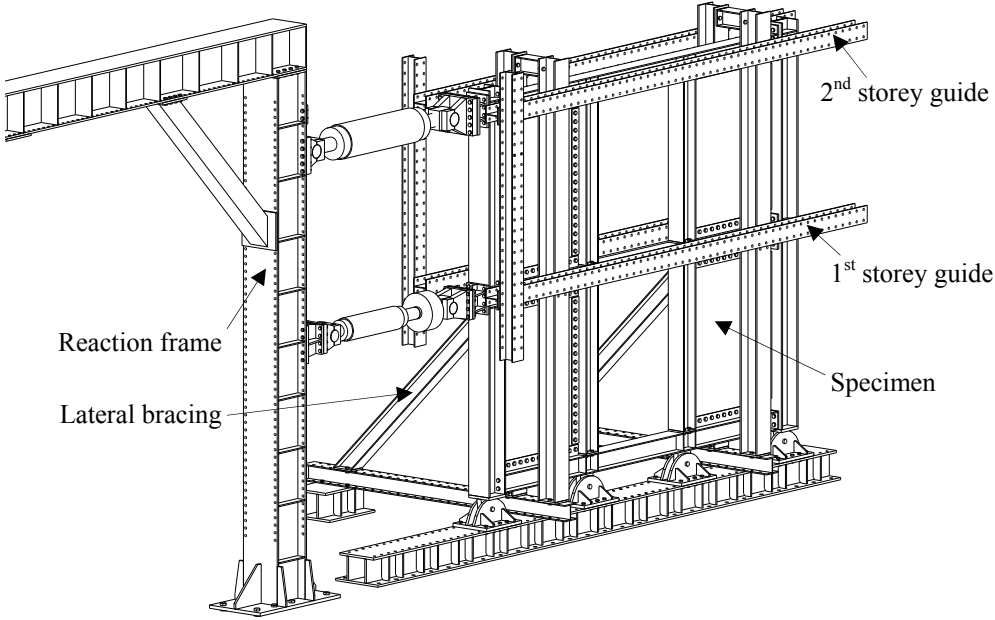
Figure 72: Test setup

Table 20: Specimen characteristics

Specimen	Infill plate[mm]	Columns	Stanchions	Beams	Beam-to-column connection	Loading
R-M-T2	2				Rigid	Monotonic
SR-C-T2	2	HEB240	HEB180	HEA180	Semi-rigid	Cyclic
R-C-T2	2				Rigid	Cyclic
SR-C-T3	3				Semi-rigid	Cyclic

(a)   (b)   (c)
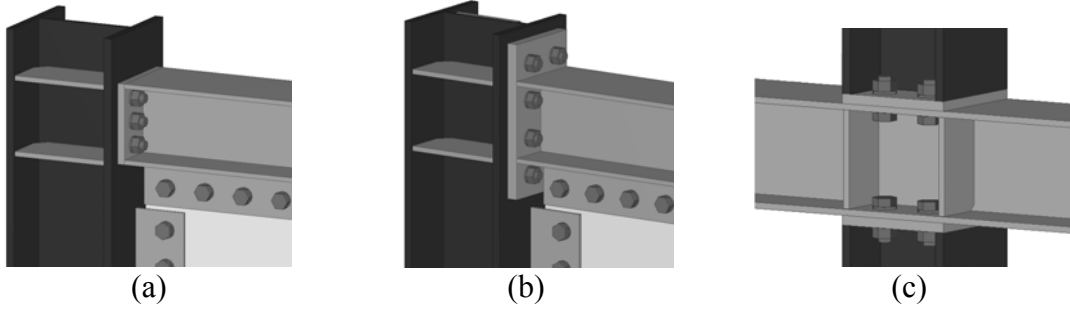
Figure 73: Typical connections: a) semi-rigid beam-to-column; b) rigid beam-to-column; and c) boundary stanchion-to-beam
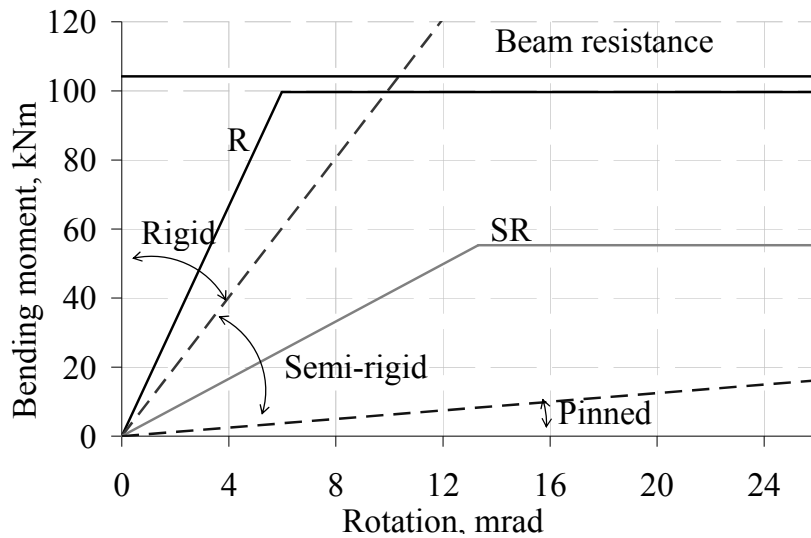
Figure 74: Classification of connections for frame specimens

Panels were bolted to boundary members at all edges using 6-mm-thick and 120-mm-wide fishplates (Figure 75). European practice recommends shop welding and site bolting for joining the steel elements. In case of very thin plates such as those used for the specimens, bolted connections were considered more appropriate than welded ones owing to the difficulties in execution and quality control of welding onsite. Moreover, with bolted connections, removing damaged panels is easier. Welding the plates together can be a solution, but the authors did not consider this as practical as compared to the bolted connection owing to the abovementioned conditions. To increase the bearing capacity of the panel, and, consequently, to reduce the number of bolts, we welded additional plates to the sides of the infill panel to obtain the same thickness as that of the fishplates. Thus, the 2- and 3-mm plates had 4- and 3-mm additional plates, respectively, welded to them by metal active gas welding. Welding current intensity was adapted to prevent the thin plate material from burning.
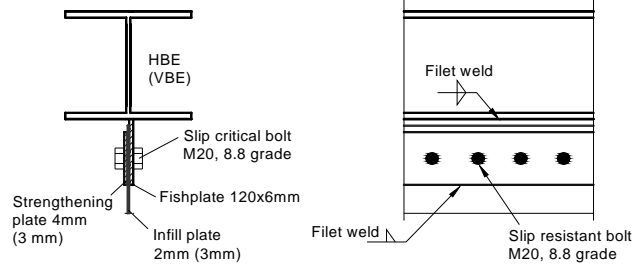
Figure 75: Connection between infill plates and boundary elements

The yield strength and tensile stress of coupons from the infill plates and boundary members are listed in Table 2 and Table 22, respectively. The actual (measured) yield strength of the infill plates was higher than the nominal values by almost 30%. This increase represents the material overstrength, which is accounted for in design by the overstrength factor γ_{ov} according to [26]. Higher material overstrength values can alter the relative strength ratio between dissipative and non-dissipative members, and consequently, the desired plastic mechanism. Therefore, real material characteristics were employed in a pushover analysis on the half-scale specimens to assess their behavior and approximate their load–displacement curves. The analysis was performed using the tension strip model, developed by Thorburn et al. [2] (Figure 76). This model has been adopted by the AISC seismic provisions for SPSW design. Each panel was represented by 10 equally spaced pin-ended strips, inclined at an angle α relative to the vertical boundary element. According to AISC provisions, based on the work of Timler and Kulak [3], the strip inclination α, is given by:

$$\tan^4 \alpha = \frac{1 + \dfrac{t_w L}{2 A_c}}{1 + t_w h \left(\dfrac{1}{A_b} + \dfrac{h^3}{360 I_c L} \right)} \tag{2}$$

where
h = distance between horizontal boundary element centerlines
L = distance between vertical boundary element centerlines
A_b = cross-sectional area of beam
A_c = cross-sectional area of column
I_c = column moment of inertia, perpendicular to the steel plate line
The area of a strip, A_s, can be calculated as follows:

$$A_s = \frac{L \cos \alpha + h \sin \alpha}{n} \tag{3}$$

where n represents the number of strips per panel (10 in this case).

The average angle of inclination α was calculated to be 40°. To simulate strip yielding, an axial hinge was placed at the midpoint of each strip. The boundary beams and columns were modeled using conventional beam-column elements. Main parameters such as yielding displacement, initial stiffness, maximum shear capacity, and ultimate displacement were evaluated.

Table 21: Material properties of rolled profiles

Element	Steel grade (ordered)	Element	Material properties (measured)		Actual steel grade
			f_y [N/mm^2]	f_u [N/mm^2]	
HEB240	S355	Flange	457	609	S460
		Web	458	609	
HEB180	S355	Flange	360	515	S355
		Web	408	540	
HEA180	S355	Flange	419	558	S420
		Web	415	542	

Table 22: Material properties of flat steel (infill plates)

Steel grade (ordered)	Thickness [mm]	Material properties (measured)		Actual steel grade
		f_y [N/mm^2]	f_u [N/mm^2]	
S235	2	305	429	S275
S235	3	313	413	S275
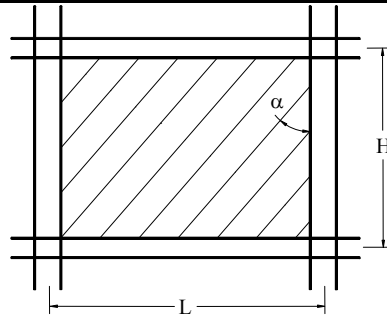
Figure 76: Strip model of steel plate shear wall

The thick line in Figure 77 denotes a plot of the base shear force against top displacement for the half-scale SPSW model with rigid connections (a) and semi-rigid connections (b). Four regions can be readily identified on the force–displacement curve:

0 to 1   elastic region
1 to 2   infill plates yielded, boundary frame elastic
2 to 3   infill plates and frame yielded, strength is increased up to peak load at point 3
3 to 4   infill plates and frame yielded strength degradation until failure.

As seen in Figure 77, it is possible to identify the contributions of individual components (i.e., the infill plates and bare frame) in carrying the lateral forces. The first infill plate yields at an approximately 0.5% storey drift for both cases. The infill plates (dashed thin line) strongly influence the overall capacity of the specimen. Owing to its higher flexibility, the bare frame (thin continuous line) has a much lower contribution to the overall capacity, and yields at approximately 2% storey drift for rigid structure and at approximately 2.4% storey drift for semi-rigid structure.

Due to the scaling process and the difference between nominal and actual characteristics of the steel, the final configuration of the specimens (elements and connections) was based on the results of the pushover analysis.
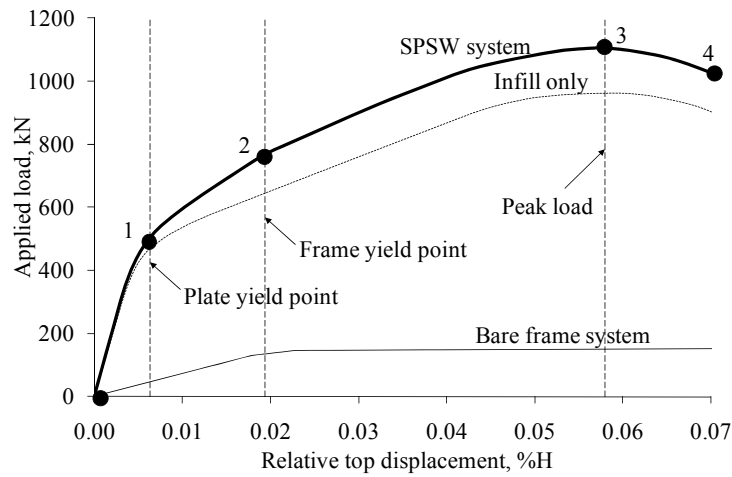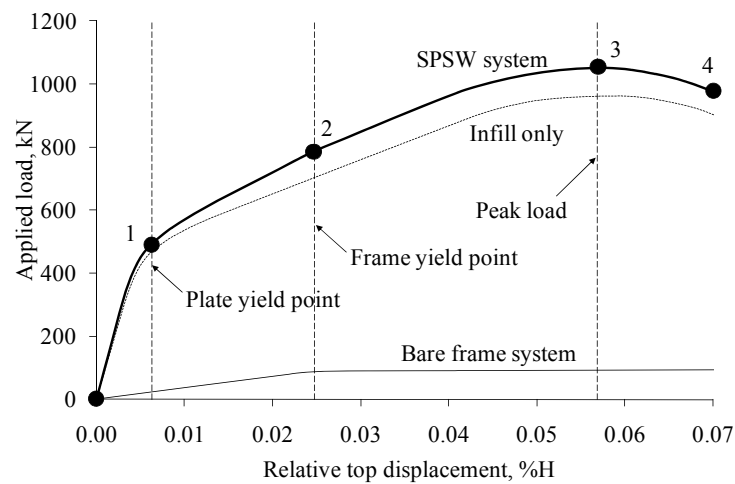
Figure 77: Base shear vs. top displacement from numerical modeling, 2-mm-thick plates:
a) rigid specimen; b) semi-rigid specimen

3.3.2.3 *Loading protocol and instrumentation*

Figure 72 shows the test setup. Two hydraulic actuators were used, one at each storey. Quasi-static cyclic testing was performed in accordance with ECCS Recommendations [27]. A monotonic test was first carried out for obtaining the force vs. displacement curve (Figure 78(a)). Using this curve, we intersected a tangent having 10% of the initial stiffness slope to the maximum force with the initial stiffness line to obtain the yielding displacement D_y. The yielding displacement is then used for establishing cyclic loading, which involves generating four successive cycles for the $\pm 0.25D_y$, $\pm 0.5D_y$, $\pm 0.75D_y$, and $\pm 1.0D_y$ amplitude ranges, followed further to failure by series of three cycles each of amplitude $\pm 2n \times D_y$, where n = 1,2,3… (Figure 78(b)).

The lateral load was applied quasi-statically under displacement control, with triangular distribution. It is important to note that D_y has no standardized or even harmonized definition for SPSW systems. The ECCS procedure for the evaluation of D_y was initially developed for testing beam-to-column joints, and therefore, because the different behavior of SPSW, D_y may be quantified using other methods. In fact, because both shear buckling and bearing work of bolted connections are included in the SPSW response, one can refer to "pseudo-yield displacement".
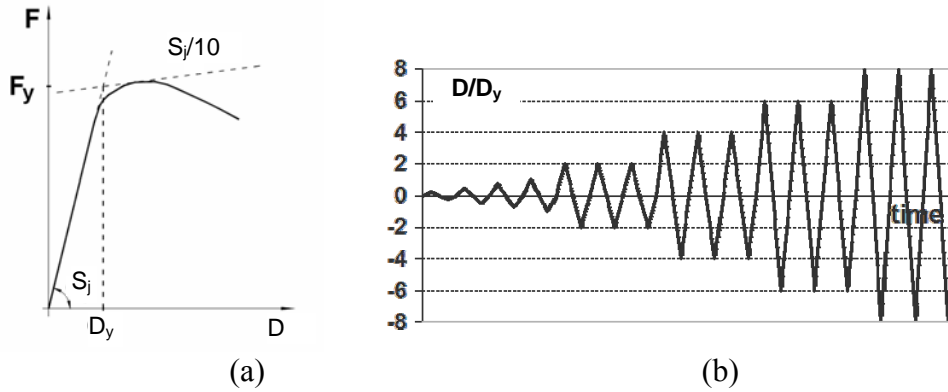
Figure 78: Loading protocol: a) determination of yielding displacement D_y; b) cyclic loading protocol [27]

The lateral loads and displacements of the system were monitored and recorded during the test. The specimens were equipped with linear and rotational displacement measuring devices. Storey displacements, including base slippage, uplift at the two main columns, beam-to-column slippage, and infill panel diagonals were monitored using linear displacement sensors. In addition, out-of plane displacements were recorded. Because the behavior of the first-storey infill panel was expected to be the most critical, a video image correlation device, VIC-3D, was used for measuring initial imperfections and out-of plane deformations within a central area of 450×550 mm (Figure 79). VIC-3D is a displacement and strain video measurement system, which uses a mathematical correlation method to analyze digital image data recorded during specimen testing. The system has a point-to-point strain accuracy of 0.02% and can provide accurate measurements of object contour and out-of-plane displacements of the infill panel in the highlighted area.

Legend:
DSWH$_0$ -base slippage
DSWH$_1$ -1st level displacement
DSWH$_2$ -2nd level displacement
DSWV$_l$ -left base uplift
DSWV$_r$ -right base uplift
DJH0$_d$, DJH0$_u$ - base beam-column connection rotation
DJH1$_d$, DJH1$_u$ - 1st level beam-column connection rotation
DJH2$_d$, DJH2$_u$ - 2nd level beam-column connection rotation
DPD1$_d$, DPD1$_u$ - 1st panel diagonal measurement
DPD2$_d$, DPD2$_u$ - 2nd panel diagonal measurement
VIC 3D - optical measuring device

Figure 79: Instrumentation of experimental frames with cable potentiometers and optical measuring devices

3.3.2.4   Monotonic test

The first specimen, R-M-T2, used rigid beam-to-column connections and 2-mm infill plates. Figure 80 shows a plot of the lateral force against top displacement. Notably, the strip model accurately modeled the specimen behavior, including strength degradation after application of the peak load. Figure 81 shows the structure and VIC-3D measurements at different stages during the testing. Initial out-of-plane deformations in the bottom left panel

were approximately $0.006\sqrt{Lh}$ or 8.1 mm (Figure 81(a), Table 23). These initial deformations occurred during fabrication as well as after test setup installation. The specimen exhibited an elastic behavior up to 0.6% of inter-storey drift. The infill plates yielded first, at a 0.6% inter-storey drift, and this was indicated by a change in stiffness (Figure 80). At this point, the base shear force reached 482 kN and the corresponding top displacement was 20.7 mm. The out-of-plane deformation of the infill panel corresponding to this drift value was $0.018\sqrt{Lh}$ or 23.6 mm (Figure 81(b)). For up to 2% inter-storey drift, there were no plastic deformations in the boundary elements and beam-to-column connections. For drifts larger than 2%, plastic deformations developed in the flange under compression at the beam end. Figure 82 shows the moment-rotation curve for first storey beam end. The development of plastic deformations at beam end for 2% inter-storey drift is in good agreement with the change in the slope of the force–displacement curve shown in Figure 80. At 2% drift, some cracks were also initiated at the panel corners (Figure 83(a)); then, these cracks propagated along the fillet welds that connected the infill plate to the additional fishplates (Figure 83(b)). There were no indications of any deterioration in the load carrying capacity owing to these local fractures. It was found that the cracks occurred mainly owing to insufficient clearance between the two adjacent fishplates, which collided when the beam rotated relative to the column. The peak capacity was reached at 6% drift (or a top displacement of 210 mm) at a corresponding base shear force of 1094 kN (Figure 80). Out-of-plane deformations in the panels corresponding to peak capacity were $0.027\sqrt{Lh}$ or 36.1 mm (Figure 81(c)). The test was stopped at 240 mm, not owing to the specimen collapse but owing to the limitation of the actuator stroke.

The specimen condition post testing is presented in Figure 84, which shows a global view of the left-hand side panels. It can be seen from Figure 84(a) that orientations of the tension field in the first- and second-storey panels are very similar, 41° and 42°, respectively. These angles are close to the 40° obtained using the AISC provisions. Figure 84(b) shows one beam-to-column connection after the test. Figure 84(c) shows the link beam of the first storey where some plastic deformations were observed. This indicates that, at large displacement cycles, plastic deformations may take place, apart from beam ends, also in the link beam. These plastic deformations represent the frame's contribution to the system's inelastic response.
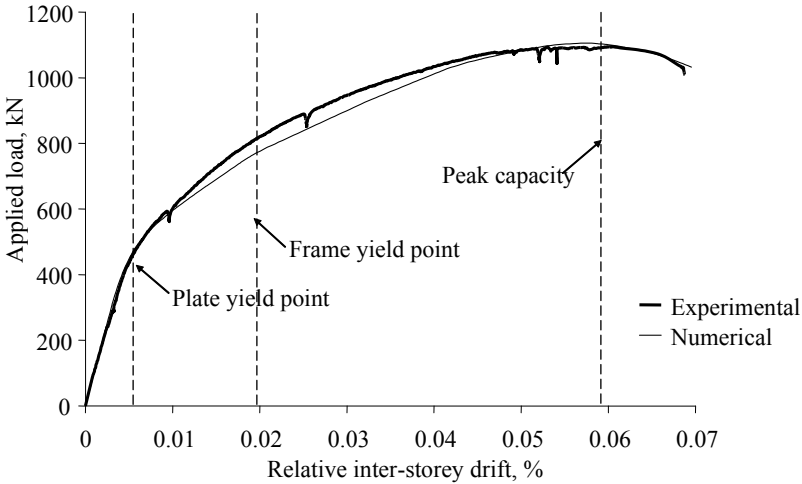
Figure 80: Experimental vs. numerical force–displacement curves, rigid specimen with 2mm-thick plates, R-M-T2
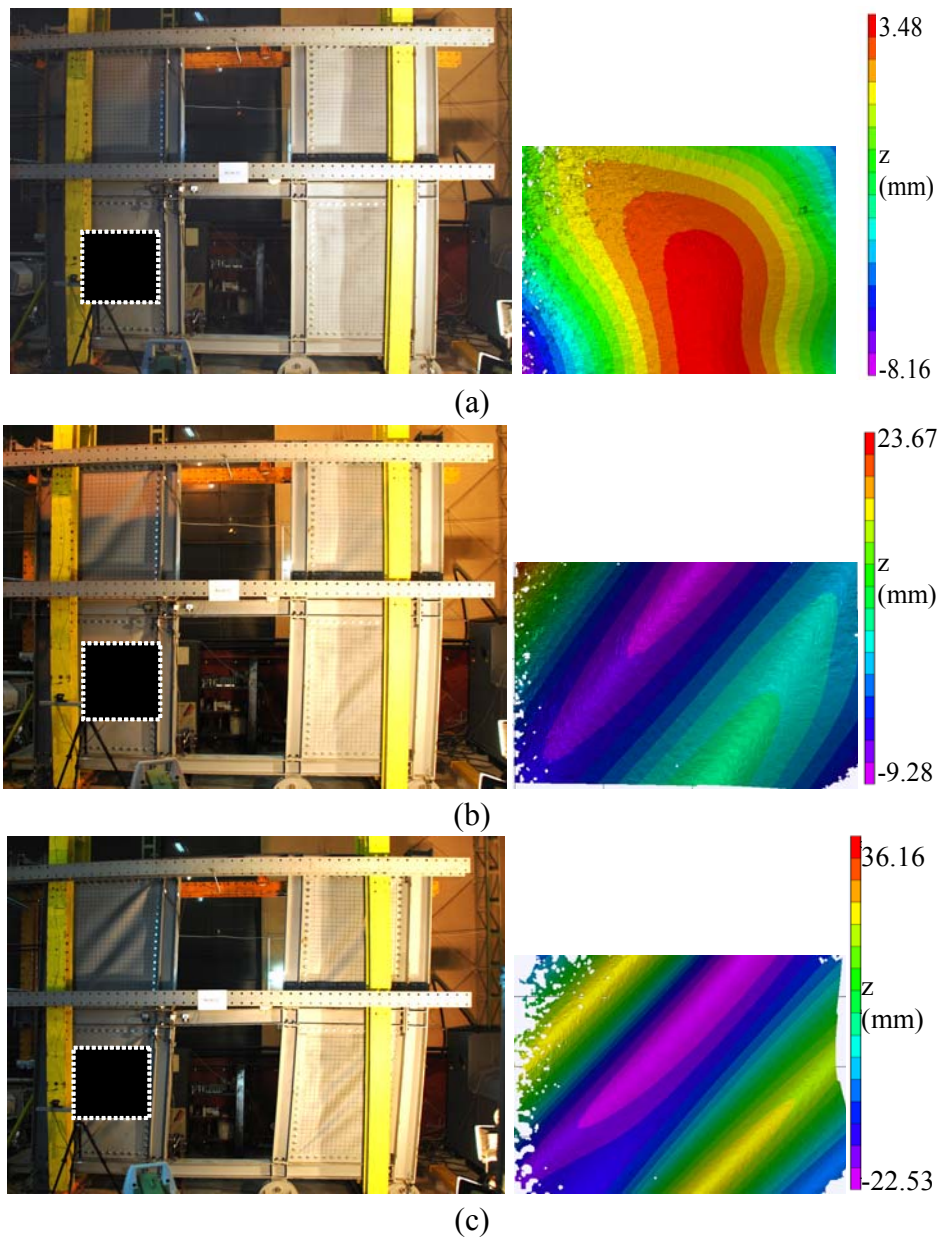
Figure 81: General view and VIC-3D out of plane measurements for R-M-T2 specimen: (a) initial state, before test; b) yielding state; c) peak capacity

Table 23: Out-of-plane deformations corresponding to yielding and ultimate load

| Specimen	e_{0w} (initial) [mm]	e_w (yielding) [mm]	e_w (ultimate) [mm]
R-M-T2	8.1	23.6	36.1
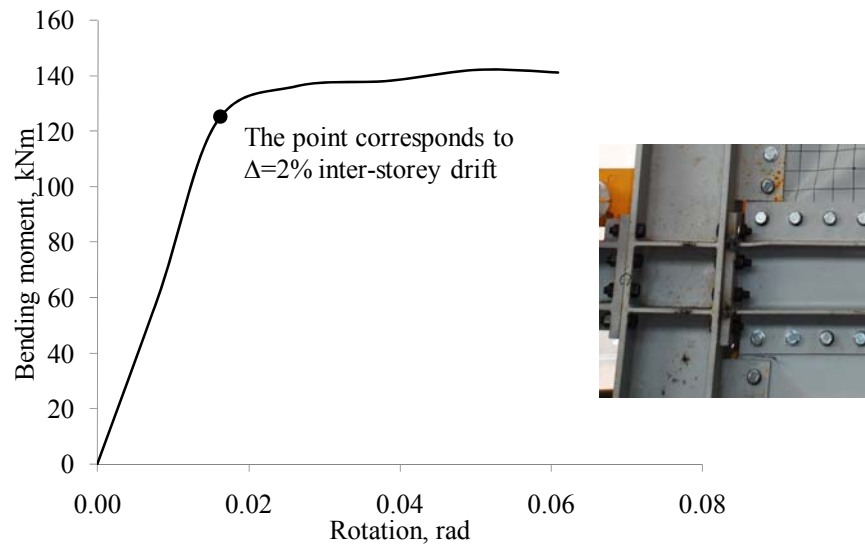
Figure 82: Moment-rotation curve for first storey beam end, rigid specimen with 2-mm-thick plates, R-M-T2

(a)   (b)

Figure 83: Damage level at plate corner: (a) 2% inter-storey drift and (b) 6% inter-storey drift

(a)

(b)

(c)
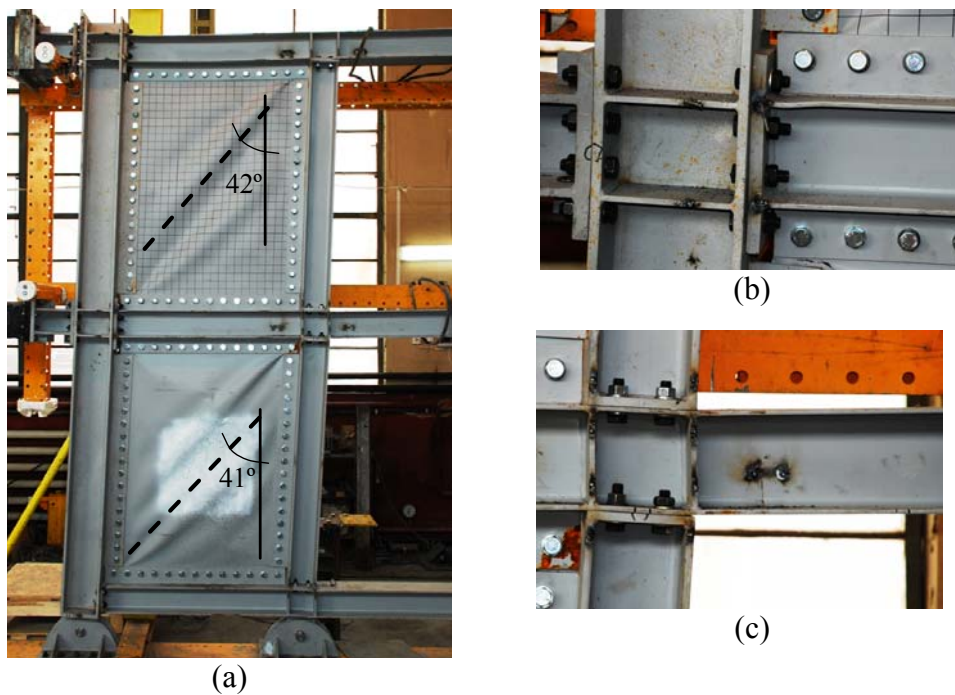
Figure 84: Specimen R-M-T2 after test: a) overall specimen view; b) beam-to-column connection; and c) link beam

3.3.2.5 *Cyclic tests*

All specimens exhibited stable force-displacement behavior, with some pinching of hysteresis loops that are line with the characteristics commonly observed in other tests on SPSW ([1]). Plots of lateral load against top displacement of the three specimens tested under cyclic loading are shown in Figure 85(a–c).

(a)

(b)

(c)
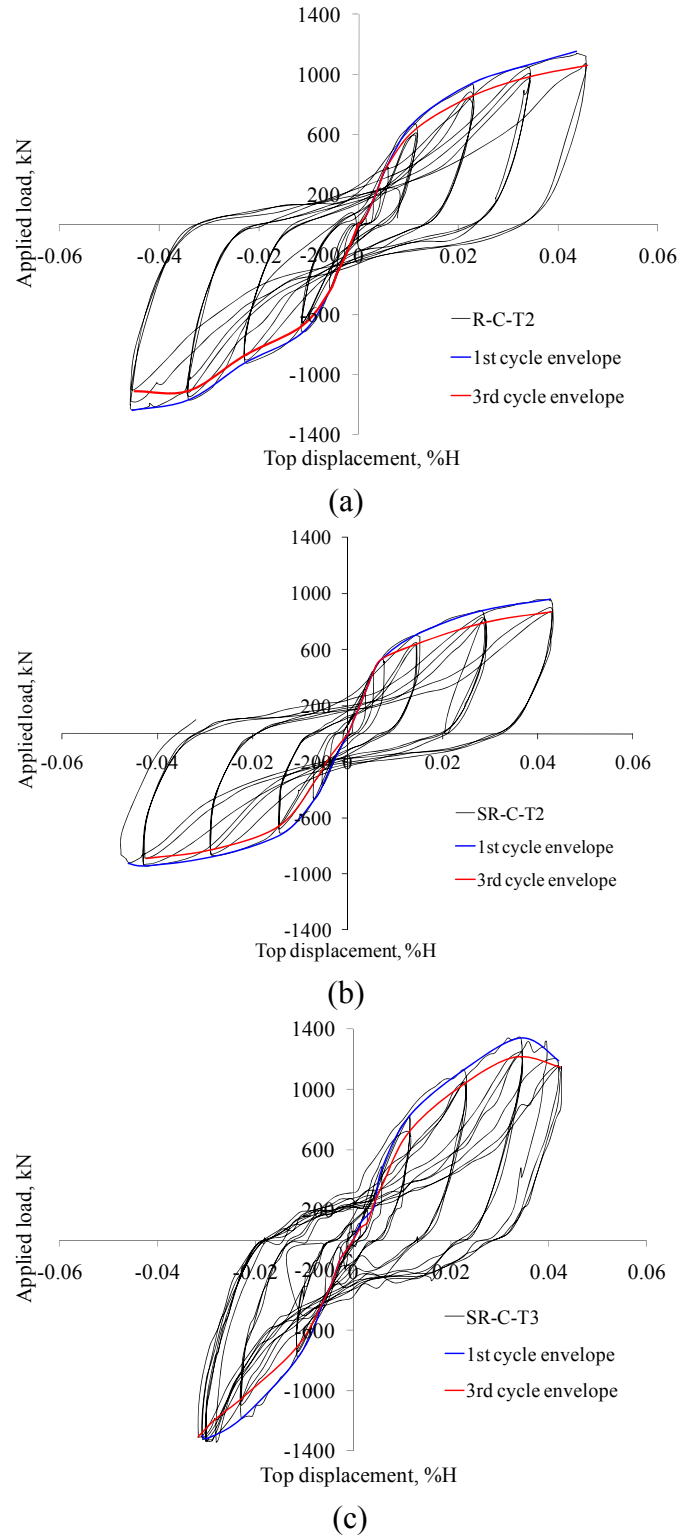
Figure 85: Results of cyclic tests: a) hysteresis curve for SR-C-T2; b) hysteresis curve for R-C-T2; and c) hysteresis curve for SR-C-T3

All specimens showed an initial out-of-flatness of less than $0.01\sqrt{Lh}$ (Table 24), which is similar to the value measured for the monotonically tested specimen, R-M-T2. These initial deflections affected the initial stiffness and yield strengths of the plates, but had a negligible effect on their ultimate capacity. Specimens of 2-mm panels, i.e. SR-C-T2 and R-C-T2, yielded at 0.65% and 0.7% drift, respectively (Table 25). This indicates that until the yielding, the rigidity of the beam-to-column joint has little effect on the behavior. The specimen with 3-mm-thick panels, SR-C-T3, yielded at approximately 0.85% drift. Some local cracks were initiated at the panel corners at approximately 2% drift, which then propagated along the fillet weld of the plate to the additional fishplate. At the same drift level, local plastic deformations were observed at the beam flange under compression for rigid connections. For the semi-rigid specimens plastic deformations were initiated in the connections because of the beam end plate in bending at approximately 2.5% drift.

All specimens exhibited stable behavior up to cycles of 4% storey drift, at which point the strength deteriorated. It should be noted that the negative direction drift for SR-C-T3 is smaller than the positive direction drift owing to the limitation of the actuator capacity, and therefore, the behavior under positive displacement is of interest. The ultimate displacement of the specimens is approximately 4.5% storey drift, not owing to the specimen collapse but owing to the limitation of the actuator stroke (Table 25). The contribution of the frame to overall response increases with lateral displacement. Thus, the difference between SR-C-T2 and R-C-T2 in terms of yield resistance and yield displacement was small, as mentioned before, but ultimate capacity decreased by 20% when connections with low rigidity were used. As for the peak drift level, there was a small difference between the rigid and semi-rigid specimens.

Table 24: Out-of plane deflections of infill plates

Specimen	e_w, [mm]		
	initial	yielding	ultimate
R-C-T2	8.7	NA*	NA*
SR-C-T2	11.5	32.6	52.6
SR-C-T3	8.9	21.3	31.9
* not available			

Table 25: Yielding and ultimate force and displacement, cyclic test (H = 3500 mm)

Specimen	F_y [kN]	D_y [%H]	F_{max}, 3rd cycle [kN]	D_{max}, 3rd cycle [%H]
SR-C-T2	450	0.0065	943	0.046
R-C-T2	500	0.007	1151	0.044
SR-C-T3	675	0.0085	1340	0.042

To further explain the differences in the hysteretic behavior of rigid and semi-rigid specimens, the 11th cycle for specimens R-C-T2 and SR-C-T2 is shown in Figure 86. The loops can be separated into three distinct regions. When the cycle starts and the applied force increases from point 1 to point 2, the specimen shows a reduced stiffness due to the permanent stretching of the plate. In this region, the main contribution to the stiffness is attributed to the frame. Therefore, when compared to the semi-rigid specimen, the rigid one shows an increase in stiffness and also a reduction of almost-zero stiffness region. After point 2, the structure deforms sufficiently to allow the development of the tension field and the stiffness increases. After point 3, the plate begins to deform plastically in tension and the stiffness decreases. The point 4 represents the peak load in the positive direction of the cycle.

It is important to note that, the almost zero-stiffness regions need to be taken into account when the total displacement D_u is calculated, because this affects the value of the ductility.
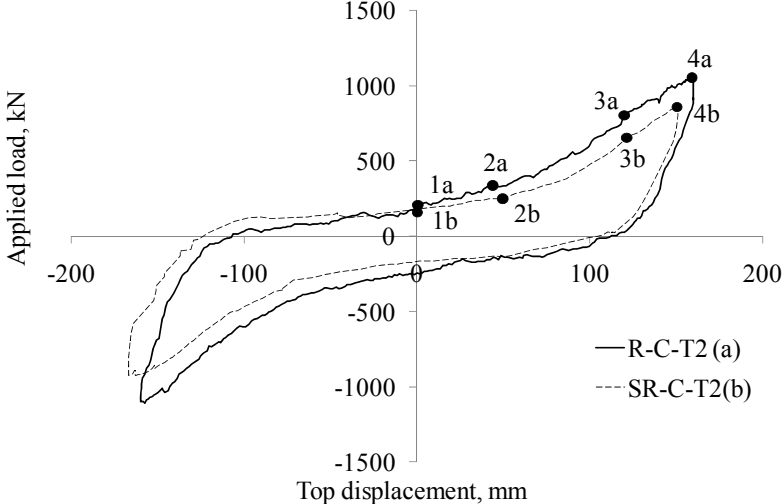

Figure 86: Behavior at the 11th cycle for R-C-T2 and SR-C-T2 specimens

Figure 87 plots the envelope of the stabilized hysteresis curve corresponding to the 3rd cycle vs. monotonic curve for rigid specimen with 2-mm panels. The results show that the monotonic curve constrains the specimen's cyclic response except the reduction of the ductility for the cyclic test. This can be explained by reduced cyclic hardening of the plates, which are the main components of the SPSW system. Thus, a static pushover analysis can be employed for evaluating the initial stiffness and yield point of the SPSW structure.
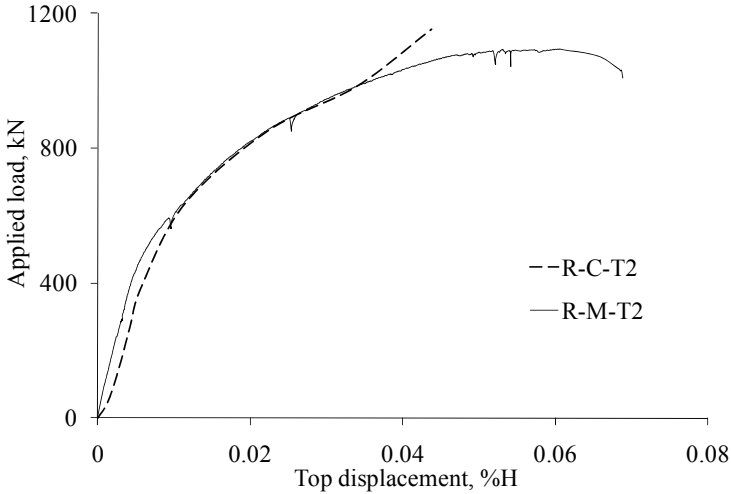
Figure 87: Envelope of stabilized hysteresis curve corresponding to 3rd cycle (R-C-T2) vs. monotonic test (R-M-T2)

Figure 88 shows some details within the specimens after the test. Figure 88(a) shows a panel of the first storey after the test, with fold lines developed parallel to the tension field in both directions. Figure 88(b) shows the left and right plate corners with crack propagation along the tension field in the plate. These plate corner fractures are larger than the cracks observed in the monotonically tested specimen. This propagation is ascribed to the tension field force, which changes orientation during a cycle and acts normal to the fracture direction.

The same orientation change of the tension field also caused the panel to tear at the intersection of the two diagonals (Figure 88(c)) owing to repeated local buckling. Bolted connections between the infill panels and fishplates showed small slippage but no plastic deformation on either the plate side or bolt side (Figure 88(d)). Figure 88(e) shows the semi-rigid beam-to-column connection, and Figure 88(f) shows the rigid connection. The flush end plate of the semi-rigid connection suffered plastic deformations owing to bending, whereas, in case of rigid connections, the beam flange under compression buckled plastically. As in case of the monotonic test, the plastic rotation demand on such connections is moderate because the corners of the infill plate act as gusset plates above and below the connection. Plastic deformations were observed in the link beam after the test, indicating the frame's contribution to the system's inelastic response (Figure 88(f)). Because no plastic deformations were recorded in the bolts and fishplates, the steel panels could be dismantled easily after the test. This fact, coupled with a small residual drift, allows for the removal of damaged panels after moderate earthquakes.

(a)   (b)   (c)   (d)   (e)   (f)

(g)
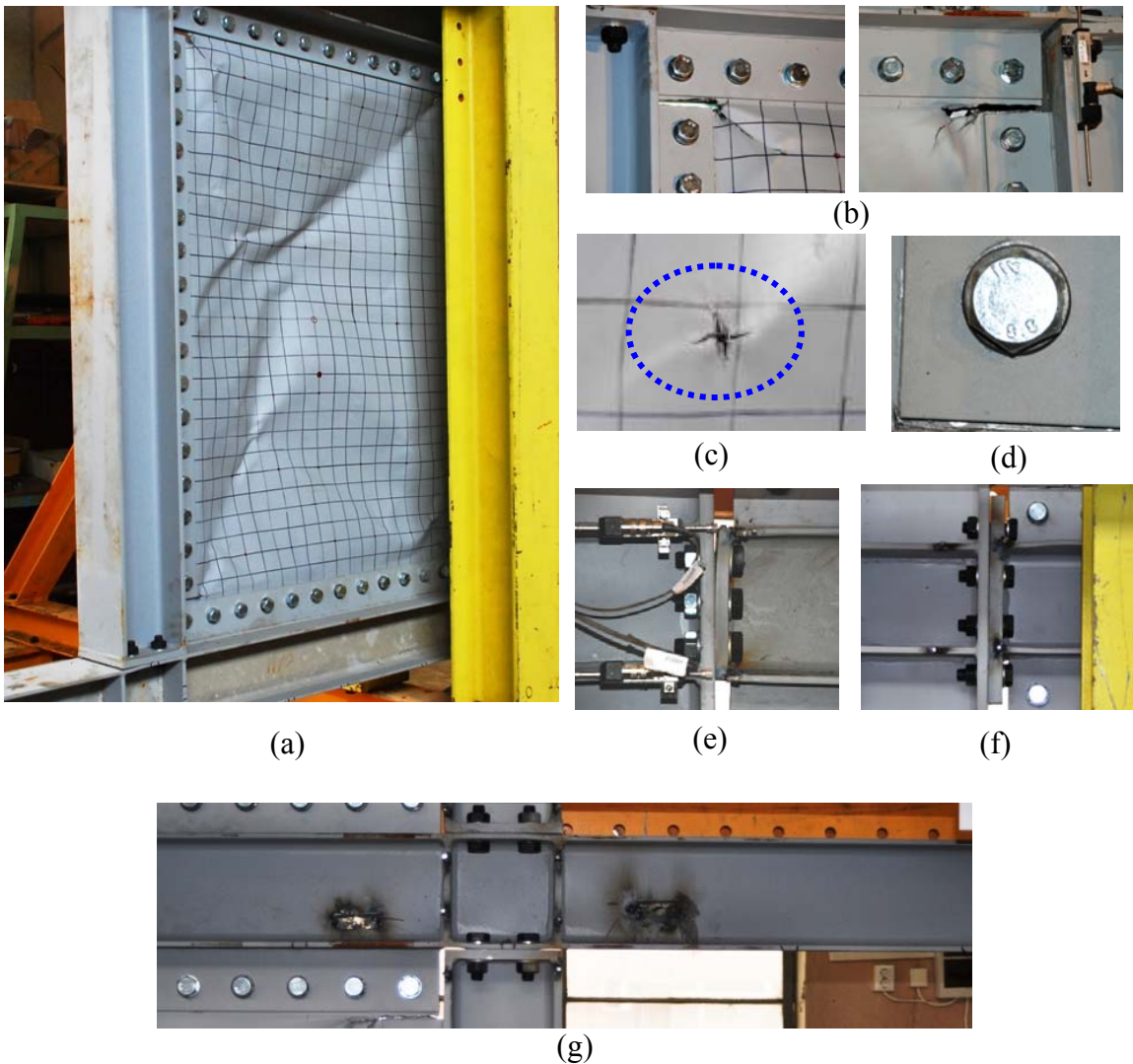
Figure 88: Specimen damage: a) first storey panel; b) plate corners; c) plate tearing at the intersection of fold lines; d) bolted connection between panel and fishplate; e) semi-rigid beam-to-column connections; f) rigid beam-to-column connections; g) link beam

Figure 89 shows the energy dissipated by the specimens during cyclic loading, and Table 26 lists the values of total dissipated energy. Increasing the thickness of the infill plates from

2 mm (SR-C-T2) to 3 mm (specimen SR-C-T3) increases the energy dissipation capacity of the system by almost 50%. The use of rigid beam-to-column connections instead of semi-rigid ones gives similar results because dissipated energy increases by almost 45%.
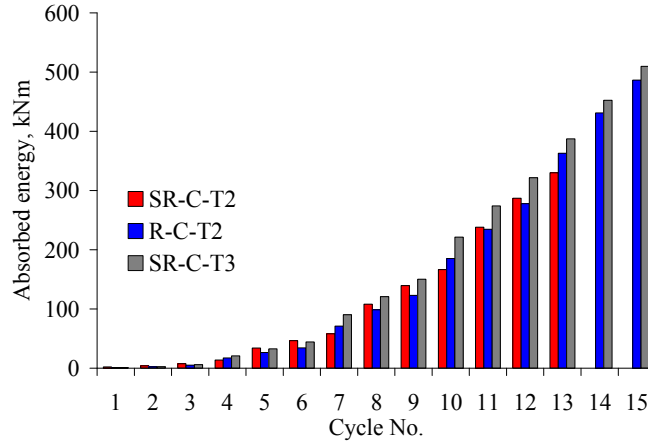
Figure 89: Dissipated energy in each loading cycle for the three specimens

Table 26: Cumulative dissipated energy

Specimen	SR-C-T2	R-C-T2	SR-C-T3
Dissipated energy [kNm]	330	485	510

3.3.2.6 Seismic force reduction factors

One goal of the experimental program was to evaluate the seismic force reduction factor, or q factor (behavior factor in EN 1998). Our test shows that SPSW systems have good ductility. This ductility can be employed for estimating the q factor. For periods $T > T_B$, where T_B is the lower-bound period of the constant branch of the design acceleration spectrum, EN 1998-1 proposes a constant *q* factor that is generally equal to a product of the reduction factor due to ductility, q_μ, and overstrength factor q_s. All factors depend on the type of the structural system and on the material.

The reduction factor due to ductility, denoted as q_μ, can be defined as:

$$q_\mu = \mu = \frac{D_u}{D_y} \tag{4}$$

where:

μ = ductility factor
D_u = ultimate displacement
D_y = yield displacement.

According to EN 1998-1, the overstrength factor, denoted here as q_s, may be taken as 1.5. Similar values are given in National Building Code of Canada [28], which recommends an overstrength factor, q_s, equal to 1.5 for limited ductility plate walls and 1.6 for ductile plate walls, respectively.

Because of the difficulties in estimating the true yield of SPSW structures, two methods were used for evaluating the yield displacement D_y (Figure 90). The first, based on the tangent of the 10% slope of the initial stiffness, follows the ECCS recommendations [27]. According to the second method, the yield point corresponds to the point where the force–displacement curve's slope changes considerably ("1st yield" method). The ultimate displacement D_u is the maximum displacement obtained during testing. To note that the test was stopped after the peak load was attained, not owing to the specimen failure but owing to the limitation of the actuator stroke.
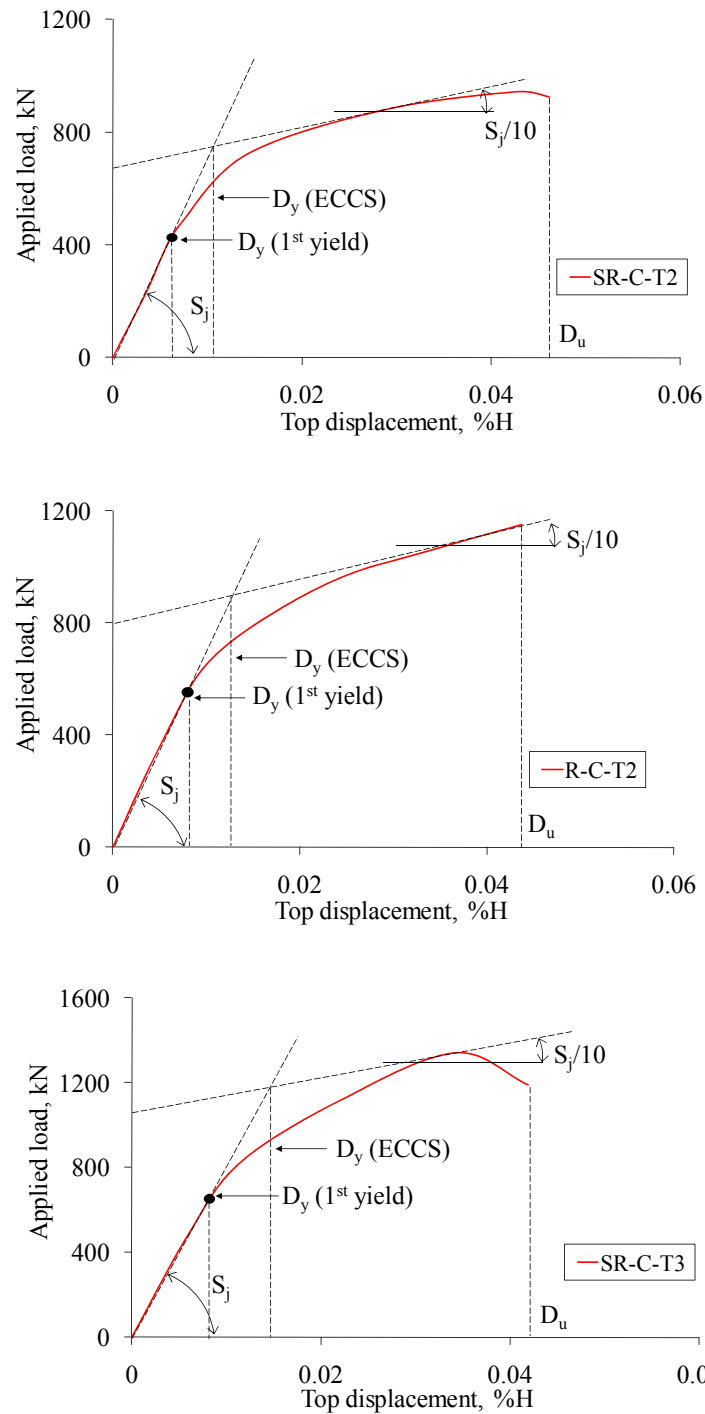
Figure 90: Yield and ultimate displacements for cyclic test envelopes, 3rd cycle

Table 27 lists the reduction factor q for each specimen as well as the average values. The average value obtained using the ECCS method is 3.3 and is lower than the 4.1 value obtained using the "1st yield" method. If the overstrength factor, q_s, is used to amplify the ductility factor, q_μ, the total value of q factor obtained using the ECCS method is 5.0, while for "1st yield" method is 6.2. The later value is close to the value of 6.5 used for structure design in this study. It is important to note the values of ultimate displacement D_u were corrected by substracting from the total displacement the almost zero-stiffness regions. Given that the number of specimens that have been tested is small, our results cannot be generalized.

However, the test results do indicate that the SPSW systems comprising link beams and slender panels are capable of dissipating large amounts of energy with stable cyclic behavior.

Table 27: Experimental values of q factor

Structure	D_y [mm]		D_u [mm]	q_u		q	
	ECCS	1st yield		ECCS	1st yield	ECCS	1st yield
SR-C-T2	33	26	119	3.6	4.6	5.4	6.9
R-C-T2	38	31	123	3.2	4.0	4.9	6.0
SR-C-T3	40	33	127	3.2	3.8	4.8	5.8
Average value				**3.3**	**4.1**	**5.0**	**6.2**

3.3.3 References

[1] Bruneau, M., Berman, J., Lopez Garcia, D., Vian, D., Steel Plate Shear Wall Buildings: Design Requirements and Research, North American Steel Construction Conference, Montreal, Canada, April 2005 - CD-ROM paper #075.

[2] Thorburn, L.J., Kulak, G.L., and Montgomery, C.J., Analysis of Steel Plate Shear Walls, Structural Engineering Report No. 107, Department of Civil Engineering, University of Alberta, Edmonton, Canada, 1983.

[3] Timler, P.A., Kulak, G.L., Experimental Study of Steel Plate Shear Walls, Structural Engineering Report No. 114, Department of Civil Engineering, University of Alberta, Edmonton, Canada, 1983.

[4] Driver, R.G., Kulak, G.L., Kennedy, D.J.L, Elwi, A.E., Cyclic Test of a Four Storey Steel Plate Shear Wall, ASCE Journal of Structural Engineering, Vol.124, No.2, p.112–120, 1998.

[5] Berman J.W., Bruneau M., Plastic Analysis and Design of Steel Plate Shear Walls, Journal of Structural Engineering, ASCE, Vol. 129, No. 11, pp1448-1456, 2003.

[6] Zhao, Q. and Astaneh-Asl, A., Cyclic Behavior of Traditional and Innovative Composite Shear Walls, Journal of Structural Engineering, ASCE, Vol.130, No.2, pp. 271–284, 2004.

[7] Qu, B., Bruneau, M., Lin, C.H., Tsai, K.C. and Lin, Y.C., Full scale steel plate shear wall: MCEER/NCREE phase II tests, Ninth Canadian Conference on Earthquake Engineering Ottawa, Ontario, Canada 26-29 June 2007.

[8] Caccese, V., Elgaaly, M., and Chen, R. (1993), "Experimental Study of Thin Steel-Plate Shear Walls Under Cyclic Load," Journal of Structural Engineering, ASCE, Vol. 119, No. 2, February, pp. 573–587, Reston, VA.

[9] CSA, CAN/CSA 16-01. Limit States Design of Steel Structures, Canadian Standards Association, Willowdale, Ont., Canada, 2001.

[10] CSA, CAN/CSA 16-09. Limit States Design of Steel Structures, Canadian Standards Association, Willowdale, Ont., Canada, 2009.

[11] ANSI/AISC 341-05, Seismic provisions for structural steel buildings. American Institute for Steel Construction, 2005.

[12] ANSI/AISC 341-10, Seismic provisions for structural steel buildings, American Institute for Steel Construction, 2010.

[13] Seilie, I., and Hooper, J., Steel Plate Shear Walls: Practical Design and Construction, Modern Steel Construction, April 2005.

[14] Berman, J.W., Seismic behavior of code designed steel plate shear walls, Engineering Structures, Volume 33, Issue 1, 2011, pp. 230–244.

[15] M.M. Alinia, M. Dastfan, Cyclic behaviour, deformability and rigidity of stiffened steel shear panels, Journal of Constructional Steel Research, Volume 63, 2007, pp. 554–563.

[16] Li, C.-H., Tsai, K.-C., Chang, J.-T., Lin, C.-H., Chen, J.-C., Lin, T.-H. and Chen, P.-C., Cyclic test of a coupled steel plate shear wall substructure. Earthquake Engineering & Structural Dynamics, Volume 41, Issue 9, 25 July 2012, Pages 1277-1299.

[17] Borello, D. and Fahnestock, L., Seismic Design and Analysis of Steel Plate Shear Walls with Coupling. Journal of Structural Engineering, doi 10.1061/(ASCE)ST.1943-541X.0000576, 2012.

[18] Berman, J.W., Clayton, P.M., Lowes, L.N., Bruneau, M., Fahnestock, L.A. and Tsai, K.-C., Development of a recentering steel plate shear wall and addressing critical steel plate shear wall research needs, Proc. of the 9th U.S. National and 10th Canadian Conference on Earthquake Engineering, July 25-29, 2010, Toronto, Ontario, Canada, Paper No 1087.

[19] Dubina, D., Stratan, A., Dinu, F., Dual high-strength steel eccentrically braced frames with removable links, Earthquake Engineering and Structural Dynamics, Volume 37, Issue 15, 2008, pp. 1703-1720.

[20] Neagu C., Dinu F. and Dubina D., Seismic performance of steel plate shear walls structures, Journal Pollack Periodica, Publisher Akadémiai Kiadó, ISSN 1788-1994, Issue Volume 6, Number 1/April 2011, Pages 47-58, DOI 10.1556/Pollack.6.2011.1.5.

[21] P100-1, Seismic Design Code, Part 1 - P100-1/2006, Earthquake Resistant Design of buildings, 2006 (in Romanian).

[22] EN 1990, Eurocode: Basis of structural design, CEN, 2005.

[23] EN 1991-1-1, Eurocode 1: Actions on structures - Part 1-1: General actions - Densities, self-weight, imposed loads for buildings, CEN, 2002.

[24] EN1993-1-1, Eurocode 3: Design of steel structures - Part 1-1: General rules and rules for buildings, CEN, 2005.

[25] EN1993-1-8, Eurocode 3: Design of steel structures, Part 1-8: Design of joints, CEN, 2005.

[26] EN 1998-1, Eurocode 8: Design of structures for earthquake resistance - Part 1: General rules, seismic actions and rules for buildings, CEN, 2004.

[27] ECCS, Recommended Testing Procedures for Assessing the Behavior of Structural Elements under Cyclic Loads. European Convention for Constructional Steelwork. Technical Committee 1, TWG 1.3 – Seismic Design, No.45, 1985.

[28] NBCC, National Building Code of Canada. Institute for Research in Construction, National Research Council of Canada, Ottawa, 2005.

4   APPLICATIONS FOR BUILDINGS:

National and international experience of the candidate related to the topic
"Applications for buildings"
(Post-PhD Thesis period)

Member of technical boards:
- Member of Technical Committee TC13 "Seismic Design" of the European Convention for Constructional Steelwork (ECCS);
- Member of AICPS – Romanian Association of Structural Engineers;
- Member of APCMR – Romanian Association for Constructional Steelwork;
- Member of AGIR – Romanian Association of Engineers.

Conference committees:
- Organization Committee of the International Conference in Metal Structures: Steel – A New and Traditional Material for Building, Poiana Braşov, Romania, 20-22.09.2006;
- Chairman of Technical Session: International Symposium "Steel Structures:Culture & Sustainability 2010", 21-23 September 2010, Istanbul, Turkey.

Supporting projects:
- Structural conception and collapse control performance based design of multistory structures under aacidental actions (CODEC), PNII-PT-PCCA, 2012-2016
- Factori de comportare a structurilor metalice in zone seismice pentru implementarea criteriilor de proiectare bazate pe performanta, MEC   Grant 33047/2004, cod CNCSIS 219, 2004-2005.
- Criterii de precalificare a îmbinărilor ductile ale cadrelor metalice necontravantuite, MEC – CNCSIS, Grant CNCSIS cod 728, tema nr.2
- Sisteme constructive si tehnologii avansate pentru structuri din oteluri cu performante ridicate destinate clădirilor amplasate în zone cu risc seismic", Acronim „STOPRISC", Proiect de cercetare de excelenta Program CEEX – MATNANTECH, PC-D04-PT23-346, 2005-2007
- Requirements for multi-storey buildings in seismic areas, RUUKKI/2009, 2009, Rautaruukki Corporation, Finland.
- **Invited papers and courses:**
- Invited lecturer at TUCSA (Turkish Association for Constructional Steelwork), 02.03.2009 (Lecture: Multi storey steel frame buildings in seismic areas. Authors: Dan Dubina, Florea Dinu).
- Invited course Cost C25/C26: Sustainability in Structures and Structural Interventions. Improving the contemporary and historical urban habitat constructions within a sustainability and risk assessment framework, Early stage researchers training school, 17-24 May 2009, Thessaloniki, Greece.

Reviewer in ISI journals:
- Journal of Structural Engineering – ASCE (http://ascelibrary.org/sto/)

Books:
- Vulnerability and damageability of constructions under impact and explosion", COST Action Final Report – Urban Habitat Constructions under Catastrophic Events, CRC Press, A Balkema Book, ISBN 978-0-415-60686-8, 2010.

4.1   Introduction

Buildings located in seismic regions shall be designed and constructed such that the no-collapse and damage limitation requirements under specific seismic hazard are met. For low

rise buildings, the design is often made from gravity loads, and therefore the designer may adopt the low dissipative seismic concept. For medium and high rise buildings, the concept that is adopted is mostly the medium or high dissipative one.

In order to avoid explicit inelastic structural analysis in design, the capacity of the structure to dissipate energy is taken into account by performing an elastic analysis based on the design response spectrum, which is reduced with respect to the elastic one. This reduction is accomplished by introducing the behaviour factor q. In case of complex structures or structures that combine different systems (i.e. dual systems) or different steel grades (eg. mild carbon steel and high strength steel), EN 1998-1 [1] does not provide confident values for q factor. Moreover, in order to achieve a favourable plastic mechanism (global mechanism), targeted structural members are designed to dissipate seismic energy (dissipative elements), while others are designed to remain predominantly elastic (e.g. non-dissipative elements). To approach as much as possible the global plastic mechanism configuration, it is necessary to control by design the history of appearance of plastic hinges in dissipative members. On this purpose, a good balance between strength, stiffness and ductility of members and connections of the structure has to be ensured. In real structures, this requirement is, in many cases, difficult or impossible to accomplish, as the lateral resisting system may be designed from conditions other then seismic one, eg. wind loadings.

Even in strong seismic areas, when high values of q factor are used, for multistory buildings of more then 25-30 stories wind forces control the design of the lateral force-resisting system. Seismic detailing is of course required and should be carefully carried out. In such cases, the seismic performance should be checked by means of nonlinear static or dynamic analysis and, if necessary, the elements sizes corrected. The candidate has been involved in the design of many types of buildings, ranging from low to medium and high rise buildings, also large span or special structures. In the following, two building structures will be presented. First one is a 26 storey building, located in Bucharest and the second one is a 6 storey building located in Constanta. Both structures have been designed using advanced nonlinear analysis and employe special systems and detailing to provide stiffnes, strength and ductility required for such systems.

Several papers related to this topic have been published during the last 10 years. A selection of these papers is presented below:

1. Dubina D, Dinu Florea, Stratan A, Ciutina A, Analysis and design considerations regarding the project of Bucharest Tower Centre steel structure International Conference on Metal Structures, Poiana Brasov, Romania, 2006, 20-22.09, 0-415-40817-2.
2. Dubina D., Dinu Florea, Stratan A. Design and performance based evaluation of Tower Centre International building in Bucharest. Part I: Structural design. Steel Construction, Willey, 2009, ISSN 1867-0520
3. Dubina D., Dinu Florea, Stratan A. Design and performance based evaluation of Tower Centre International building in Bucharest. Part II: Performance based evaluation Steel Construction, Steel Construction, Willey , 2010, ISSN 1867-0520.
4. D. Dubina, F. Dinu, A. Stratan, Performance based evaluation seimic response of bucharest tower center international, Proc. Of the 5th European Conference on Steel and Composite Structures, Eurosteel 2008, 3-5 september 2008, Graz, Austria, Ed. R. Ofner, D. beg, J. Fink, R. Greiner, H. Unterweger, ISBN 92-0147-000-90, 1317-1323.
5. F. Dinu, Gh. Dima, Presentation de la structure Bricostore Orchideea Bucharest, Colloque International, 2eme edition, Lácier dans la construction moderne, A. Ciutina and A. Lachal Eds, ed. Politehnica, Timisoara, ISBN 978-973-625-682-0, p. 181-189, 2008.
6. D. Dubina, V. Ungureanu, F. Dinu, C. Molnar: Proiectul structurii metalice de rezistenţă a imobilului D+P+5E, zona Port Constanţa, Revista AICPS Nr. 2-3 / 2010, pg. 14-22.

4.2 Design and performance based evaluation of a 26 storey building located in Bucharest

The building is a 26 story steel structure office building and is located in Bucharest. Bucharest is the European capital with the highest seismic risk. The local site conditions and the specific features of the source (i.e. deep source with several acceleration peaks) aggravate the seismic risk in Bucharest area, particularly for medium rise frame buildings. The city has been shattered by several strong earthquakes during the last 35 years. Therefore, one important concern is the safety of these tall buildings under strong ground motions.

In order to check the seismic behaviour, a performance-based methodology PBA was considered, using three performance levels: serviceability limit state (SLS), ultimate limit state (ULS) and collapse prevention (CPLS) limit state and three seismic hazard levels, which are frequent rare and very rare ground motions. Seismic demands were evaluated using non-linear incremental analysis and a set of seven time histories. Due to the irregular shape of the building, the building was also tested in the wind tunnel. Both rigid and aeroelastic models were constructed and tested, in order to evaluate the distribution of pressure coefficients on the building envelope and the dynamic behaviour of the building.

Finally, in order to evaluate the robustness of the structure in case of abnormal loadings, like blast, impact or fire after earthquake, a complex risk scenario was done. It included loss of several columns, located at the bottom part and mid-height of the building.

4.2.1 Description of the structural system

The location of TCI building neighbours the city centre of Bucharest, in a very dense construction area, has 26 storeys and for the time being, is the tallest civil building in Bucharest (Figure 91:). The building has 3 basements, 26 floors and a total height of 106.3m. In 2007, the project was awarded by the European Convention for Constructional Steelwork ECCS. Figure 92: presents typical transversal and longitudinal frames, typical floor plans and foundation system. The storey height is 4.0m, except for the first storey, which is 5.4m tall, and the 2nd to 4th stories, which are 4.2m high. Between 7th and 11th stories, the floors are cantilevered on one side, for about 4.5 meters. The building is 25.5m by 41.5m in plan and has a total construction gross area of approx. 24 000 m^2. The lowest basement has a technical destination; the other basements are arranged as parking areas. The ground floor and the first two floors are arranged for the bank operation. The remaining floors are arranged as offices.

The foundation system is made by mat foundations and concrete piles that were driven 28 meters below surface. Settlements of the nearby buildings (located at more than 10 meters from the excavation), were continuously monitored during construction. Measurements indicated values less than 6mm when the building was completed. The building frame system uses steel braced and unbraced frames (dual structural configuration) (Figure 93:).

The cruciform cross sections columns, made of hot rolled profiles were partially encased in reinforced concrete to increase the strength, stiffness and fire resistance. Columns cross-section varies along the height of the building, from 2xHEM800 at the base to 2xHEA800 at the top for square sections and from HEB1000xHEM500 to HEB1000xHEB500 for rectangular sections. Beams and braces are made of I hot rolled sections (Figure 94:). S355J2 steel was generally used for frame members, excepting the braces designed as dissipative members, which are of S235J2 steel.

Figure 91: Rendering, location of the building
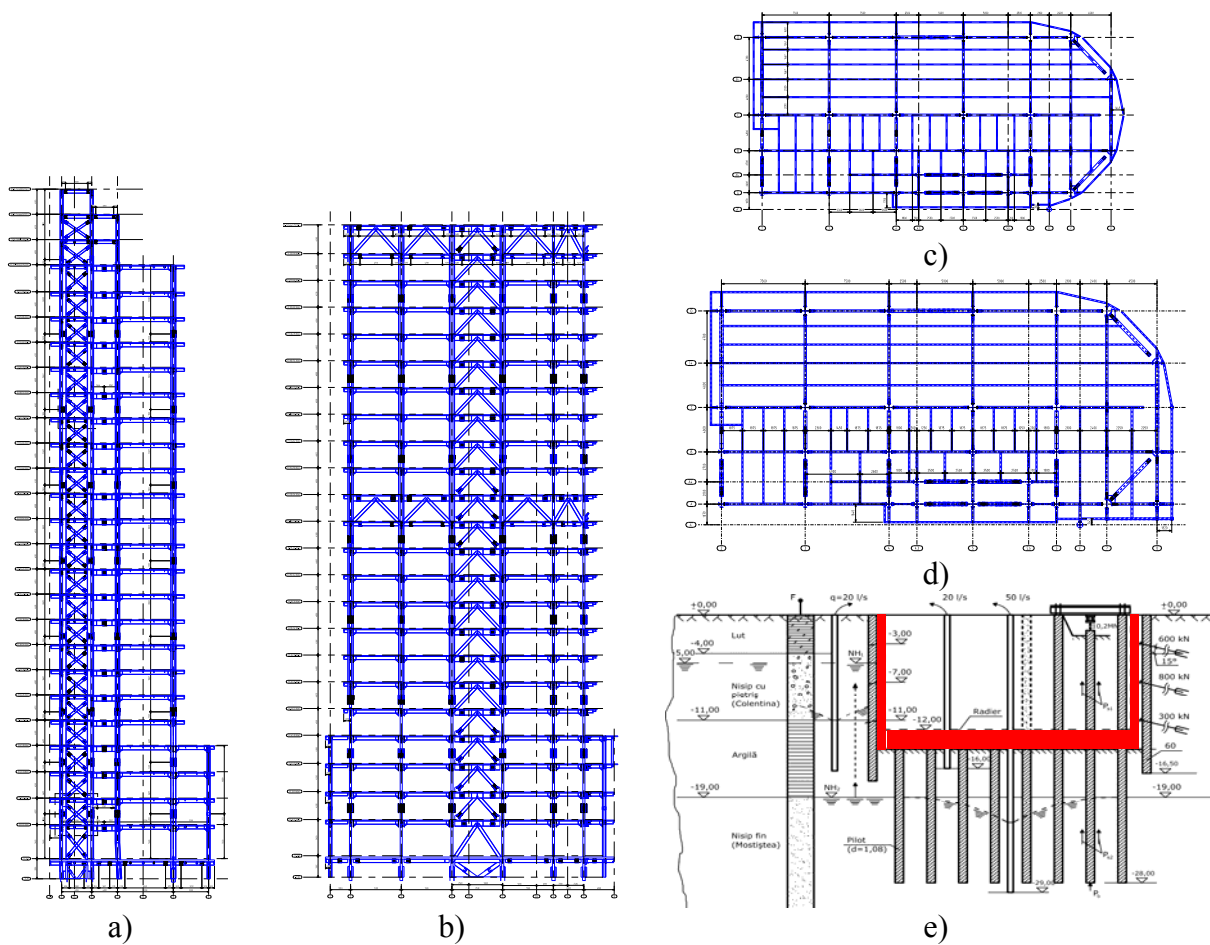
Figure 92: Structural system: a) transversal frame; b) longitudinal frame; c) current floor plan; d) floor plan between 7th and 11th stories; e) infrastructure and soil layers

Figure 93: View of frame system
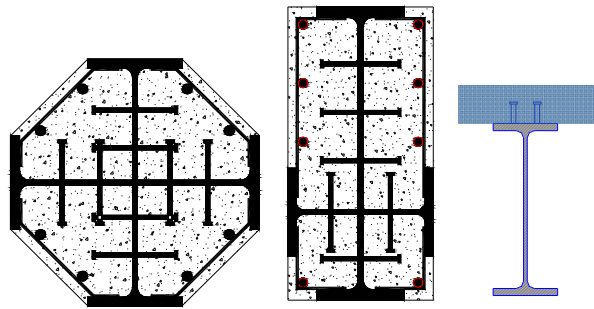
Figure 94: Columns and beams cross-sections

All site connections, including column splices were bolted connections (Figure 95:).
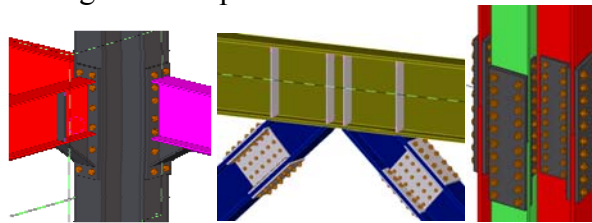

Figure 95: Typical connections

4.2.2   Construction

The original design project was developed in 1997, and afterwards the works of infrastructure began. Between 1997 and 1998, the infrastructure was 95% ready, with some minor works at the level -3.20m. Afterwards, the construction works were halted. In 2006, after a pause of eight years, the works at superstructure started again, but based on a different project. This new project was developed based on the existing infrastructure but adapted to new design codes, came into operation during the period 2004-2006, including the new seismic code P100/1-2006 [2], adapted to EN1998-1.

Before starting the works, the infrastructure was verified and strengthened due to the new loading conditions, considering also the level of degradation due to weather conditions that affected it. In this new project, for reasons of easy assembly and good quality control, site welding connections were avoided and were preferred bolted connections. Columns were continuous over three stories, and as a result, the number of splice connections was reduced.

Figure 96: Columns are continuous over three stories
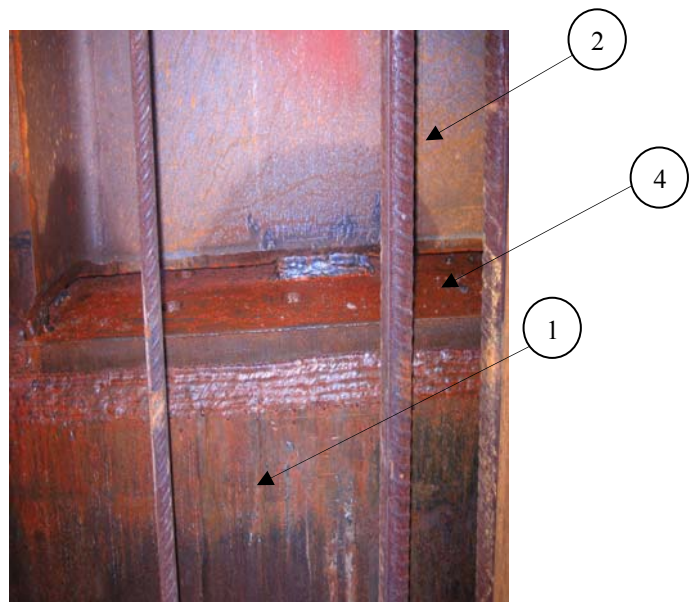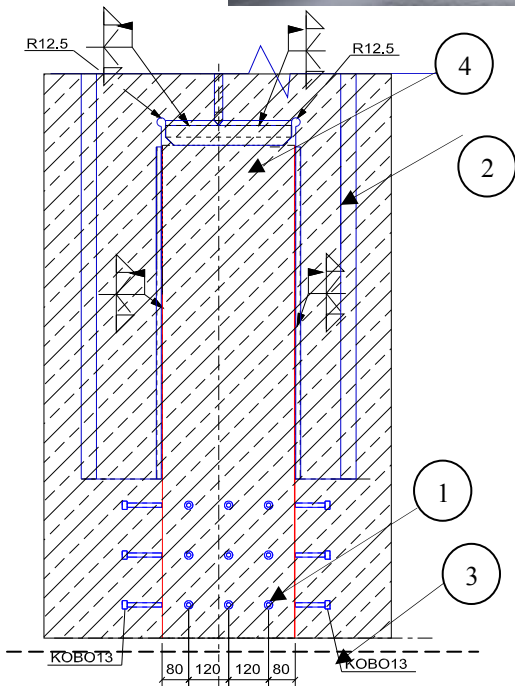
Figure 97: Connection between columns of infrastructure and superstructure

Row	Welding procedure	Dimension of deposit material	Intensity of electrical current	Voltage	Type of current	Welding wire speed	Welding speed cm/min	Thermal energy
1-12	111	4	140-160	22-24	CC+	-	8-10	-
3…18	111	2,5	75-85	20-22	CC+	-	8-10	-
19…	111	3,25	110-120	21-23	CC+	-	8-10	-
Post-weld heat treatment				Welding procedure				
Type	Not necessary			Edge preparation		Thermal + mechanical		
Temperature	-			Root support		nb		
Time	-			Oscillation		(1-2)d		
Cooling	-			Root grove		Chipping		
Heating/cooling speed	-			Cleaning between layers		Grind		
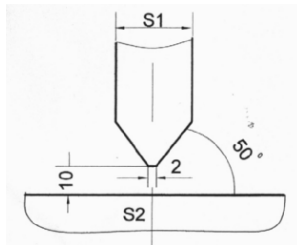
The edges of the plates chamfered to an adequate bevel to facilitate access to the root of the weld.
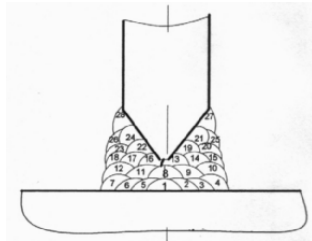
Welding sequence

Metallographic analysis
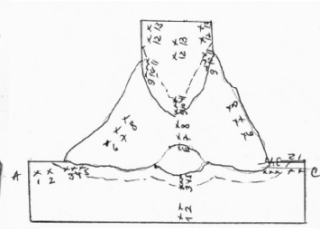
Hardness measurements

Figure 98 Welding details and quality control

This had also a beneficial effect on the precisions at the assembly, as the splices are prone to deviations. Complexity of the structure required an extensive quality control program in every phase: engineering (steel detailing), fabrication and construction. Thus, a complete 3D CAD-CAM computer model was produced and then interactively adjusted during fabrication, by taking into account the deviations of the structure from the original position. This enabled also the interoperability between the design model and cutting, drilling and welding operating programs used by the steel fabricator. Columns of the existing infrastructure (Figure 97) were made by steel hollow sections (1) encased in concrete (3) and were connected through concrete beams. The superstructure building frame system used steel braced and unbraced frames (dual structural configuration). The original column cross-section was replaced by cruciform cross sections, made of hot rolled profiles (2) which were partially encased in reinforced concrete to increase the strength, rigidity and fire resistance (Figure 94:).

Connection between infrastructure and superstructure columns was made by welding, including thick cap plate at the top of the hollow section column (4). Due to the large gaps between columns of existing infrastructure and the new ones and taking into account for the tensile stress in the cap plate (some columns are loaded in tension) and the stress concentration in the welding, the welding and the cap plate material were strictly controlled to avoid lamellar tearing and micro-cracking of welds. For each connection, detailed welding procedures were detailed and qualified based on both destructive and non-destructive testing (Figure 98).

Modern and accurate GPS systems were used, in order to ease the control of the beams and columns positions. Even the total deviation from the vertical position allowed for this structure was at about 70 mm, the measurements shown horizontal deviations were limited to 10 mm.

Figure 99 GPS system to control the position of members

Construction of steel structure was completed in November 2006. Building was officially opened in May 2007 and started to operate in the same year. During the last three years, the building remained the tallest civil building in Bucharest.

Figure 100: Views of building during construction

4.2.3 Design considerations

Multi-storey buildings of 25 to 30 stories should be designed to accommodate both wind and seismic loads. In general, for taller buildings, designed will be governed by wind load, even if seismic design philosophy (structural system, local detailing, etc.) should be considered. As the TCI structure was at the border between earthquake and wind resistant structures, both actions contributed to the final sections of the members (Figure 101:) [4]. This last statement challenged the design team, as some outcomes of wind design were in contrast with the seismic outcomes. As an example, in order to assure an adequate lateral stiffness (i.e. to limit the lateral drift) against wind load, there were necessary heavy bracings, much higher then those resulting from seismic design (both stiffness and strength). The solution adopted by the design team was to keep the bracing cross sections and therefore to assure and adequate level of stiffness but to reduce the yield strength f_y from 355 N/mm^2 to 235 N/mm^2 and thus to reduce the level overstrength in the same bracings. Static and dynamic calculations were done using the computer code Etabs, version 9 [3]. The seismicity of the Bucharest area was one of the main important aspects in design. The idea was to obtain a building with a fundamental period large enough to reduce the base shear force but in the same time to keep the lateral displacements under wind load in the acceptable limits (i.e. H/500). Perimeter belt trusses mounted at mid-height and top of the building have a beneficial effect, as they reduce the top lateral displacement under wind and seismic actions. They also reduce the torsional effects on the structure and improve the seismic behaviour.
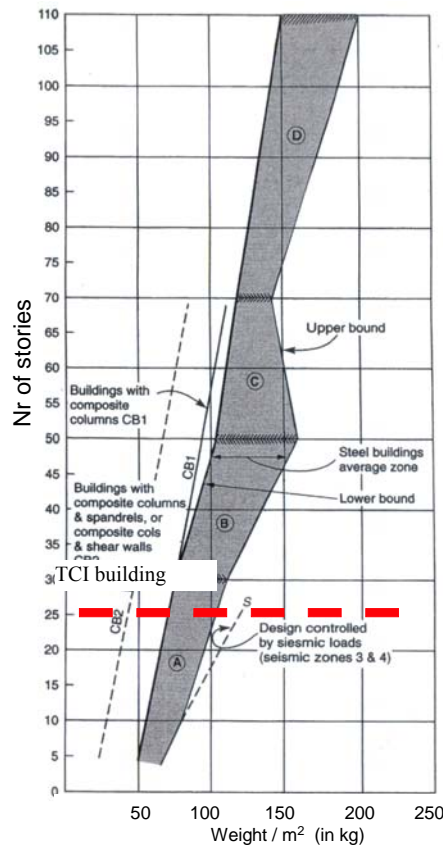
Figure 101: Wind load vs. seismic load [4]

The first two modes of vibration were translational, with $T_1 = 2{,}86$sec and $T_2 = 2.68$sec, and with low contribution from torsional modes ($T_3 = 1{,}76$sec).

As the seismic design concept was dissipative, the target of the design was to locate the

107

plastic hinges in beams, near their connections to the columns (for moment resisting frames MRF), or in the braces (for centrically braced frames CBF). Therefore, to avoid the development of plastic hinges in the connections, they must be provided with reasonable overstrength. According to seismic code (e.g. P100-1/2006 and EN1998-1), bolted non-dissipative connections of dissipative members must have a moment capacity higher than 1.375 plastic resistance of the member. For extended end plate bolted connections, it is difficult to achieve this high level of over strength. Therefore, in the case of TCI structure, the solution was to use haunches at beam ends (Figure 95:). Non-dissipative connections of dissipative braces, made by means of full penetration butt welds are deemed to satisfy the overstrength criterion. Shear studs were welded to the column webs near the beam-to-column joints, to ensure a composite action in the column and the transfer of the shear forces from column web to the concrete.
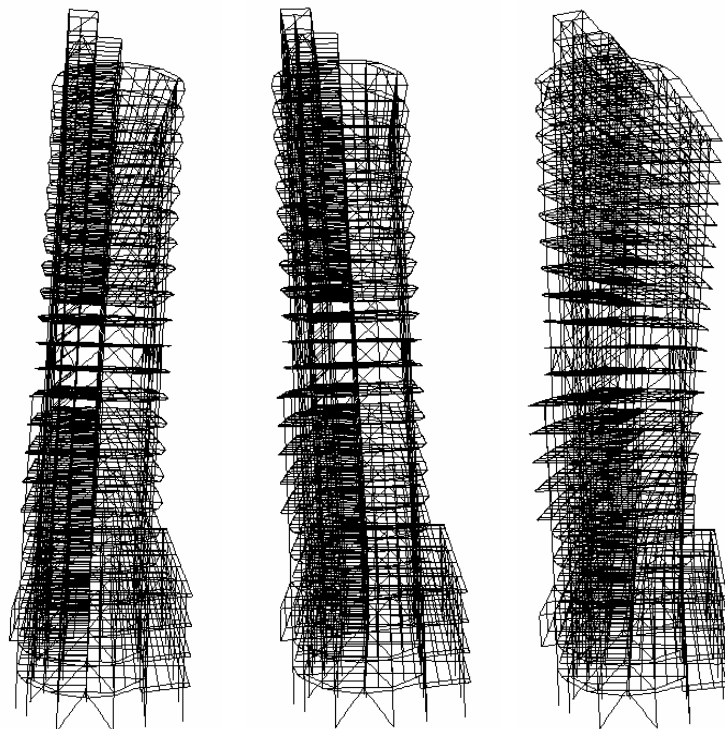
Figure 102: First three modes of vibration

Beams and braces are made of I hot rolled sections. S355 steel was generally used for frame members, excepting the braces designed as dissipative members, which are of S235 steel. Since dissipative elements are made by lower yield strength steel ("dual-steel" configuration), over strength requirement to non-dissipative elements (Ω factor) are reduced without affecting the stiffness against the lateral wind load. This was an innovative solution and, besides the provision considerations [5], had to be checked by a proper PBA. The actions considered in design were considered as follows:

- dead load: 6.2kN/m^2
- live load: 2.0kN/m^2
- snow load: $g_z = 1.50$kN/m^2
- wind load: base pressure $g_v = 0.55$kN/m^2
- base shear force, P100-1/2006:
  - $a_g = 0.24$g (Bucharest)
  - q = 4 (dual frame structure)
  - $T_B = 0.16$ s; $T_C = 1.6$ s; $T_D = 2.0$ s;
  - $\beta_0 = 2.75$ (see Figure 103)
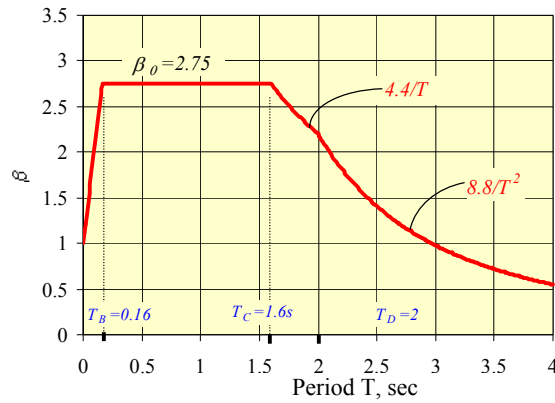
Figure 103 Normalised elastic response spectrum for Bucharest

Tall buildings may experience high winds. Resonant dynamic response in along-wind or cross-wind is a feature of the overall structural loads experienced by these structures. Moreover, extreme local pressures may be experienced on their walls or glass facades. In case of TCI building, due to its irregular shape, there were no precise relations in the code to evaluate the wind pressure (pressure coefficients), and therefore a boundary-layer wind-tunnel testing was carried out with a rigid model [6]. The length scale of the model was 1:100. The mean wind velocity profile was described by Davenport's power law (Figure 104):

$$U(z) = G\left(\frac{z}{\delta}\right)^{\alpha} \tag{1}$$

where:
- G is the gradient wind speed
- z is the altitude
- α is the Davenport exponent; $\alpha = 0,23$
- δ is the thickness of the boundary layer in the area of the building site; $\delta = 300$ m.
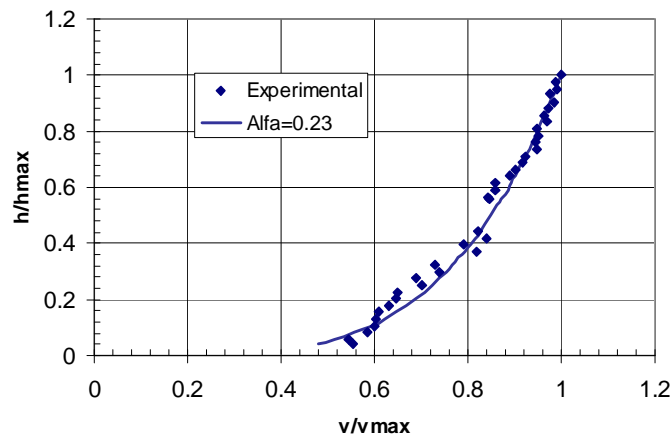
Figure 104 Mean wind profile, experimental vs. theoretical
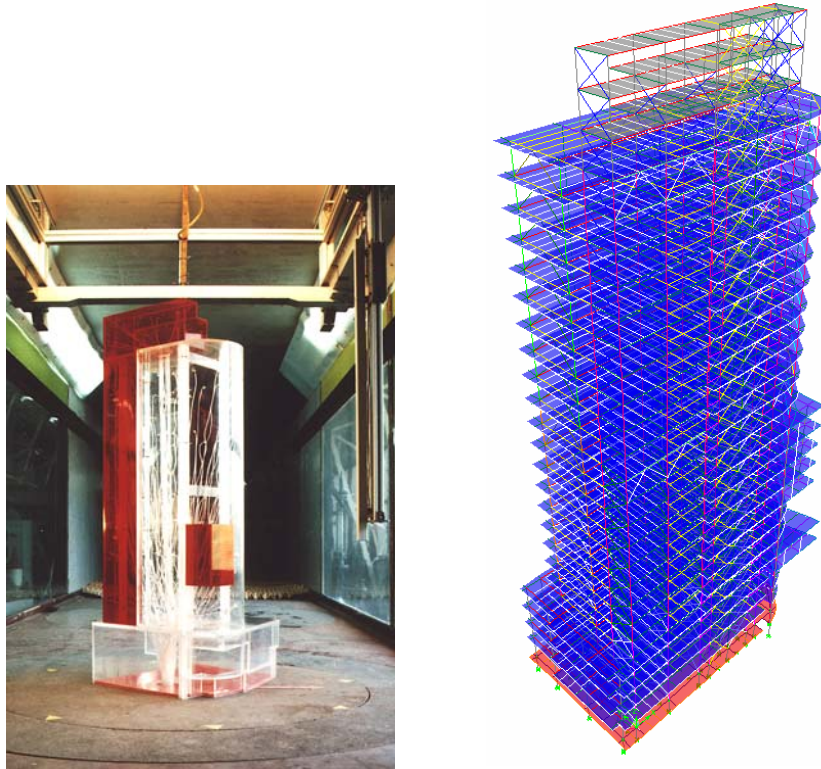
Figure 105 Rigid wind model, length scale 1:100

Eight different wind directions were considered, between 0^0 and 360^0, at every 45^0 (Table 28). Wind tunnel test confirmed the values of pressure coefficients given by code recommendations (Figure 106 , Figure 107). Attention should be paid at transition between round and flat areas, where pressure tends to intensify significantly. In order to obtain a more estimation of the wind effect, aeroelastic model tests in the boundary-layer wind tunnel were done. These tests provide the overall mean and dynamic loads, displacements, rotations, and accelerations.
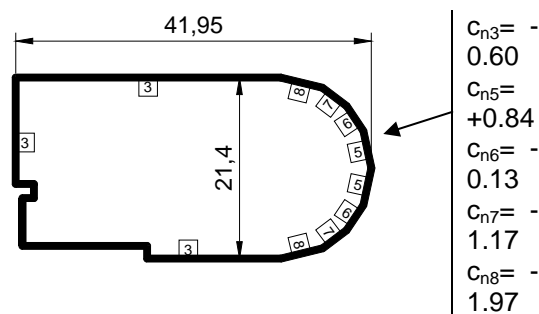
Figure 106 Design pressure coefficients, E-V

Table 28. Wind direction on the scaled model

Wind direction	N	NE	E	SE	S	SV	V	NV
Wind – model incident angle θ	230^0	185^0	140^0	95^0	50^0	5^0	320^0	275^0

110
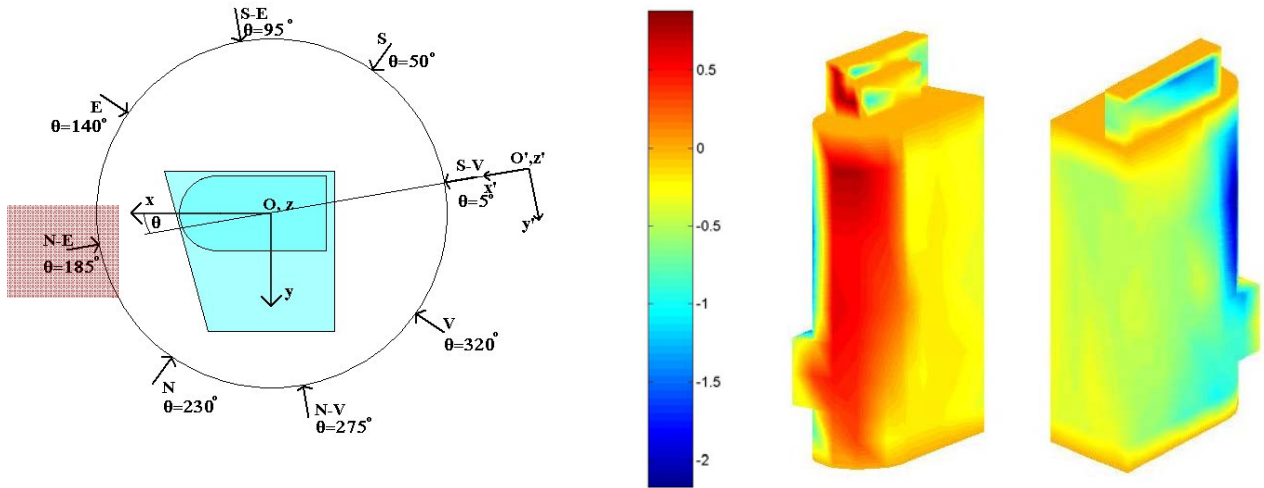
Figure 107 Distribution of the pressure coefficients on the envelope of the rigid model scaled to 1:100, NE direction of the wind
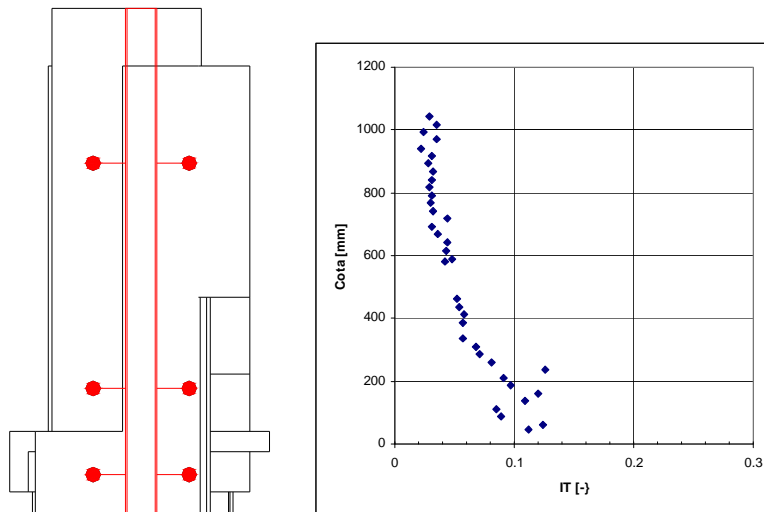
Figure 108 Eddies generators and surface roughness treatments

In order to have a correct evaluation of the wind effects, it is necessary to have a good similarity in behaviour between the model and the full-scale structure. This may be done by means of a group of variables. This group of variables should be numerically equal for the model (wind tunnel) and prototype situation. In case of TCI building, a set of

8 variables were considered, which are:
- U   is the mean wind speed at some reference position.
- ρ   is density of air.
- μ   is the dynamic viscosity of air.
- ℓ_s is characteristic length of the structure.
- E_s is Young's modulus.
- δ_s is logarithmic decrement of structural damping.
- g is acceleration due to gravity.

     With the similarity conditions selected, the scaled model was tested in the turbulent boundary-layer flow.

     In order to obtain the appropriate turbulence intensity and roughness, five eddy generators and discrete surface roughness treatments were installed (Figure 108). Results have shown accelerations and displacements are bellow acceptable levels according to the destination and construction type.

4.2.4   *Performance based seismic evaluation*

In order to evaluate the performance of the structure under seismic actions, a performance based procedure was employed. Three performance levels were considered: serviceability limit state (SLS), ultimate limit state (ULS) and collapse prevention (CPLS) limit state. Intensity of earthquake action at the ULS is equal to the design one (intensity factor $\lambda = 1.0$). Ground motion intensity at the SLS is reduced to $\lambda = 0.5$ (similar to $\nu = 0.5$ in EN 1998-1), while for the CPLS limit state was increased to $\lambda = 1.5$ ([7]). Based on FEMA 356, the following acceptance criteria were considered in the study:

- for braces in compression, plastic deformations at SLS, ULS and CPLS are $0.25\Delta_c$, $5\Delta_c$ and $7\Delta_c$, where Δ_c is the axial deformation at expected buckling load.
- for braces in tension, plastic deformations at SLS, ULS and CPLS are $0.25\Delta_t$, $7\Delta_t$ and $9\Delta_t$, where Δ_t is the axial deformation at expected tensile yielding load.
- for beams in flexure, the plastic rotation at ULS and CPLS are $6\theta_y$ and $8\theta_y$, where θ_y is the yield rotation.
- for columns in flexure, the plastic rotation at ULS and CPLS are $5\theta_y$ and $6.5\theta_y$, where θ_y is the yield rotation.

Beams and columns were modelled with fibre hinge beam-column elements, with plastic hinges located at both ends. In order to take into account the buckling of the compression diagonal, the post buckling resistance of the brace in compression was set $0.2N_{b,Rd}$ (*Figure 109*), where Af_y is the tensile yield resistance and $N_{b,Rd}$ is the buckling resistance for compression [7]. A strain-hardening ratio of 0.03 was used for all of the analysis in this study. In order to assess the structural performance, nonlinear dynamic analyses were performed. A set of seven ground motions were used in the analysis (see Figure 110). Spectral characteristics of the ground motions were modified by scaling Fourier amplitudes to match the target spectrum [2]. This results in a group of semiartificial records representative to the seismic source affecting the building site and soft soil conditions in Bucharest.
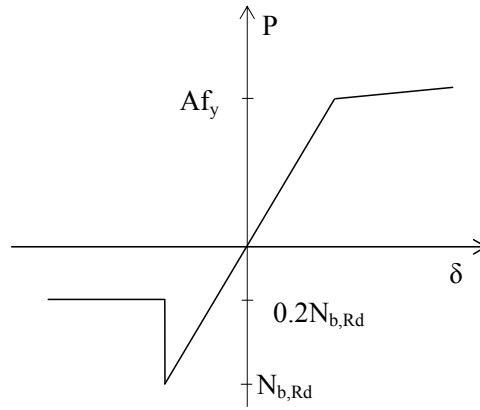
Figure 109 Response of bracing members
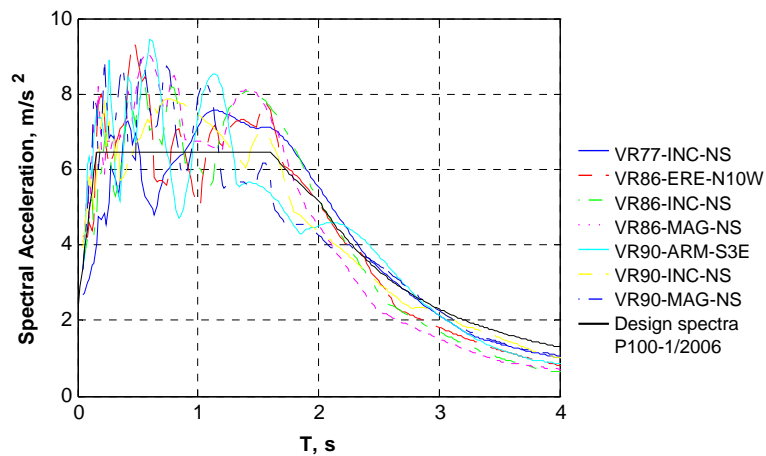
Figure 110 Elastic acceleration response spectra of the semi artificial accelerograms and design spectra (P100-1/2006, a_g=0.24g, TC=1.6s)

The results obtained from nonlinear timehistory analyses shown that the frames progress in post-elastic range, towards a "full plastic mechanism" configuration, as it was considered in the design strategy and effectively realised by the detailing of the steel/composite members and connections of the structure (Figure 111, Table 29). It can be observed that structure has adequate performance at the SLS (λ=0.5), ULS (λ=1.0) and CPLS (λ=1.5) limit states. In the dual configuration structure, the higher energy dissipation capacity of MRFs brings important benefits to the overall energy dissipated by the structure by plastic deformations. Plastic deformations in braces and beams indicate an incipient damage to the structure at SLS (ag = 0.16g), while plastic deformations in non-dissipative elements (columns) are completely avoided. For the ground motion scaled to the design acceleration (a_g = 0.24g), the maximum plastic rotation in the beams of MRF is of 0.01rad and this rotation demand increases to 0.015rad for a_g = 0.36g.

The distribution of the maximum interstorey drifts in transversal direction is shown in Figure 112, for the SLS (S_a = 0.16g), ULS (S_a = 0.24g) and CPLS (S_a = 0.36g). For frequent earthquakes, associated to SLS, the maximum interstorey drift is less than 0.005, which was the limit adopted in design. Again should be mentioned the effectiveness of the perimeter truss belt in reducing the top lateral displacement.

113
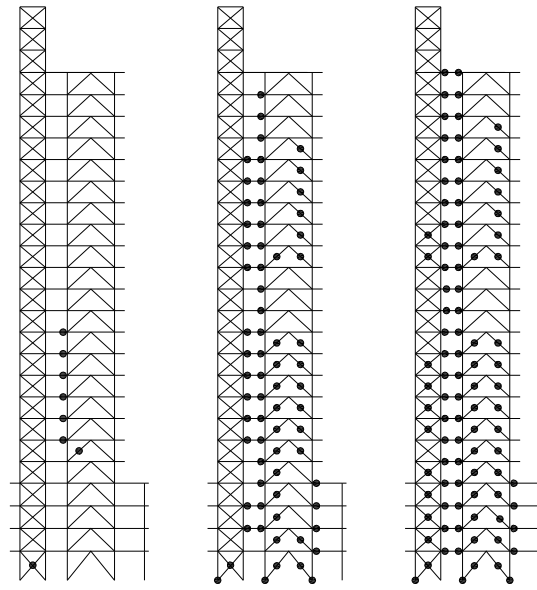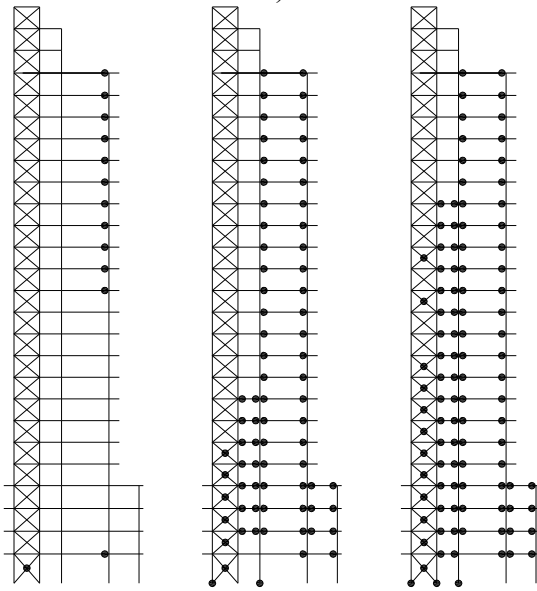
Figure 111 Plastic hinges: a) side transversal frame; b) current transversal frame

Table 29. Plastic rotation in beams and columns (in rad) and plastic deformation in braces (in %) at SLS, ULS and CPLS, average of records

	braces	beams	columns
SLS	0.002	0.002	-
ULS	0.006	0.01	0.002
CPLS	0.009	0.015	0.0035
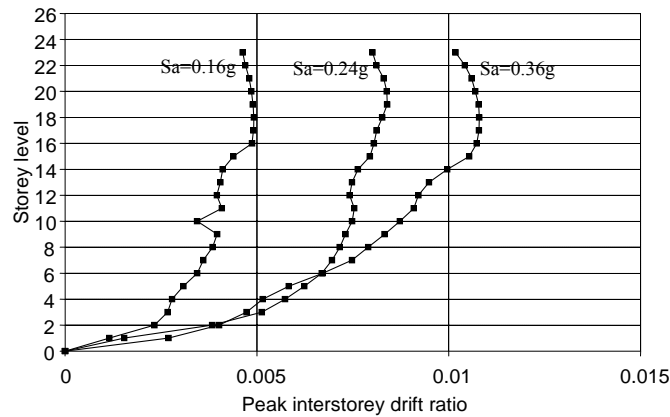
Figure 112 Peak interstorey drift ratio vs. storey level for transversal direction, average of records

4.2.5 *Study of structural robustness in case of column loss*

When subjected to extreme loadings, like blast or impact, multi-storey buildings may fail in a very specific manner, called progressive collapse. Progressive collapse refers to the spread of an initial local failure from element to element, eventually resulting in a disproportionate extent of collapse relative to the area of initial damage. Localized damage due to direct air-blast effects may or may not progress, depending on the design and construction of the building. Previous studies showed that seismic resistant structures may survive to such events, mostly due to the redundancy incorporated in the structure.

In order to evaluate the robustness of the structure in case of column loss, alternate load path method was used. The alternate load path method provides a formal check of the capability of the structural system to resist the removal of specific elements, such as a column at the building perimeter. The method does not require characterization of the threat causing loss of the element, and is, therefore, a threat independent approach. An advantage of this approach is that it promotes structural systems with ductility, continuity and energy absorbing properties that are desirable in preventing progressive collapse. This method is also consistent with the seismic design approach. The seismic codes promote regular structures that are well tied together. They also require ductile details so that plastic rotations can take place. The alternate load path approach assumes a hypothetical damage state that ignores all other damage to the structural members that may accompany the loss of critical column support in the real situation. The transition from the original structural configuration to the damaged state is assumed to be instantaneous, exposing the structure to a dynamic effect. Dynamic effects are taken into account in different ways depending on the analytical technique used. Because it is not reasonable to require a structure to respond elastically to the effects of an instantaneous column removal, structures are permitted to develop plastic hinges and sustain significant inelastic deformations when subjected to these extreme-loading conditions. This enables the structure to dissipate significant amounts of energy that would otherwise impose much greater dynamic loadings to the individual members. In case of this study, it was used an inelastic static analysis, or push-down method.

The nonlinear static approach generally simulates a dynamic enhancement through a load factor and incrementally applies the gravity load reaction of the removed columns. Dynamic effects coming from the instantaneous removal of the column are taken into account by the use of a dynamic amplification factor for dead load only. In the literature, this amplification amounts a value of 2.

The gravity loads are incrementally applied resulting in a push-down analysis. The load combination for analysis is: $2 \times (D + 0.5L) + 0.2 \times W$, where D, L and W are dead, live and

wind loads. Dead and live loads are amplified only on the floors above the affected area. The columns are removed one by one in order to see how many columns the structure can loss till global collapse initiate. The aim is to prevent progressive collapse by limiting the rotations in plastic hinges to the rotation capacity of the elements and connections. Two scenarios were considered in the study:

- case 1: loss of 1st floor interior columns
- case 2: loss of 14th floor interior column.

The development of collapse mechanism may prevent the total collapse if the beams and their joints may develop large plastic deformations without fail. Therefore, the rotation demand in the plastic hinges may indicate the state of damage in the structure and the potential to global collapse. In the study, the beams may be considered failed when the plastic rotation exceeds 0.035rad.

4.2.6 *Analytical results*

The static nonlinear analyses for different hazard levels (columns removal), shown the structure is capable to support vertical loads in case of the loss of 15 to 20% of all columns of the first floor. In case of 1st scenario, structure was stable after the loss of 5 interior columns. Plastic hinges occurred in beams located on 1st to 13th storey, with maximum rotation reaching 0.015rad, for 5 columns removal. In case of 2nd scenario, structure was also stable after the loss of 5 interior columns but maximum plastic rotation reached 0.007rad, only, due to the lower amount of vertical loads to be imparted in the remaining structure. These plastic rotation demands are similar to those coming from a strong ground motion associated to collapse prevention limit state (475 yrs. in P100-1/2006).
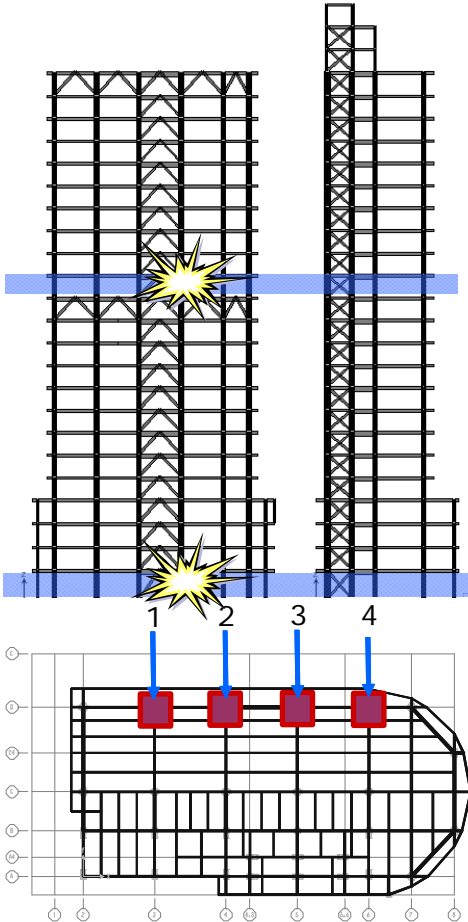
Figure 113 Location of member loss: case 1: 1st floor; case 2: 14th floor

In the beams where a catenary effect is induced by the missing columns, significant increases of axial force occur. The level of axial forces in the dissipative members should be very strictly monitored, as it may limit the plastic rotation capacity of members. According to seismic provisions (EN1998-1), for elements in bending, there is no reduction in plastic rotation capacity if axial force N_{Ed} is less than $0,15N_{pl,Rd}$. As was mentioned earlier in the introduction, the use of mega-truss or hat bracings would increase the resistance to progressive collapse. This is clearly seen in Figure 114a, where the presence of the intermediate perimeter belt trusses isolates the plastic hinges to the lower half of the structure and distributes more evenly the plastic rotation demands in beams.

In order to see the importance of truss system, the belt trusses were removed, both from mid-height and top of the structure. In Figure 115 plastic hinges in the structure in the new configuration are plotted. It may be seen that in case of 1st scenario, plastic hinges spread now on the entire height of the structure and rotations amount 0.013rad. Also very important, the structure is no more stable after the removal of 5 columns, like it was when the belt trusses were in place, and it can survive with 4 column loss, only.

a)

b)
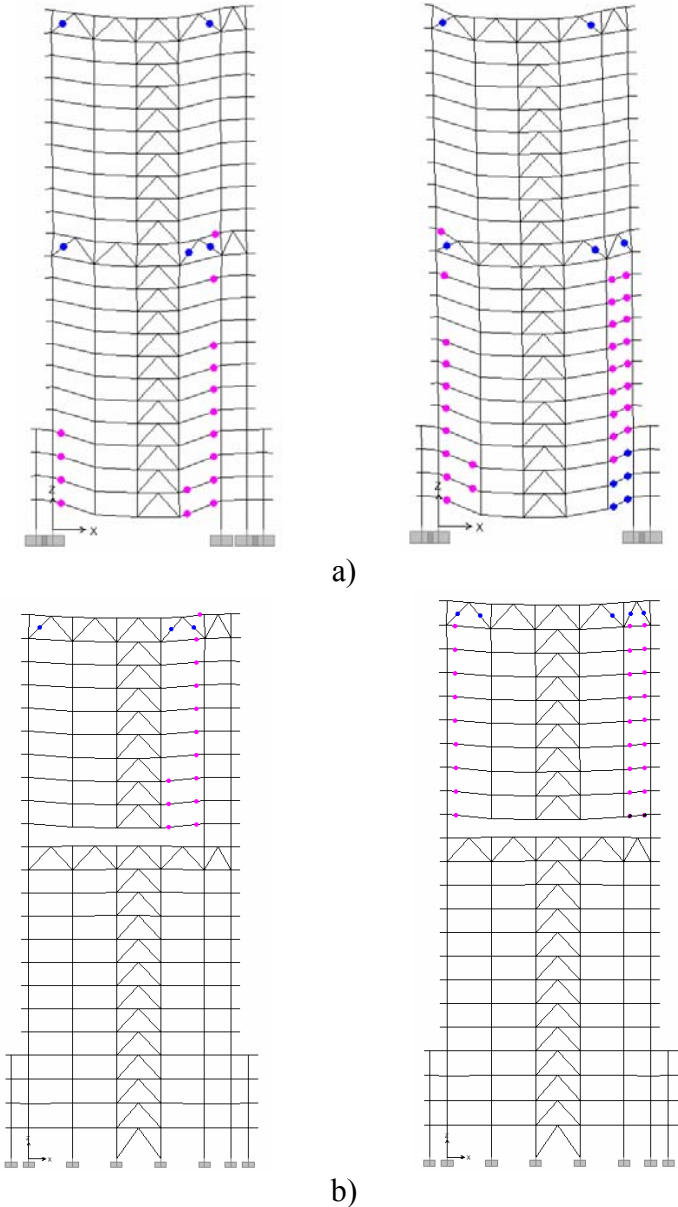
Figure 114 Plastic hinge in the structure for three and four column loss: a) case 1; b) case 2

117
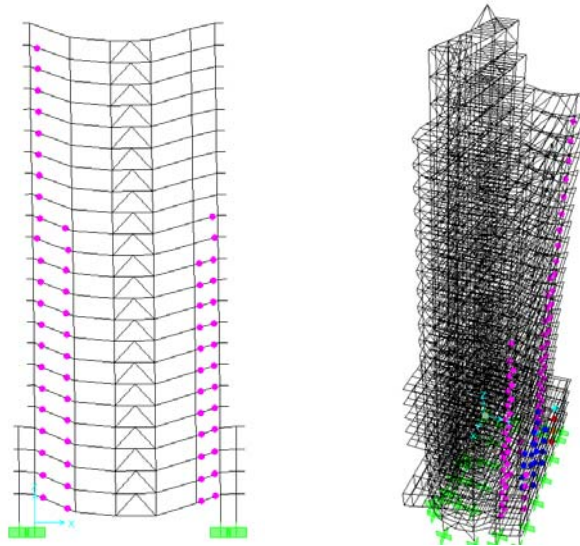
Figure 115 Plastic hinge in the structure for 1st scenario, 4 columns loss and belt trusses removed

4.2.7 References

[1] Eurocode 8: Design provisions for earthquake resistance of structures - 1-1: General rules - Seismic actions and general requirements for structures, CEN, EN1998-1-1, 2004.

[2] Cod de proiectare seismică P100: Partea I, P100-1/2004: Prevederi de proiectare pentru clădiri, 2006.

[3] Etabs version 9. Computers & Structures Inc, CSI, CSI Berkeley, Inc. Structural and Earthquake, 2005.

[4] B. S. Taranath. Wind and Earthquake Resistant Buildings: Structural Analysis and Design, Ed. M. D. Meyer, 2004.

[5] Dubina D. and Dinu F., Seismic performance of dual- steel multistorey building frames, Proceeding: Int. Seminar devoted to the activity of Prof. Rene Maquoi, Liege, Belgia, 14-15 December 2007.

[6] L. Sandu, M. Degeratu, L. Hasegan, A. Georgescu, C. Cosoiu. Design report Modelarea acţiunii vântului asupra clădirii Bucharest Tower Center International, Contract nr. 427 / 2004 (in Romanian)

[7] FEMA 356, Prestandard and commentary for the seismic rehabilitation of buildings; Washington (DC): Federal Emergency Management Agency, 2000.

4.3 Design and performance based evaluation of a 6 storey building located in Constanta

4.3.1 Description of building

The case study building is a 6-storey office building (see Figure 116). The lateral load resisting structure is made of moment resisting frames on both directions. The flooring system is realized with in situ concrete slab. The exterior walls of the building are made with framed glass windows. The basic dimensions of the building in plane are 9.05m×17.65m, the storey height is 3.8 m and the total height is 26.75m. The foundation design is not required but it can be assumed that RC foundations will provide a rigid support. The building was constructed in 2010, and since 2011 is in operation.
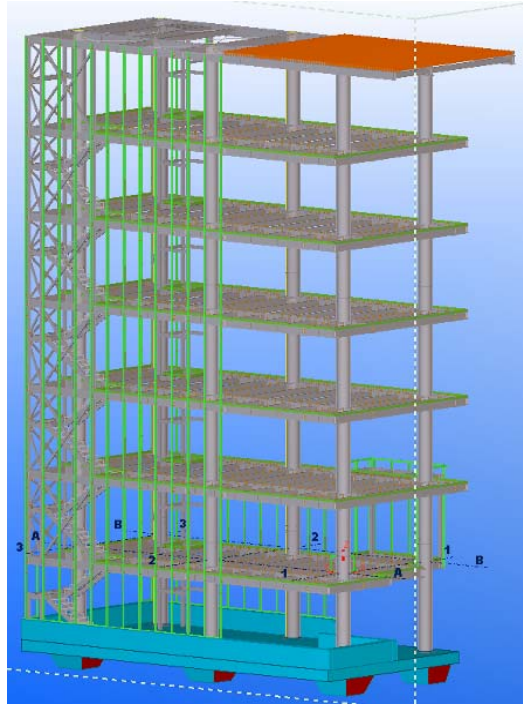
Figure 116. General view

4.3.2 Structural system

Structural system is made of transversal and longitudinal moment resisting frames. Main girders and secondary beams are made of hot rolled profiles. Shear studs are welded on main girders and secondary beams. The composite action is considered for secondary beams only, while for main girders the shear studs have the role of preventing the out of plane deflection of the top flange in compression. Columns are made of concrete filled tubular columns with circular hollow steel section CHS (ϕ610x20mm, concrete C30/37, longitudinal reinforcing 12ϕ25). The CHS column-to-beam diaphragm connection is shown in Figure 117.

| Plan of the current floor | Transverse frame, line 2 | Longitudinal frame, line B |
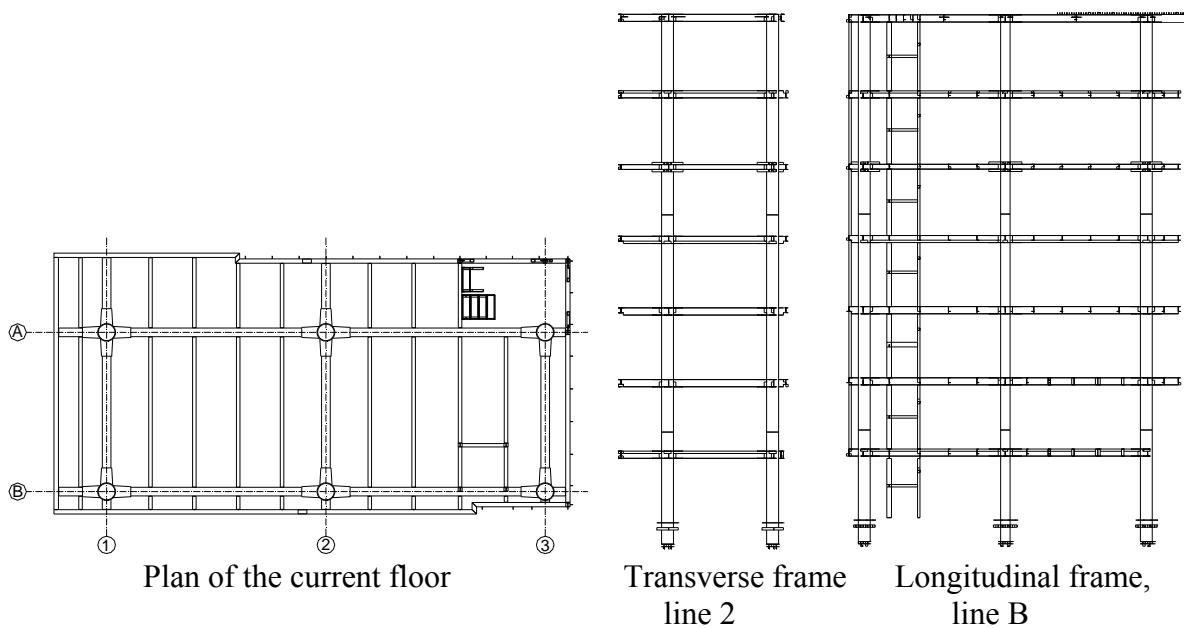
Figure 117. Building structure
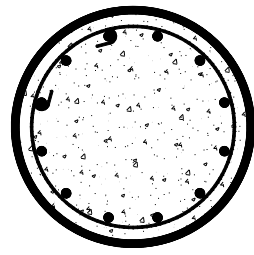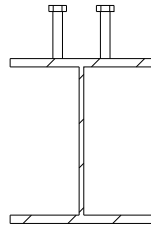
| circular column | main girder | secondary beam |

Figure 118. Typical cross section of the members
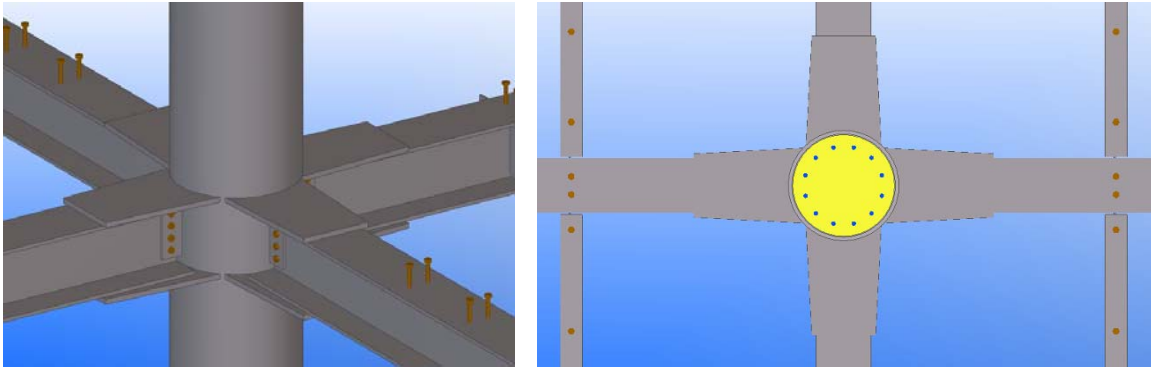
Figure 119. Typical CHS column-to-beam diaphragm connection

4.3.3 Structure design

4.3.3.1 Design loads

Loads are evaluated according to the relevant parts of EN 1991, while the combination of loads is done according to EN 1990 provisions.

Dead load
Dead load (G) includes the self-weight of the structure and permanent fittings and equipment and is equal to 4kN/sqm.

Live load
Live load (L) includes the weight of the structure's occupants and contents and is equal to 3kN/sqm.

Snow load
Characteristic value for snow loading on the roof (S) is 2.0 kN/sqm.

Wind load
Wind loading on the walls (W) is calculated with $V_{b,0}$ = 29m/s and an urban area. Wind has been considered both on transversal (WX) and longitudinal (WY) directions.

Seismic design
The EN 1998 type 1 spectrum constructed for soil type C has be used for the design. Design was done considering a seismic acceleration a_g = 0.30g for the ultimate limit state (10%

probability in 50years) event. The characteristic periods of the design spectrum are those indicated in the table below:

Soil Type	S	T_B (s)	T_C (s)	T_D (s)
C	1.15	0.20	0.60	2.0

The behavior factor (q factor) was reduced to 3 mainly due to the vertical irregularities, but also due to a reduced number of spans.

4.3.3.2 Load combinations

Partial safety factors are as follows:
- $\gamma_{M0} = 1,0$
- $\gamma_{M1} = 1,0$ (1.1 for seismic combinations)
- $\gamma_G = 1,35$ (permanent loads)
- $\gamma_Q = 1,50$ (variable loads)
- $\psi_0 = 0,70$ (live, snow)
- $\psi_0 = 0,60$ (wind)
- $\psi_1 = 0,50$ (live)
- $\psi_1 = 0,20$ (wind)
- $\psi_2 = 0,30$ (live)
- $\psi_{Ei} = 0,24$ (live) [$\varphi = 0.8$, $\psi_{Ei} = \varphi \times \psi_2$]

ULS combinations

→ Fundamental combinations (persistent or transient design situations):

$$1.35\sum_{j=1}^{n} G_{k,j} + 1.5 Q_{k,1} + \sum_{i=2}^{m} 1.5\psi_{0,i} Q_{k,i}$$

→ Seismic design situations

$$\sum_{j=1}^{n} G_{k,j} + \gamma_I A_{E,k} + \sum_{i=2}^{m} \psi_{2,i} Q_{k,i}$$

According to the seismic design concept of EC8, brittle failure or other types of undesirable failure mechanisms shall be prevented, assuming that plastic hinges are formed in dissipative members and primary seismic columns satisfy the following capacity design requirements:
- ESLU = 1.0G + 0.3Q + $A_{E,K}$ (dissipative members - beams)
- ESLUO = 1.0G + 0.3Q + 3$A_{E,K}$ (non-dissipative members - columns , excepting the base of the column, where the dissipative combination is used)

SLS combinations:
→ Non-seismic combinations

$$\sum_{j=1}^{n} G_{k,j} + Q_{k,1} + \sum_{i=2}^{m} \psi_{0,i} Q_{k,i}$$

→ Seismic combination
ESLS = 1.0P + 0.3Q + $q \cdot v \cdot A_{E,K}$

The dissipative zones were located in the beams. Therefore, the connections of the dissipative parts to the rest of the structure have been designed with sufficient overstrength to allow the

development of cyclic yielding in the dissipative beams. For non-dissipative connections, the following expression should be satisfied:

$$R_d \geq 1{,}1 \, \gamma_{ov} R_{fy}$$

where

R_d is the resistance of the connection in accordance with EN 1993;

R_{fy} is the plastic resistance of the connected dissipative member based on the design yield stress of the material as defined in EN 1993.

γ_{ov} is the overstrength factor and is equal to 1,25.

The analysis of the structure has been performed with SAP2000 computer code. The diaphragm effect of the concrete slab has been considered in the analysis.

The design for ultimate limit state and serviceability limit state, seismic design situation included, has been done according to EN1993-1-1, EN1993-1-8, EN1994-1-1 and EN1998-1.

4.3.4 *Performance based seismic evaluation*

The evaluation procedure of building structure for multiple performance objectives used the N2 method, which connects pushover analysis with the response spectrum approach. Beams and columns were modeled with concentrated plastic hinges located at the element ends.

A pushover analysis was first performed, under an inverted triangle lateral force pattern, accounting for P-Delta effects. The displacement demand corresponding to the ultimate limit state (life safety performance level) associated to a return period of 475 years (peak ground acceleration a_g = 0.30g) was determined using the N2 method (EN 1998-1, 2004). The top displacement demand amounted to D_t = 0,252 m (see Figure 120, Figure 121). At the target displacement, the maximum value of the plastic rotation in the beam is of 5 mrad, well below the EN1998-1 acceptance criteria of 35 mrad. First yielding in beams occurs on Y direction at a top displacement of 0,18 m, which is below the target displacement of 0,252 m. There are no plastic hinges in columns. Plastic hinge pattern at the target displacement is shown in Figure 124. Under rare earthquakes, the structure is in the post-earthquake damage state, the level of damage is moderate but some margin against either partial or total structural collapse remains. This indicates that the Life Safety performance level is not exceeded.

The results of the analysis for seismic intensity of 0.10g, corresponding to 63% probability of exceedance in 50 years (return period of 72 years) shows no plastic hinges developed in beams before the attainment of SLS target displacement (see Figure 120, Figure 122). This indicates that, under frequent earthquakes, the structure does not suffer any structural damage in members and the Immediate Occupancy performance level is not exceeded.

The structure should be designed with some margins against failure, in order to avoid partial or global collapse under very rare earthquakes, with a probability of exceedance of 5% in 50 years (or a return period of 975 years). As shown in Figure 120, the Collapse Prevention performance level is not exceeded even on X direction it is very closed to the point of failure.
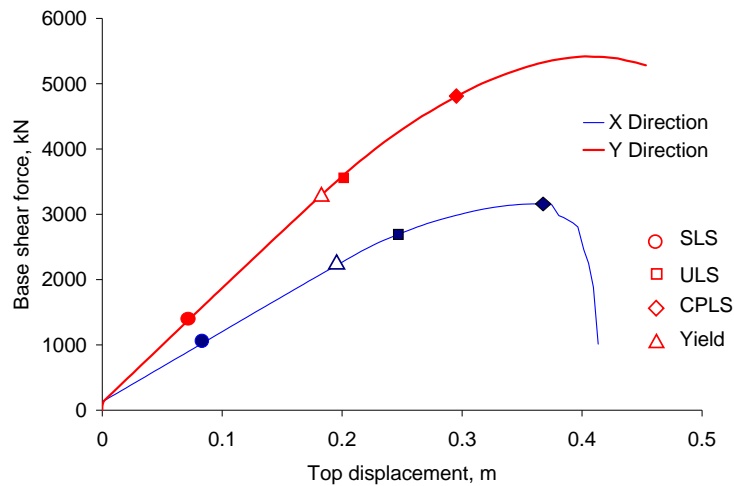
Figure 120. Push-over curves, X and Y directions
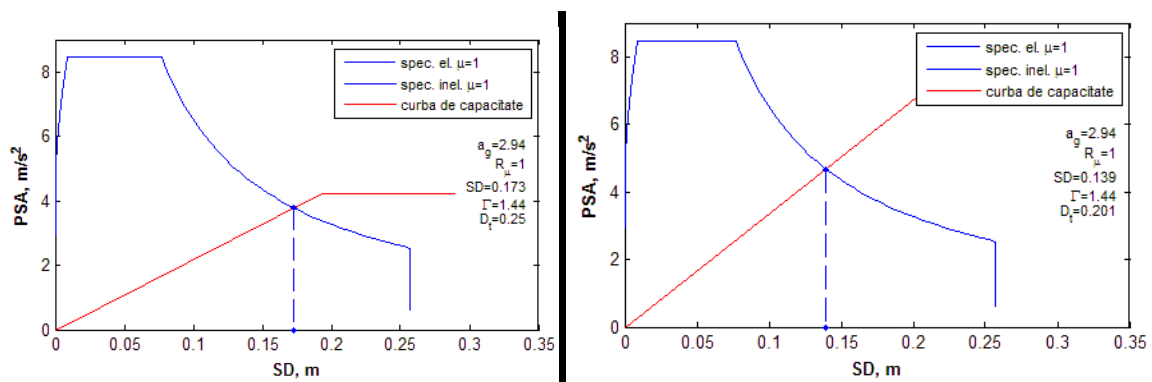
Figure 121. Target displacement for ULS, X direction (left) and Y direction (right)

Figure 122. Target displacement for SLS, X direction (left) and Y direction (right)

Figure 123. Target displacement for SLS, X direction (left) and Y direction (right)

Figure 124. Plastic hinges at ULS, X direction (left) and Y direction (right)

4.3.5 *Steel construction, views during construction*

Figure 125. Views during construction

4.4 Scientific and technical contributions of the author to the actual state-of-knowledge

Regarding the subjects presented above and based on the studies done by the author and the obtained results, the personal contributions include:

- Advanced design based on non-linear static and dynamic analysis, for earthquake situations and other extreme loading (column loss scenarios). Structural systems have been tested using advanced non-linear analysis for evaluating the plastic mechanism and the behaviour according to a performance based methodology. Also for important buildings, systematic robustness evaluations have been performed, which represents an important step forward.
- Designed assisted by testing of beam-to-column connections, macro-components and welding details: connection assemblies have been validated using full scale experimental tests, both under monotonic and dynamic loading, at room and elevated temperatures. Also, numerical models have been validated and parametrical analyses were performed.
- New systems for multi-storey buildings (dual steel systems, dual steel connections, new hysteretic devices). Dual-steel frames have dissipative members made of lower yield strength steel and non-dissipative members are made of higher steel grade. Dual steel connections have components of different steel grades, to allow a better hierarchy of components for optimizing the strength, stiffness and ductility properties. This activity has been very much appreciated and the candidate was awarded with several national and international prizes: Romanian Association of Structural Engineers, 2004, for the project: Bancpost building in Timisoara; Romanian Association of Structural Engineers, 2005, for the project: Shoping Center Bricostore Bucharest; Romanian Association of Structural Engineers, 2007, for the project: Tower Center International, Bucharest; Romanian Association of Structural Engineers, 2010, for the project: 6 storey office building located in Constanta; European Steel Design Award, 2007, for the project: Tower Center International, Bucharest.

(b-ii) Scientific, professional and academic future development plans

As presented in (b-i), the future research that will be done by the candidate will follow three main directions that are detailed below. First and second topics continue in fact the recent activities, and are mostly related to improving the robustness of structures under extreme loading. Third one is a new topic and aims at predicting, controlling and reacting to the structural reliability and durability issues caused by the climate change.

In the following these research directions are detailed:

Robustness based design of buildings
- Experimental program on beam-to-column joints under column loss scenario

For experimental tests investigating the connection behaviour a subassembly with following scheme has been designed (Figure 126). Figure 127 shows the test set up with the specimen. **The test should investigate four different types of connections (Figure 128). First two connections are partial strength and semirigid and the last two connections are rigid and have overstrength compared to the beams. Some preliminary numerical simulations have been performed in an attempt to evaluate the behavior and the main characteristics (ultimate deflection, ultimate base reaction forces, lateral restraining system), see** Figure 129, Figure 130. **The results wil be used to validate the models and provide acceptance criteria for robustness analysis of framed buildings under extreme loading.**

Figure 126. Subassembly static scheme
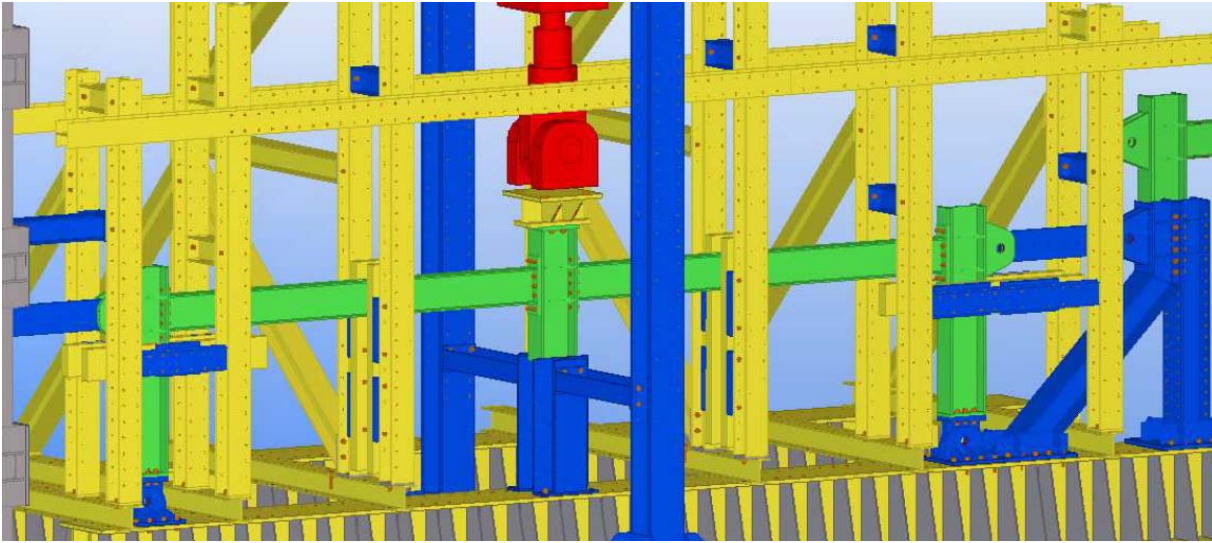
Figure 127. Subassembly 3D model

| a) | b) | c) | d) |
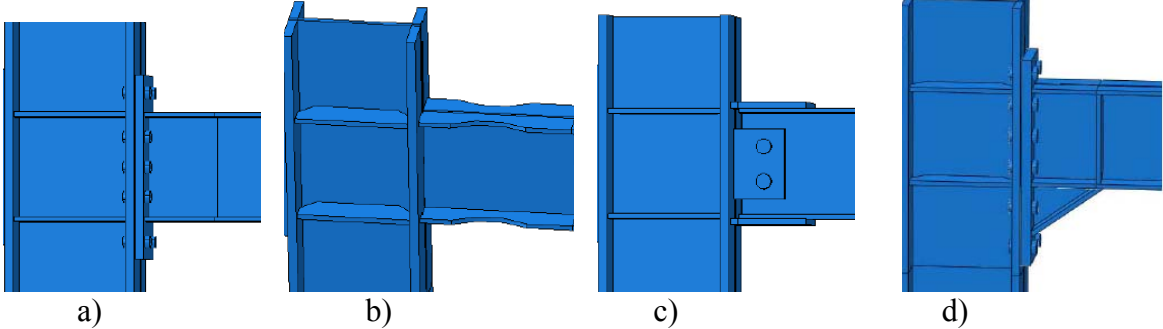
Figure 128. Connections typology: a) extended end plate bolted connection; b) reduced beam section connection; c) cover plate welded connection; haunch end plate bolted connection

a)

b)
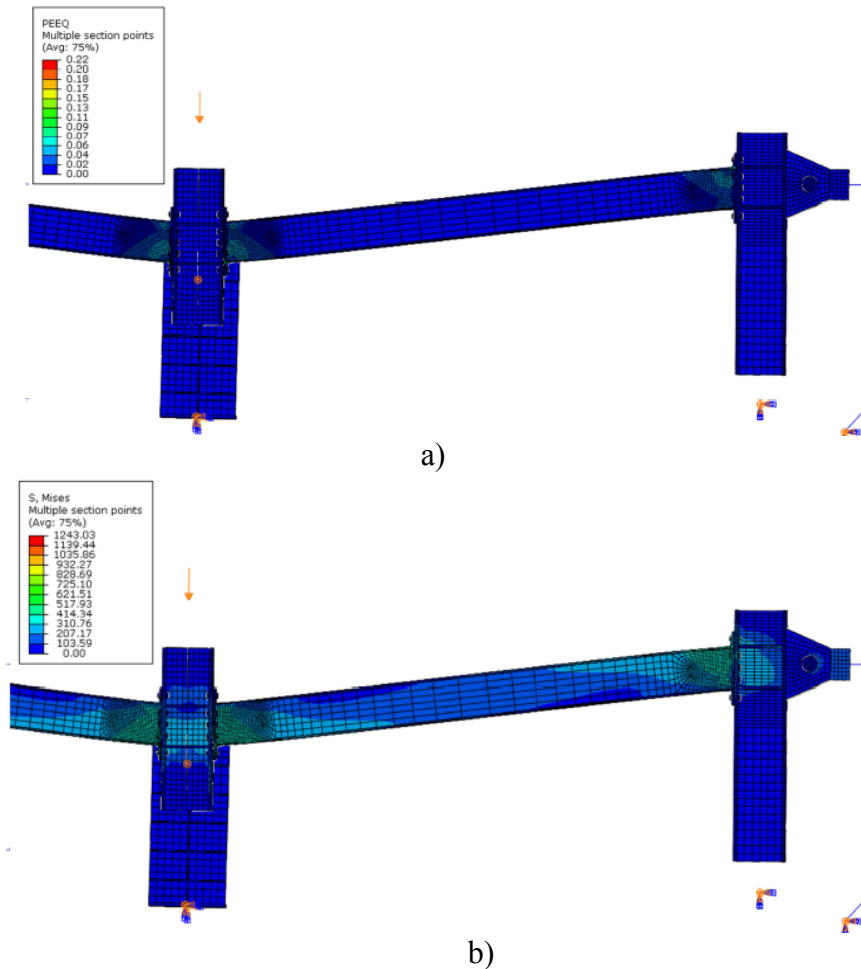
Figure 129. Numerical simulations on EP connection: a) plastic deformations; b) von Mises stresses
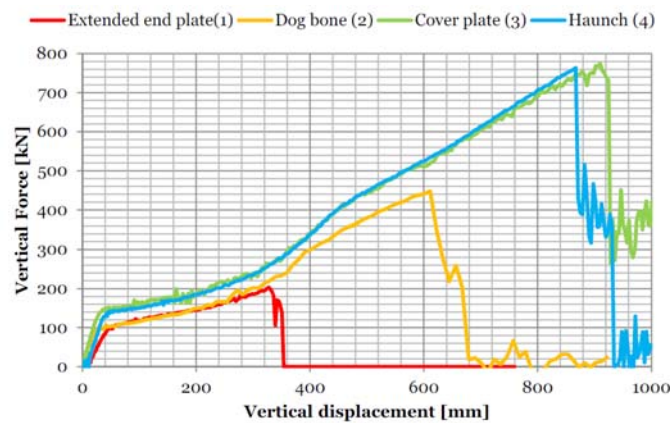

Figure 130. Comparison between force – vertical displacement curves for the connections

- Experimental program on 3D assemblies under column loss scenario

The experimental sub-assemblies are extracted from a reference building, ensuring that the support and connection conditions are equivalent to those in the reference building. A total of four typologies will be designed, constructed and teste experimentally under increasing vertical force till the complete failure ():

- Only steel structure - reference
- Composite beam structure

- Composite beam and composite slab structure
- Prefabricated slab structure.

All specimens have extended end bolted connections (Figure 133).

Some preliminary numerical simulations have been performed in an attempt to evaluate the behavior and the main characteristics (ultimate deflection, ultimate base reaction forces, and influence of shear studs on main and secondary beams, restraining system), see Figure 134, Figure 135, Figure 136. The results will be used to validate the models and provide acceptance criteria for robustness analysis of framed buildings under extreme loading.
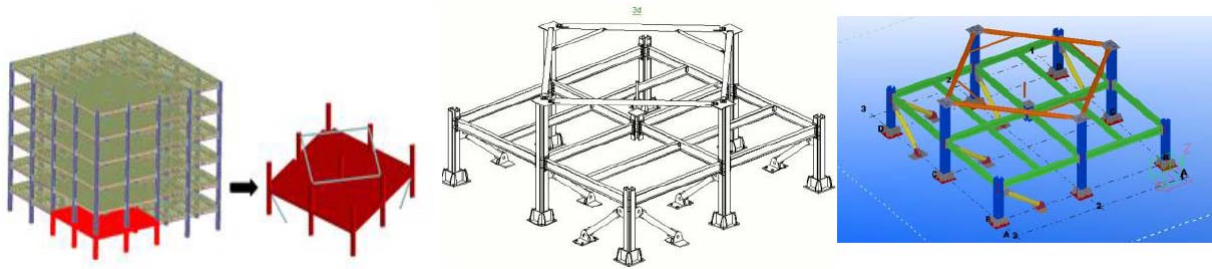
Figure 131. Extraction of sub-assembly specimens from the reference structure
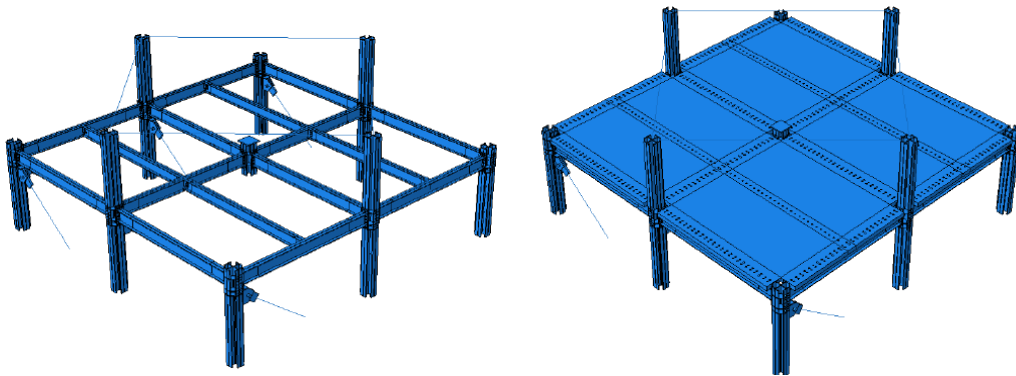
Figure 132. Sub-assembly specimens: pure steel structure (left); composite structures (right)
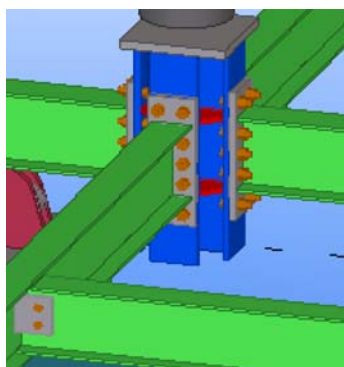
Figure 133. Central column with the beam-to-column connection
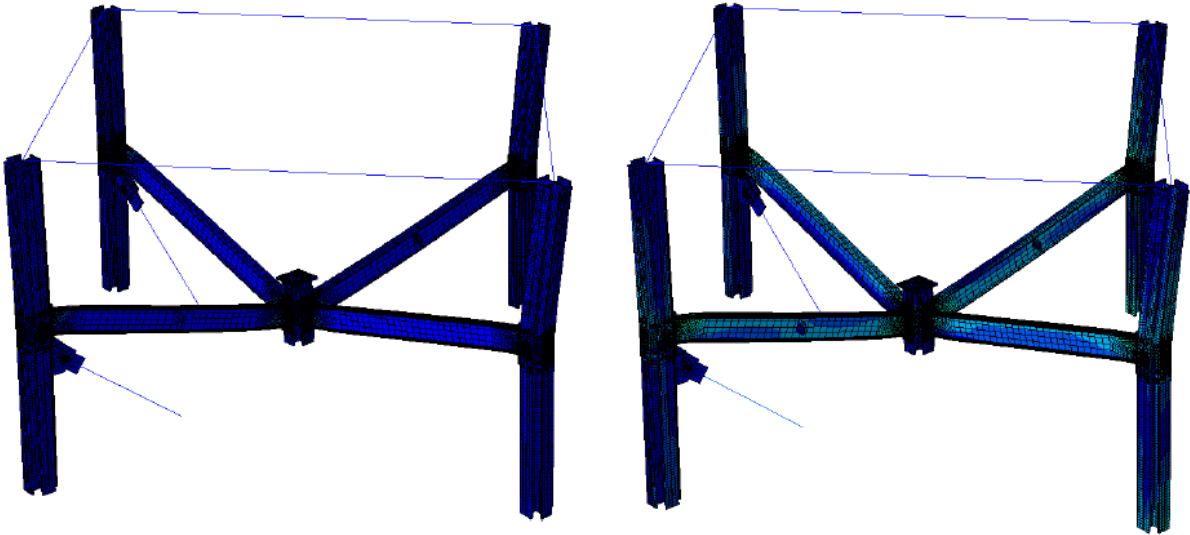
Figure 134. Deformed shape of the structure
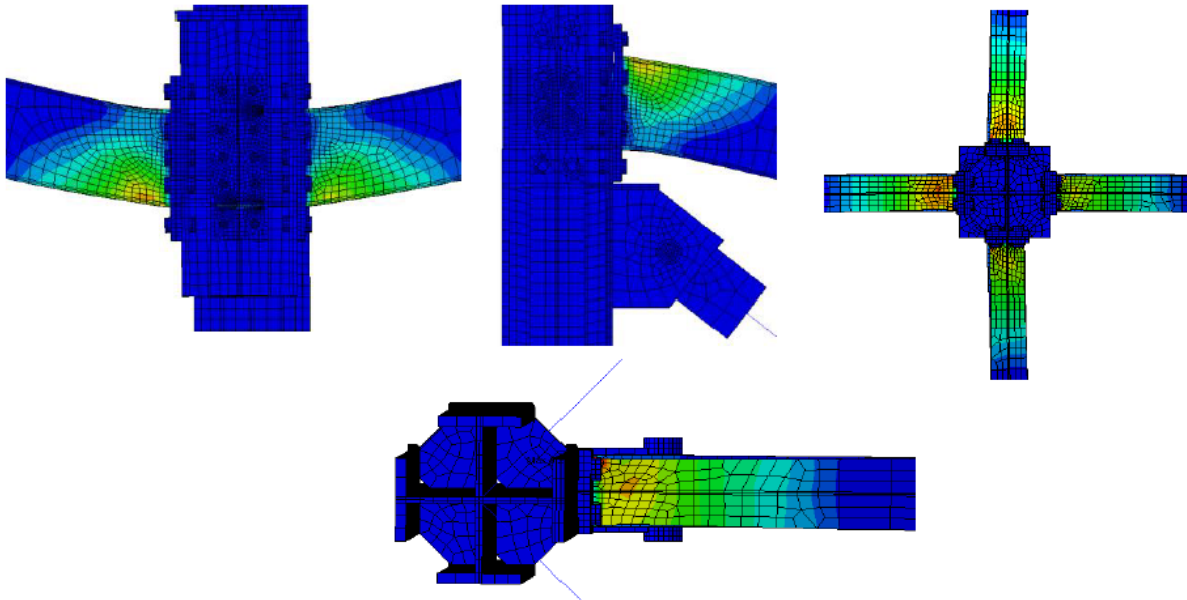
Figure 135. Development of plastic hinges in members
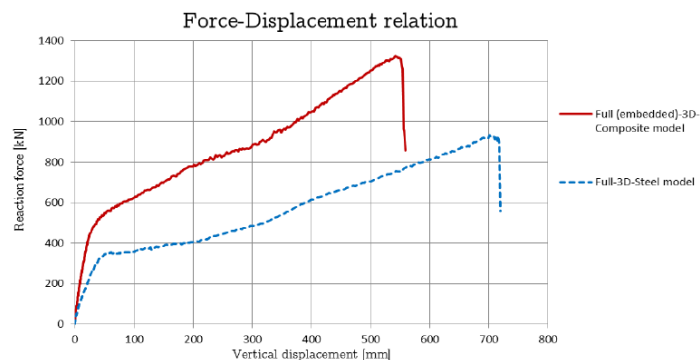
Figure 136. Comparison of force-displacement curve for full 3D steel model and 3D composite model

- Experimental program on macro-components and welding details under extreme loading

This program will continue the activity related to the local ductility and factors that have a potential effect on the ultimate deformation capacity of connections. The test will also use external blast as loading, and will vary the size of the charge and the distance to the element.
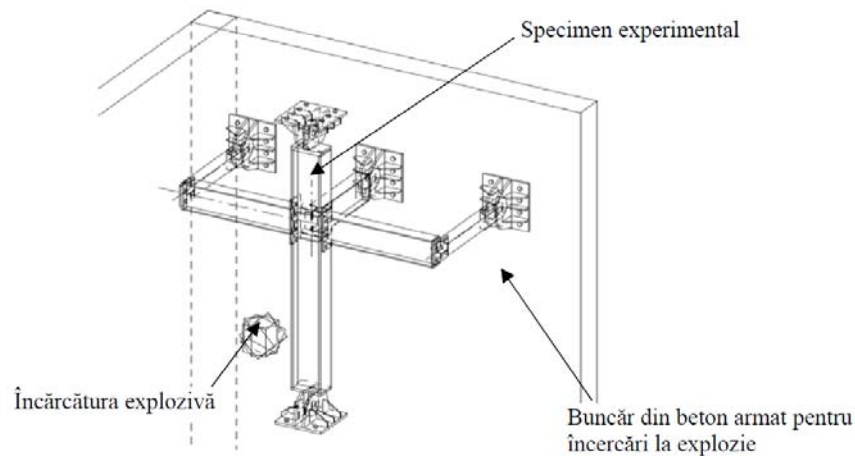


Figure 137. Direct blast specimen

Figure 138. Direct blast test: a) 3D specimen; b) effect of 1 kg TNT at 50 cm from the specimen, ELS simulation

- Validation of numerical models for members and connections to evaluate the progressive collapse resistance of framed buildings

Some reference to the numerical simulation program has been made in the previous sections. Based on the large experimental program that will be developed at CEMSIG Research Centre, it is also important to validate numerical models that may be further used for advanced numerical analysis.

- Improved details for progressive collapse resistance

Redistribution of forces, especially by the development of catenary action (steel structure only) in beams and membrane action (composite structure) in the slab provide an important gain for the progressive collapse resistance under extreme loading. When there is an initiation of progressive collapse occurs, the connections are subjected to significant tension, which is different from their behavior in normal load condition. This is because the ductile joints allow for redistribution of internal forces within the structural system by enabling large deformations so that they are suitable for progressive collapse mitigation by transition from flexural loading to axial loading in the members and joints and initiating of a catenary action.
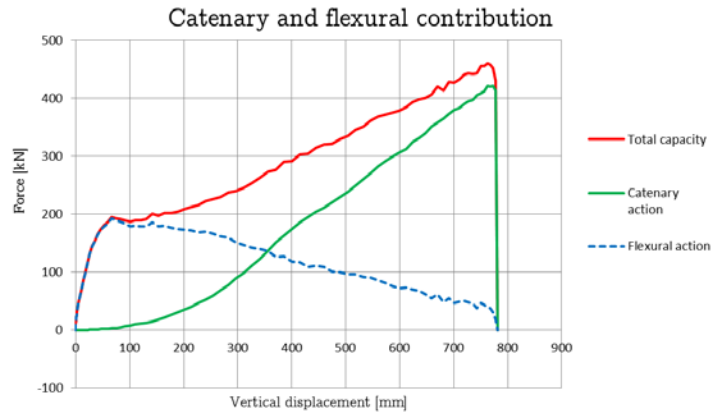
Figure 139. Catenary and flexural action

- o Guidelines for the collapse control performance based design of multi-story frame buildings against accidental actions

The activity is devoted to a review of research on progressive collapse, related guidelines and recommendations as well as to the gaps in knowledge and research needs following the latest developments in the field. Case studies that can offer some insight into the problems of progressive collapse and lessons to be learned are also investigated. The benefits of seismic design philosophy on the integrity of the multi-storey structures will be identified.

Improved structural systems and application to buildings
- New structural systems based on removable dissipative members
- New hysteretic devices with improved damping characteristics (eg. visco-elastic dampers)
- Application of new braced systems (steel panels, buckling restrained braces) to design of new buildings
- Application of new braced systems (steel panels, buckling restrained braces) for refurbishing existing buildings.

All these topics refer to the application of new concepts and special devices for improving the robustness of framed buildings against extreme loading. These devices were mainly designed for improving the seismic behavior but they may be effective for other loadings too. Of specific interest in the application of new braced systems for refurbishing existing buildings.
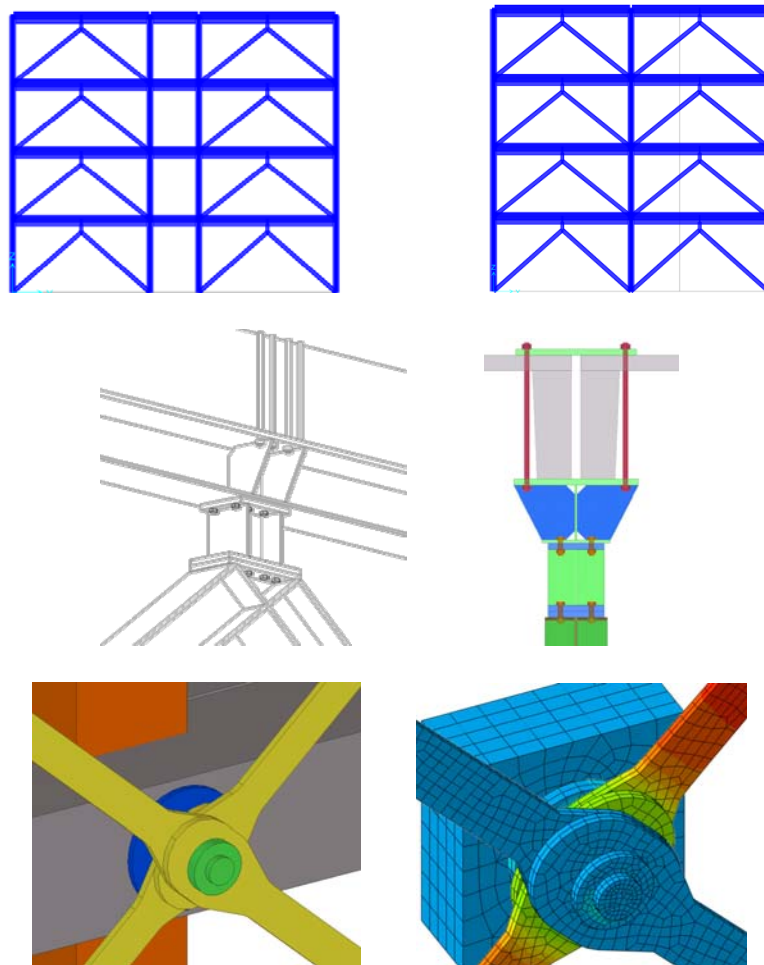
Figure 140. Application of a vertical link system for refurbishing existing structures

<u>Durability of structures under climate change effects</u>
- evaluation of the reliability and durability of structures along the designed lifetime
- methodologies for Performance Based Evaluation / Design of construction for progressive climate action exposures;
- intervention strategies and adaptive building technologies

Load effect E_d and resistance R_d are influenced by the climate change. Climate change may influence the return period of extreme weather events (heavy loads of snow or extreme winds) which results in an increase of loads Ed, while changes in temperature, humidity, levels of precipitation, wind, frequency of extreme weather and emissions reduce the durability of the materials and their resistance R_d. Moisture associated with temperature variations affects the mechanical properties and durability of building materials, finally with impact on building safety and health. It is necessary to initiate the systematic survey of climate change effects against constructions, on the aim to provide a coherent approach, starting with definition and characterization of actions, observation and quantification of the climate-affected material properties, evaluation of the reliability and durability of structures along the designed lifetime, providing reference criteria, and background studies for technical regulations and, finally, proposing intervention strategies.